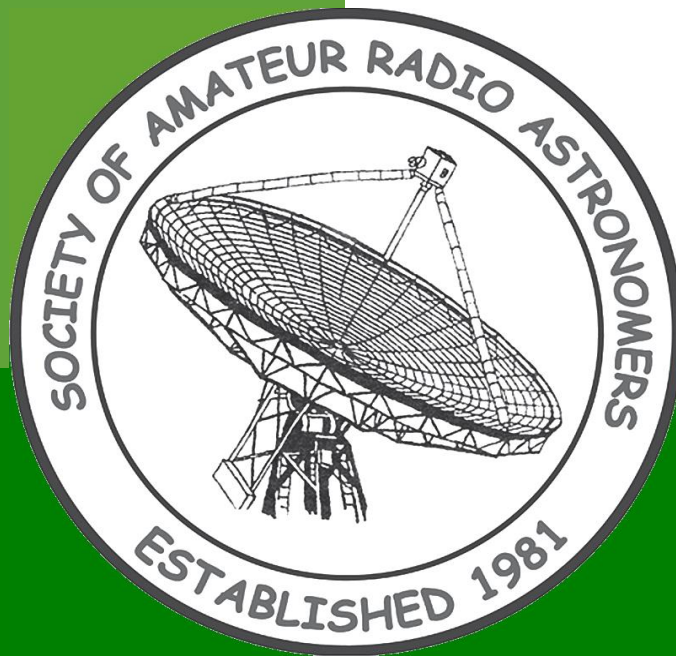# Proceedings
of the 2014 Conference
of the Society of Amateur Radio Astronomers

June 29- July 2, 2014

National Radio Astronomy Observatory
Green Bank, West Virginia

Mission Statement

It shall be the Mission of the Society of Amateur Radio Astronomers

(SARA) to:

- Facilitate the flow of information pertinent to the field of Radio Astronomy among our members.

- Promote members to mentor newcomers to our hobby, and share the excitement of radio astronomy with other interested persons and organizations.

- Promote individual and multi station observing programs.

- Encourage programs that enhance the technical abilities of our members to monitor cosmic radio signals, as well as to share and analyze such signals.

- Encourage educational programs within SARA and also educational outreach initiatives.

- The Society of Amateur Radio Astronomers, Inc. is a membership supported, non-profit [501(c)(3)], educational and scientific corporation.

~ The President's Page ~

I would like to welcome all of our members and guests to the Society of Amateur Radio Astronomers Society 2014 Annual Conference. This is my last year as President of SARA and it looks like we will have one of the biggest SARA Conferences ever. With two Nobel Laureates on the schedule, the great papers from members and the Radio JOVE team we are seeing a huge interest in radio astronomy. Although I will no longer be president, I will continue to support the growth of SARA and look forward to progress made by our members and this great organization.

We have been meeting at the great facilities of the National Radio Astronomy Observatory in Green Bank, WV for twenty-nine years. Thanks to Sue Ann Heatherly and all of the staff for hosting our annual meeting and making us all feel so welcomed.

I want to thank Vice President Tom Crowley for his leadership in getting our keynote speaker and putting together this conference. It is a huge task that requires a lot of planning and preparation.

Thanks also to the members presenting papers, without them we would not have a conference. I encourage our members that no matter what their level of experience to consider presenting at next year's conference. This is your conference and we want to know what radio astronomy projects you are doing, your methods and results.

I hope you enjoy the fellowship and information exchange at this year's conference and that you will make plans to attend again in 2015.

Bill Lord

KJ4SKL

FROM THE VICE PRESIDENT:

Welcome members and guests to the 29th Annual Conference at NRAO Green Bank, WV of the Society of Amateur Radio Astronomers (SARA). This is SARA's 33rd year of operation, interest in radio astronomy continues to increase all over the world with SARA being the leader in amateur radio astronomy.

We have the pleasure of having not one, but two Nobel Laureates speaking during the conference Dr. Joseph H. Taylor and Dr John C. Mather.

Joseph H. Taylor Jr and Russell A. Hulse were awarded the Nobel Prize in Physics in 1993 for the discovery of a new type of Pulsar, a discovery that has opened up new possibilities for the study of gravitation. A copy of the Nobel lecture "Binary Pulsars and Relativistic Gravity will be included on the Proceedings CD.

Joe Taylor is also an avid ham radio operator and has written several programs for hams dealing with weak signal. www.pysics.princeton.edu/pulsar/k1jt

John C. Mather and George F. Smoot were awarded the Nobel Prize in Physics in 2006, for their discovery of the blackbody form and anisotropy of the cosmic microwave background radiation. A copy of the Nobel Lecture "From the Big Bang to the Nobel Prize and Beyond" will also be included on the Proceedings CD.

In addition to the two Noble Laureates the SARA amateur radio astronomers are presenting their work. Much of this work will provide you the attendee with a wealth of knowledge. This year's SARA Proceedings is the largest yet produced.

I hope you have an enjoyable time while at the SARA Annual Conference and have an opportunity to enjoy all the NRAO facility and the surrounding Pocahontas County have to offer.

Tom Crowley KT4XN

SARA Vice President

Table of Contents

2014 SARA CONFERENCE SCHEDULE

Sunday 29 June- Wednesday 2 July, 2014

| Day	Time	Speaker	Title
Sunday June 29	12:00 PM	Melinda Lord	Registration at NRAO Dorms
Sunday			
29 June	12:30 PM	Tom Hagen	Radio Astronomy Beginner Session
Sunday	3:00 PM	Tom Crowley	40 FT Radio Telescope Workshop
Sunday	5:15 PM		Dinner NRAO Cafeteria
Sunday	6:30 PM		Set Up Outside Experiments
Sunday	8:00 PM		Social at Drake Lounge
Monday June 30	7:30	Lynn Crowley	Ladies meet in residents dorm lobby for car pool to Greenbrier for Breakfast
Monday	7:45 AM		Breakfast in NRAO Cafeteria
Monday	9:00 AM	Tom Crowley, VP	Introductions and Opening Remarks
Monday	9:15 AM	Bill Lord, President	SARA Announcements
Monday	9:45 AM	Jon Wallace	Microwave antenna demonstration
Monday	10:15 AM		Coffee Break and Poster Session
Monday	10:30 AM	David Fields	Radio Astronomy with RASDR2
Monday		Paul Oxley	RASDR2 Control and Analysis Software
Monday		Bogdan Vacaluic	Production Manufacturing for the RASDR2

Day	Time	Speaker	Title
Monday	12:30 PM		Lunch NRAO Cafeteria
Monday	1:30 PM	Bill Lord	Call for Nominations
Monday	2:00 PM	Paul Shuch	SETI New Horizons
Monday	2:40 PM		Coffee Break and Poster Session
Monday	2:55 PM	Tom Hagen	Measuring the Field Strengths of VLF Stations
Monday	3:40 PM	John Mather	COBE
Monday	4:10 PM	Jon Wallace	VSRT Demonstration
Monday	4:45PM	Curt Kinghorn	12.2-12.7 GHz Radio Telescope
Monday	5:15 PM		Dinner at the NRAO Cafeteria
Monday	6:15PM		Flea Market in Dorm Parking Lot
Monday	6:15 PM		Setup Outside Experiments
Monday	7:00 PM		SARA Board of Directors Meeting
Monday	8:00 PM		Social at Drake Lounge
Tuesday July 1	7:45 AM		Breakfast at NRAO Cafeteria
Tuesday	9:00 AM	Bill Lord	Elections
Tuesday	9:30 AM	Bill Lord	Business Meeting
Tuesday	10:00 AM		Coffee Break and Poster Session
Tuesday	10:15 AM	Joe Taylor	Key Note Speaker

Day	Time	Speaker	Title
Tuesday	11:15AM	Chip Sufitichi	SID Monitoring using Raspberry Pi
Tuesday	11:50 AM	Ken Redcap	611 MHz Total Power Radio Telescope
Tuesday	10:00 PM	Lynn Crowley	Ladies meet in residents dorm lobby for car pool to Cass Railway
Tuesday	12:30 PM		Lunch NRAO Cafeteria
Tuesday	1:30 PM		Group Picture
Tuesday	1:45 PM	Sue Ann Heatherly	NRAO High-Tech Tour
Tuesday	3:15 PM		Snack Break and Poster Session
Tuesday	3:30 PM	Mohammed Hassan	The Role of Mass Produced Antennas and feeds on the future of Radio Astronomy Development
Tuesday	4:15 PM	Chuck Higgins	An Overview of the Radio Jove Project
Tuesday	5:00 PM	Tom Crowley	2014 Conference Plans
Tuesday	5:15 PM		Dinner at NRAO Cafeteria
Tuesday	6:15 PM		Setup outside experiments
Tuesday	8:00 PM		Social in Drake Lounge
Wednesday July 2	7:45 AM		Breakfast in NRAO Cafeteria
Wednesday	9:00 AM		Conference Ends
Wednesday	9:00 AM		Radio Jove Conference Begins

MICROWAVE ANTENNA DEMONSTRATIONS BASED ON THE IEEE *PRESENTATION* BY JOHN KRAUS – JON WALLACE

Abstract: The presenter has had a fascination with non-visual astronomy for over 25 years and has developed and built devices to share this with students and other teachers. After seeing a video of John Kraus giving a demonstration on radio antennas many years ago to the IEEE, the presenter was so inspired that he sought to reproduce as much of it as he could. Many of the ideas were unknown to the presenter and a couple were thought provoking and required exploration. It is hoped that these demonstrations will educate and inspire others to explore as well. The equipment consists of a Gunn diode source with horn antenna and a horn antenna with crystal detector, instrumentation amplifier, and VCO so that changes in intensity will be heard as pitch changes. The demonstrations cover topics which include: beam width, inverse square law, polarization, reflection, refraction, interference, diffraction, absorption, gain, wave guides, and more.

The Equipment: The equipment consists of a transmitter (a Gunn diode device) with a larger horn antenna and regulated 8V power supply; a receiver with a small horn antenna, crystal detector, instrumentation amplifier, voltage controlled oscillator, powerful speaker, and powered by a 9V battery. The transmitter and receiver are mounted in such a way as to allow them to be rotated 90º to allow polarization to be explored. The various demonstration devices will be described in each section.
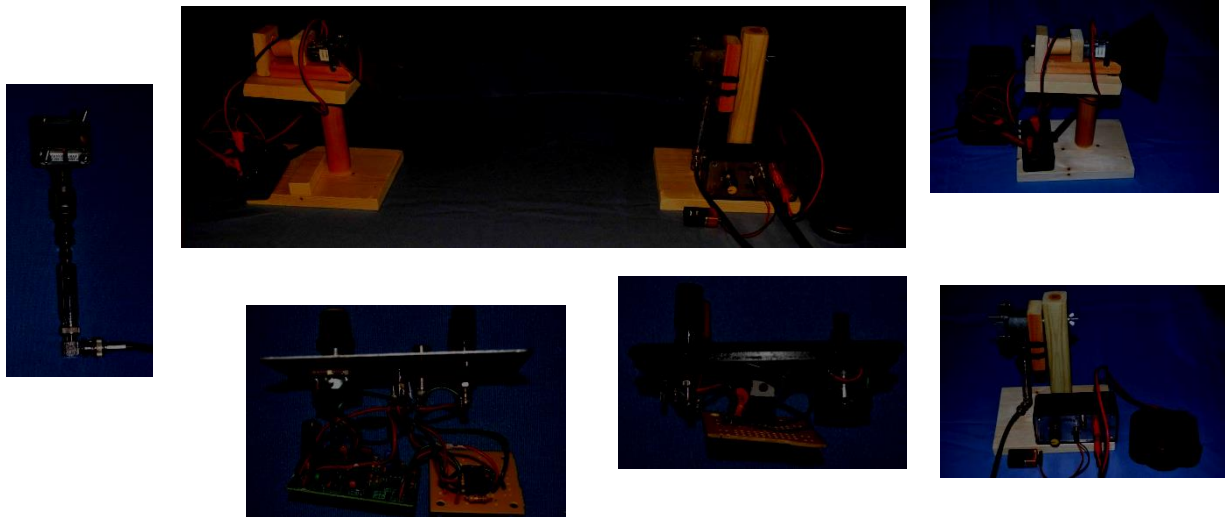
Pictures clockwise from top: the transmitter and receiver; the transmitter with power supply and meter; the power supply opened up; the receiver with instrumentation amplifier, VCO, speaker and 9V battery; the receiver electronics opened up; the horn antenna and crystal detector.

<u>The Demonstration:</u> For most of these demonstrations we will be at far-field. If the maximum linear dimension of an antenna is d and you are $2d^2/\lambda$ or farther from an antenna, you are in the far-field. For us, the maximum dimension is 9.42 cm (transmitter horn) yielding a far field of about 59 cm.

<u>Beamwidth</u>: There are many "beamwidths" defined for various reasons. In our case, using the receiver as a power detector we will use the measure of an angle from the first null on one side of the beam to the first null on the other side of the beam. We will explore the relationship between the small horn on the receiver and a large horn placed over it and show that the beamwidth for a larger horn is narrower. For a more mathematical expression we can use the approximation for half power beam width (HPBW - the beam width at 0.5 peak power or 0.707 peak voltage) also known as the -3dB beamwidth:

(HPBW) Beamwidth = 70λ / D where,

λ	=	Wavelength
D	=	Diameter

λ = 0.3 / frequency = 0.03 (for 10GHz)

Small horn and large horn

For the small horn (maximum d = 3.6 cm); the HPBW = 58.3º.
For the larger horn (maximum d = 9.42 cm); the HPBW = 22.3º.

<u>Gain</u>: Gain is a measure of the antenna's directivity and electrical efficiency. Gain is related directly to antenna area and therefore a larger horn not only has a smaller beamwidth but a larger gain which we can hear in our demonstration. Gain can be expressed as:

$G = [(4\pi A)/\lambda^2]e_A$ where,

A is the area of the aperture,

λ is the wavelength,

e_A is called the aperture efficiency and ranges from 0 and 1. For a pyramidal horn antenna it is generally around 0.5.

For our small horn (A=6.84) G=4.8.

For our large horn (A=64.8) G=45.2.

Antenna gain is usually expressed as dB = 10 log (G); so our values become: 6.8dB and 16.6dB respectively.

<u>Inverse Square Law:</u> We are detecting the power transmitted and received by our horn antennas and this is then governed by the inverse square law which states that the power received is directly proportional to the inverse of the square of the distance. This can be heard with our demonstration.

<u>Linear polarization:</u> This generally refers to the orientation of the electric field along a single plane − in our case vertical. Rotating the receiver horn shows maximum signal at vertical orientation while no signal at 90 degrees (horizontal) and decreasing signal from 0 to 90 degrees. Placing a grid between the transmitter and receiver shows the effect as well. With the grid vertical you get no signal through (the electric field is vertical, it comes to the grid which is parallel and the electric charge runs along the grid and doesn't pass through). With the grid horizontal you get maximum signal through (the electric field can't move much in the thin grid wires so most of the signal passes through). If you rotate

the grid to 45 degrees, then part of the signal passes and it basically rotates the polarization so that the horn can detect the signal at 90 degrees. The grid must have a separation distance of around λ/2, which in our case is 1.5 cm and the metal grid must be a small fraction of the λ.(see cut-off frequency below).

Reflection: Remember that the angle of Incidence equals the angle of Reflection. Many things will reflect the 10 GHz radiation including a hand and a metal sheet. By placing three metal plates mutually perpendicular to each other a three-corner reflector is made and this device has the effect of reflecting any signal which enters back in the direction it came from. An absorber will also be shown and the effect is quite dramatic, no signal is reflected.


Three-corner reflector (left) and absorber (right)
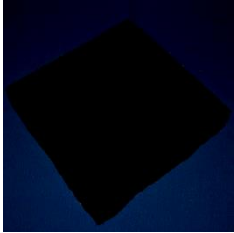
Interference/Standing Waves: By placing the receiving horn where it can detect the transmitter signal directly as well as from a reflected source creates an interference pattern. In this demonstration a flat metal sheet is moved toward the transmitter and aimed toward the receiver. In some instances the signals arrive in phase (for example both at peak – they both add together) and a maximum signal is heard while when the two signals are out of phase (for example one at peak and one a trough – they both cancel) and no signal is heard. As the flat metal plate is moved, a pattern is seen such that every λ/2 (1.5 cm) a peak is heard. This is called a standing wave pattern.

Refraction: Radio waves can bend as well and lenses can be made to take advantage of this property. A polyrod antenna (in this case a 3/8" acrylic rod) will be demonstrated and the effect is obvious! Polyrods are used in the human eye, where over 100 million polyrods in the retina are used to gather light and form images but are millions of times smaller than our 10 GHz version. The polyrod has a narrow beamwidth and behaves as if the effective aperture is much greater.
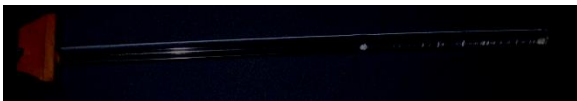
Acrylic   polyrod

A good lens material is paraffin wax and convex and concave lenses and prism of paraffin will be demonstrated. Polystyrene can also be used to form lenses and prisms of various types and these will be explored. The forms demonstrated include: a polystyrene half sphere, polystyrene lenses (convex/concave), and a polystyrene prism.

11
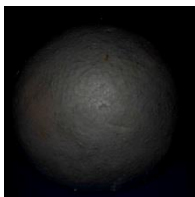
Wax prism, convex and concave lenses; wax prism on stand; polystyrene half sphere; polystyrene lenses and prism

Waveguides: A waveguide is a device that 'guides' the electromagnetic radiation. In this demonstration, pipes will be used. Starting with a large diameter pipe and noticing that the signal is passed through the pipe we continue to decrease the size of the pipe opening until we see no signal. This is known as the cut-off frequency and is calculated with the following formula:

Waveguides – metal pipes

> Cut-off frequency = c/2a where,
> c = speed of light (300,000,000 m/s)
> a = largest side length (2.2cm = 0.022m)

For the receiver waveguide, the cut-off frequency is about 6.8 GHz. The rule of thumb for rectangular waveguides is that they operate at between 125% and 189% of the cutoff frequency. Thus for our WR-90, the cut-off is about 6.8 GHz, and the band of operation is about 8.2 to 12.4 GHz. For the pipes used, the smallest has an inside diameter of 1/2 inch which is equal to about 1.25 cm = 0.0125m. Thus our cutoff frequency for this pipe is about 12GHz so our 10GHz signal will not be passed through. Inserting a polyrod antenna will allow the signal through because the polyrod increases the effective aperture as mentioned above.
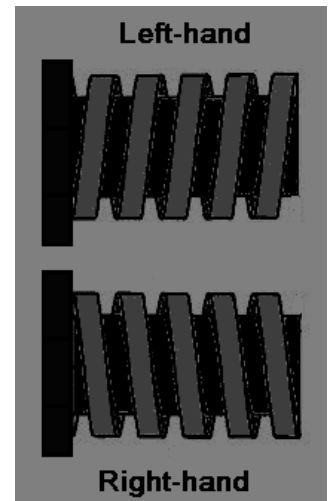
Circular Polarization: In this case the orientation of the electric field is rotated in a circular motion by a helical (spiral) antenna. There are left-handed and right-handed helices. The demonstration uses left-handed helices since they were easier to make but have no bearing on the performance of the demonstrations.

With the polyrod antenna in place a helix is pulled over the rod and the receiving horn is now circularly polarized and the signal can be detected in all orientations as the horn is rotated.

Left-hand

Right-hand

forum.flitetest.com/showthread.php?2169-How-to-build-a-5-8GHz-Helical-Antenna/page2

Aluminum Ground Plane: Placing a sheet of aluminum foil over the table we create a ground plane and radiation can be reflected as in the interference demonstration done earlier. This simulates the real-world antenna situation with a transmitter tower a long way off and the radiation not only comes directly to your receiver but the signal is reflected off the ground and interferes with the incoming direct signal creating the standing wave pattern again. As the receiving horn is raised the standing wave pattern can be heard. By placing a helical antenna on both the transmitter and receiver a circularly polarized signal is created and the standing wave pattern is theoretically eliminated. This is due to the fact that the reflected circularly polarized signal is oppositely polarized from the incoming signal and can't be detected by the left-handed helix being used for this demonstration. Only the direct signal is detected. This of course is theoretical. In our case there is some mismatch of the impedances, the placement in the horn is not a very good method for coupling, and the helices aren't made very accurately. With this in mind the demonstration shows the ideas mentioned here reasonably well.
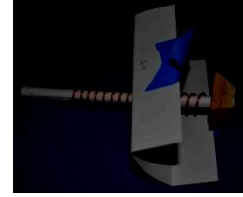
Helical coil placed in horn

Parabolic Reflectors: Using a parabolic shape to focus the signal more tightly greatly increases the gain and narrows the beamwidth. The effect is so great that the demonstration has to be done at some distance from the transmitter.

Other Antennas Demonstrated: A true helical antenna, log-periodic, and Vivaldi antenna are shown and compared to the horn used in this demonstration. The helical was wound by me so doesn't quite live up to its 13dB calculation. Two other antennas built by Kent Britain are the log-periodic which has a gain of about 6 dB and the Vivaldi which has a gain of about 8-10 dB. The last antenna is a patch antenna from a microwave DRO (Dielectric Resonant Oscillator) with a gain about 5dB.
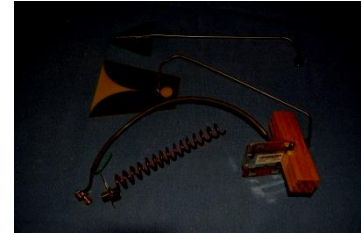

Antennas from top: log-periodic; Vivaldi; patch; helical

Diffraction: Tilting the transmitter and receiver so that the electrical field is oriented horizontally, we can set-up three diffraction demonstrations. First is the knife edge effect where the microwaves are diffracted around an obstruction. This is observed when radio waves encounter a building or mountain. Signal will be detected in an interference pattern by the receiver. Second is the single slit experiment where the signal is diffracted through a single slit and produces an interference pattern. The slit should be on the order of the wavelength of radiation. In our case a 1.5 cm wide slit is used and the interference pattern will be detected. Third is the double slit experiment. By placing metal sheets about 13cm wide in the center with a 1.5 cm gap on both sides followed by metal sheets on the ends. These sheets are placed about half way between the

Knife-edge diffraction set-up

two units and the receiver is moved back and forth in front of the sheets. A diffraction pattern with a large peak in the center and lower intensity peaks every 10-15 degrees on either side of the central peak. This satisfies the equation for diffraction: $\theta = \sin^{-1}(n\lambda/d)$, where θ is the angle, n is an integer, λ is the wavelength (about 3cm), and d is the width between openings (in our case above about 14.5 cm). Plugging in for the first peak we get about 12 degrees, second at about 24 degrees and so on.
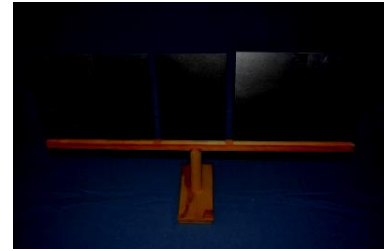
Double slit diffraction set-up

RADIO ASTRONOMY WITH RASDR2[1]

D. Fields[2], P. Oxley, B. Vacaliuc[3], C. Lyster , S. Kurtz[4], Z. Tamosevicius[5] and S. Berl
Tamke-Allan Observatory[6]
Roane State Community College
276 Patton Lane
Harriman, TN 37748

ABSTRACT

The RASDR design team is releasing a software-defined receiver (SDR) for radio astronomy called RASDR2[7]. The receiver consists of two high-density circuit boards -- a wide-band femtocell[8] chip on the front end analog interface MyriadRF board[9] linked to a DigiRed digitization and function control board -- coupled to a computer via either a USB2 or USB3 interface. RASDRViewer software runs in a Windows environment and performs receiver control, FFT analysis, spectrum averaging, power monitoring and other functions. Depending on the specific application, RASDR2 is used with an antenna, filter, preamplifier, optional upconversion or system control devices, and external frequency/time reference signals. The team has three RASDR2 units in operation and is working to make units available to SARA members.

RASDR2 software, firmware and hardware are discussed in other conference presentations. This presentation covers RASDR2 application to solve some common experimental challenges encountered by members of the community of amateur radio astronomers. Results of operation in several RF spectral bands will be shown and discussed.

---

1 Presented at the annual meeting of the Society of Amateur Radio Astronomers to be held at National Radio Astronomy Observatory, Green Bank, WV, June 29-July 4, 2014.

2 fieldsde@aol.com

3 Spallation Neutron Source (SNS); SNS is managed by UT-Battelle, LLC, under contract DE-AC05-00OR22725 for the U.S. Department of Energy.

4 UNAM, Morelia Campus, Mexico

5 Lime Microsystems, Ltd.

6 www.roanestate.edu/TAO

7 RASDR – Radio Astronomy Software Defined Radio; http://rasdr.org

8 Lime Microsystems Field Programmable RF (FPRF) Transceiver IC; https://github.com/myriadrf/LMS6002D-docs

9 Component 1434-1001-ND available from Digi-Key, Inc.

INTRODUCTION: THE RASDR PROJECT

The SARA development of an SDR that is optimized for Radio Astronomy, RASDR and which is applicable to a wide variety of SARA projects, includes a front end digital package (RASDR2) and a software-driven desktop computer back end[1][2]. The front end uses a computer chip containing the entire RF digital receiver chain, designated LMS6002d [3][4]. The back end computer controls the front end hardware and permits the user to control receiver functions, display signals and perform analysis functions (averaging, computation of spectrograms, determination of power time-spectrum, and generating output files).

Signal processing permits dealing with low S/N data, and presents data as spectral plots and data files, and metadata. Current RASDRviewer software [5] for the Windows OS, performs parameter optimizations, user control, spectra output, power characterization and output data formatting via a Graphical User Interface (GUI).

This design evolution is based on the need to have widest possible data pipeline speed for radio astronomy applications, and to make this available to SARA members[6]. The software is described at this conference in a second sister paper. [7]. The following sections describe initial tests to evaluate the radio spectrum environment. In all cases, a USB2 connection was made to a 5-y old PC laptop running Win XP.

Operation of RASDR2 in Various Radio Astronomy Bands

The FCC spectral designations from 3 KHz to 30 GHz [8] are shown in Table 1:

Band Number	Symbol	Frequency Range	Wavelength Range
4	VLF	3 to 30 kHz	10 to 100 km
5	LF	30 to 300 kHz	1 to 10 km
6	MF	300 to 3000 kHz	100 to 1000 m
7	HF	3 to 30 MHz	10 to 100 m
8	VHF	30 to 300 MHz	1 to 10 m
9	UHF	300 to 3000 MHz	10 to 100 cm
10	SHF	3 to 30 GHz	1 to 10 cm

TABLE 1. FCC BAND PLAN FROM 3 KHZ TO 30GHZ.

Development of these bands for radio astronomy research is shown in the following table. It is taken from various sources and contains comments by the author. The Jovian kilometric band is not often considered, but it has been observed by Voyager and other space probes, and may be a valid radio astronomy band from earth under certain circumstances.[9][10]

16

RASDR2 operates in bands 9 and 10 (up to 4 GHz), but with additional components the coverage may be considerably extended, as will be discussed.

Ionospheric Monitoring		ULF-VLF	0.00030 to 0.003
Jovian VLF [10,11]	Jovian kilometric	VLF	.015 to .025
Jovian and Solar	RASDR upconverter F<400MHz	HF	10 to 35
Solar / Solar Wind		VHF	70
Pulsar	1 second for pulse shape	VHF	70
	0.05 Seconds bin width	VHF	150
	Clock Disipline 0.1 Second	UHF	322
		UHF	406
Continuum, VLBI, Solar	Consider Dicke Switching	UHF	608
21 cm Hydrogen	Galactic doppler +/- 1.4 MHz	L-Band	1420
	Extra Galactic +/- 5 MHz		
Solar Contininuum		L-Band	1420
OH spectral	galactic doppler +/- 1.6 MHz	L-Band	1665/1667
OH spectral, SETI		L-Band	1702
Continuum, Solar		S-Band	2655
		S-Band	2690
	Calibration to NOAA obs	S-Band	2800
Continuum, Solar		S-Band	3260
		S-Band	3332
		S-Band	3345
	LNB required for RASDR	C-Band	4800
	operation above 3800 MHz	C-Band	4990
		C-Band	5000
		C-Band	6650
		X-Band	10600
Methanol / Doppler	Doppler +/- 12 MHz LNB Req	C-Band	6670
		KU-Band	12178
Methanol Maser Activity	Narrow Band LNB Required	KU-Band	14500

TABLE 2 CANDIDATE RADIO ASTRONOMY RESEARCH BANDS. BANDS SHOWN IN AND ABOVE HF ARE DESIGNATED. THE BAND SHOWN AS VLF IS PROPOSED FOR MONITORING [11]

HYDROGEN HI SPECTROSCOPY. L-BAND (1420 MHz)

Using RASDR2 for observing an HI hydrogen cloud signal requires a suitable antenna, a high-gain preamp (LNA) and signal averaging to extract the HI signal from the RF noise.

One may ask how much sensitivity is needed. A popular special-purpose spectrometer that works well for observing HI emissions from distant hydrogen clouds is SpectraCyber II[12], which was invented and constructed by RASDR team member Carl Lyster.

As a point of reference, the SpectraCyber bin width is about 5 KHz. If we desire to cover 10 MHz of HI spectrum then we probably require about 2000 frequency bins or about 2048 samples/FFT. One may choose the higher number of samples/FFT observe more detail, although more averaging would be required. One of the significant advantages of RASDR2 is that it has a high bandwidth.

RASDR2 control data consist of only a few values and they are discussed by Paul Oxley in a related paper.[7] Based on the preceding discussion, an initial data screen for HI spectroscopy is shown in Figure 1, with non-default values shown in red.

FIGURE 1 INITIAL CHOICES OF RASDR2 CONTROL PARAMETERS FOR COMPARISON WITH TYPICAL SPECTRACYBER RESULTS. SEE TEXT FOR CHOICE OF VALUES SHOWN IN RED.

The first tests with these settings provided a noisy graphical output. The LNA gain used in this series of tests was 15dB and skies were cloudy. In general, one expects to average over many samples. Initial runs with 99 and 999 samples produced the output shown in Figure 2. It is clear that more samples must be included in the averaging process, which will require a small software change from the current program. Note that the noise spurs (that appeared only after averaging) are about 9 dB above the floor and they are present in both tests.
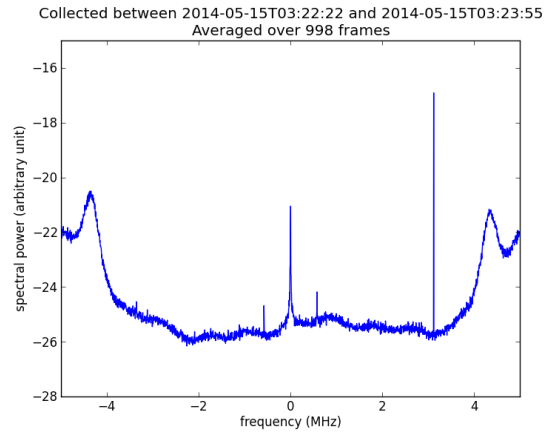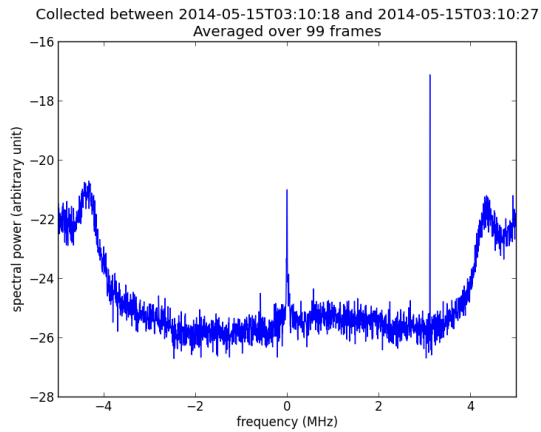
FIGURE 2 THE IMPORTANCE OF SPECTRAL AVERAGING IS SHOWN WITH PROCESSING OF 99 FRAMES (LEFT) AND 999 FRAMES (RIGHT). CONTROL SETTINGS WERE AS SHOWN IN FIGURE 1. USB2 CONNECTIVITY WAS USED TO AN IBM LAPTOP RUNNING WIN XP, AND USING A USB2 INTERFACE.

A second necessity is to remove the background noise and normalize for system response. Figure 2 shows the result of subtracting the two files shown Figure1 to removing the common baseline variation and the 9 dB spurs, but leaving only random noise component. This component is not present in the 999 FFT average.
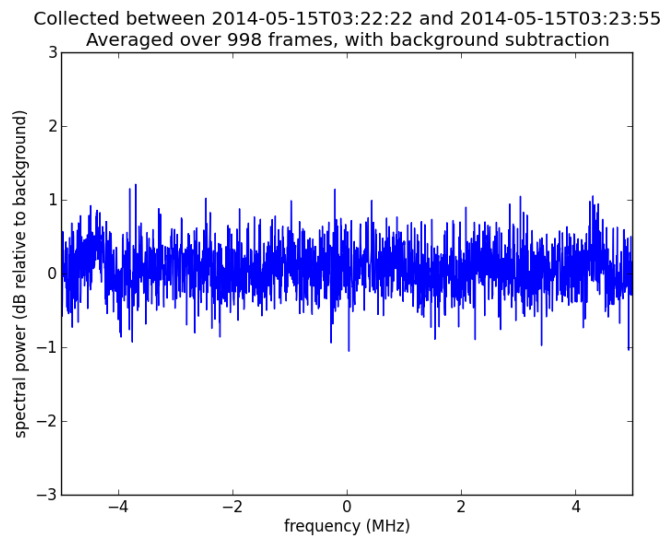

FIGURE 3 THIS FIGURE IS THE DIFFERENCE FILE USING THE 99 FILE AVERAGE AND THE 999 FILE AVERAGE SHOWN IN FIGURE 2. THE 2DB NOISE COMPONENT FROM FIGURE 2 (LEFT) IS ALL THAT REMAINS. THE COMMON FEATURE IS REMOVED, AND THE SAME METHOD CAN BE USED TO REMOVE SYSTEM RESPONSE FROM THE HI SPECTRA MEASUREMENT.

19

Radio Astronomy in the VHF band (80-190 MHz)

It is highly desirable to extend RASDR2 coverage to lower-frequency RF bands. Such an extension makes it far more useful to SARA members.

This section will consider extension of operation to the VHF band, specifically 80-190 MHz. This band is useful for solar monitoring and for meteor detection and it also contains an AM aircraft band, amateur radio activity, commercial FM band that are interesting for performance verification, and the output Intermediate Frequency (IF) band for the 40' Green Bank Radio Telescope.[13] Application to the Green Bank 40' radio telescope is planned for the 2014 SARA conference.

To add functionality below the intrinsic RASDR2 band, an upconverter was designed and constructed.

The basic LM6002d covers a wide frequency range from 300-4000MHz but RASDR2 has been used initially above 400 MHz. The VHF upconverter extends reception to an input frequency band between 100-200 MHz. Filters were included to reject incoming signals that upon mixing would have been upconverted to below 400MHz, to avoid the third harmonic of the local oscillator (LO) that was used for mixing, and to remove the LO fundamental frequency component.

Our VHF upconverter uses the third harmonic of a 100MHz oscillator [14][15]. The 3rd harmonic (300MHz) is mixed with the input signal. The following basic components are also required, and there are about 25 additional components:

Crystal oscillator	Raltron CO19025-100.000MHz [15]
Low Pass Filter	LFCN-225 [16]
Mixer,	IAM81000 [17]

Output Bandpass filter combination   PHP-400[18]

LFCN-225 [16]

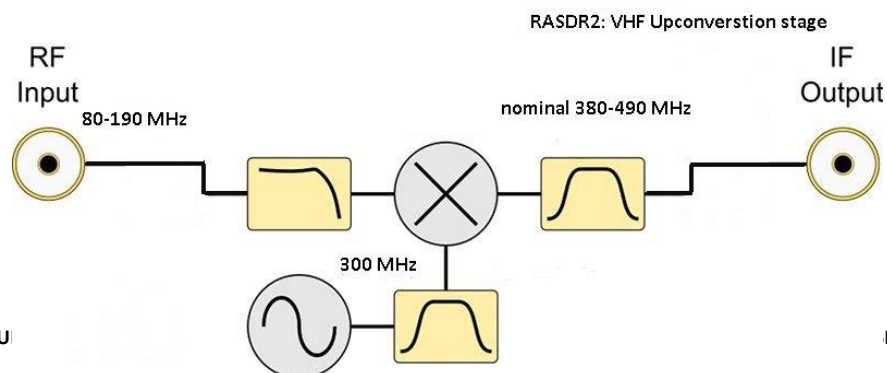Figure 4 shows the functional diagram of the VHF upconverter constructed for RASDR2 tests.

FIGURE 4. BLOCK FU...   ...DR2 INPUT BAND

Several filters are shown, the input low pass filter to avoid VHF components in the input from reaching the mixer; the 300 MHz bandpass filter to clean up the third harmonic of the oscillator, and the output bandpass filter (two filters are used in our unit) to select just the frequency components desired from the mixer stage.

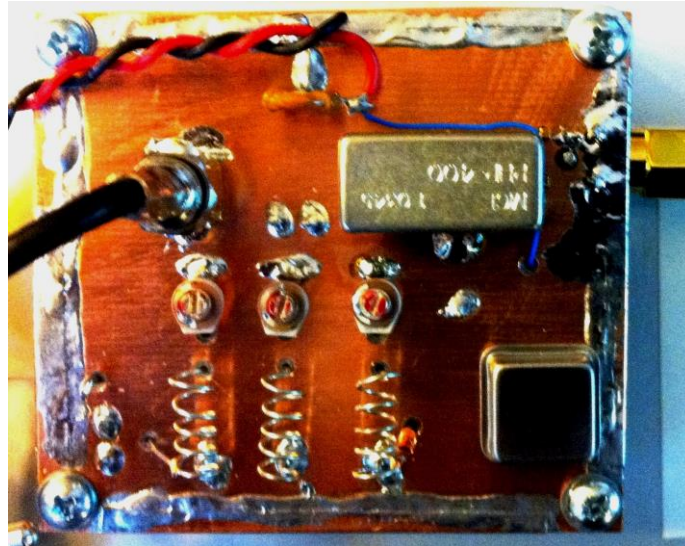Figure 5 shows the completed VHF converter stage that upconverts inputs from 80-190 MHz to 380-490 MHz:

FIGURE 5   COMPLETED VHF CONVERTER USED WITH RASDR2. INPUT IS VIA THE COAX CABLE WHILE THE OUTPUT IS VIA THE SMA CONNECTOR SHOWN ON THE UPPER RIGHT.

The circuit shown has a mixer with about 10dB gain resulting in no overall signal loss for the unit. The noise floor is about -120 dBm.

The unit is intended for several applications, including meteor detection, spectroscopy with the NRAO 40' antenna, and solar monitoring. A convenient test signal is the commercial FM band, using a random wire antenna about one wavelength long. A random length of hookup wire was connected to the input of the upconverter

Figure 7 shows a 10 MHz section of the band taken directly from the RASDR2 GUI video output, using a 2m piece of hookup wire for an antenna, and the upconverter of Figure 5.
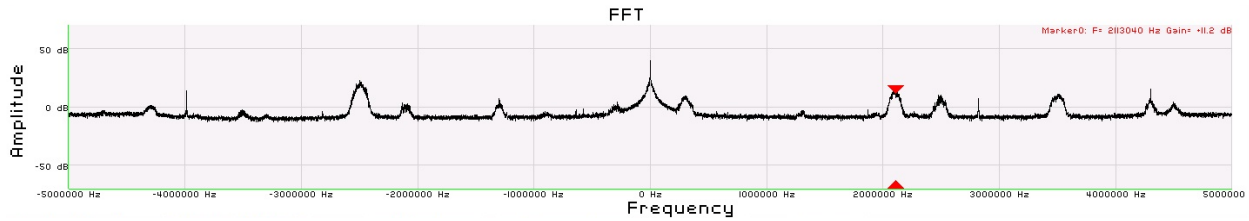
FIGURE 6 COMMERCIAL FM BAND. THE ANTENNA WAS A RANDOM WIRE ABOUT 2M LONG, CONNECTED TO THE VHF UPCONVERTER, THEN TO RASDR2. THE RED MARKER WAS ADDED ON THE RASDR2 DISPLAY TO DENOTE A LOCAL FM STATION BROADCASTING AT 102.113 MHZ.

Selecting RASDR2 internal filters to narrow the band to 2.5 MHz width, demonstrates a practice that is useful to reject interfering signals outside the region of interest and avoiding any intermodulation. The result of setting the bandwidth to 2.5 MHz is shown in Figure 7.
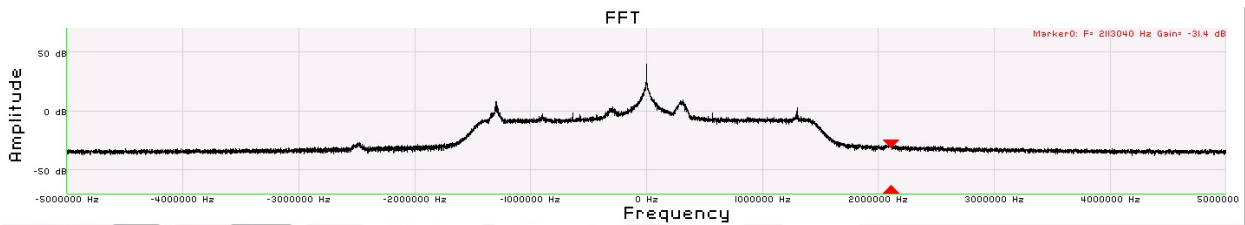
FIGURE 7 RASDR2 INTERNAL NARROW-BANDING WAS CHOSEN TO SELECT A REGION OF INTEREST. IN PRACTICE, NARROW BANDING IS USE-FUL TO REJECT UNWANTED OUTLYING SIGNALS (NOISE).

RASDR2 output is more information-rich than suggested here. Figure 8 shows the complete primary-window display of a 10MHz-wide band centered at 90 MHz, with the RASDR2 marker function used to denote a couple of interesting local FM stations. Additional windows provide "Tools" and "Define Output". As data were taken, the writer was listening to 91.9 MHz (red triangle marker) on the stereo.

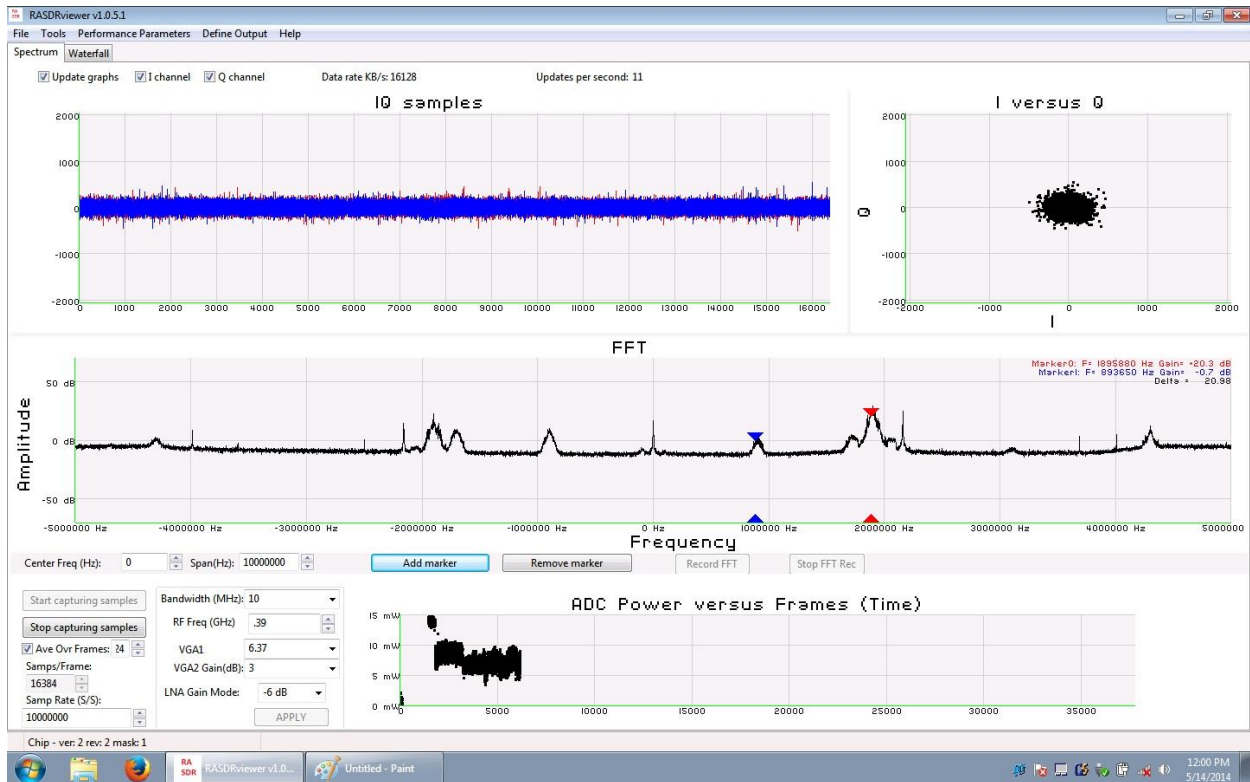**FIGURE 8 THE COMPLETE RASDR2 VIDEO OUTPUT WITH VHF INPUT SHOWS THE INPUT SIGNAL STREAM AS DIGITIZED (I AND Q VALUES); THE I VS. Q PLOT (A CIRCLE IF THERE IS A SINGLE COHERENT SOURCE, THE FFT SPECTRAL DISPLAY WITH MARKERS IF SELECTED, DIGITIZATION AND INTERNAL GAIN SETTINGS, AND A POWER VS. TIME PLOT. THE RATTY POWER VS. TIME PLOT ON THE LOWER RIGHT SHOWS THE RESULT OF MOVING THE ANTENNA.**

Radio access to signals collected by the NRAO 40' telescope are restricted to using the local IF feed. This VHF upconverter was designed with this challenge in mind. Study of HI using RASDR2 at NRAO, might be done by dialing in the 40' telescope local oscillator to 1315 MHz and measuring the signal at the output IF feed (1420 -1315 MHz), which would be at 105 MHz. This could be upconverted to 405MHz and examined with RASDR2. That is a future project and we are looking forward to performing this measurement at the 2014 SARA conference.

RASDR Spectroscopy in HF band (2-80 MHz)

RASDR2 operation has been described as applied from 400MHz to 4GHz, and with the VHF upconverter, to the input range from 80-190 MHz. To demonstrate functionality in the HF band from about 2-66 MHz, we used an upconverter obtained from Nooelec[19] that upconverts this HF input band to a 102-166 MHz output band. Thus the output is compatible with input of the VHF converter described earlier.

The Nooelec upconverter functionality is shown in Figure 9. The device shown has a measured internal loss of about -10 dB of signal. The noise floor is about -80 dBm. This device was used with a 100 MHz crystal oscillator, but one can also obtain it with a 125 MHz oscillator. If this component selection is made, then the output will be shifted by 125 MHz, and avoid the commercial and aircraft bands.

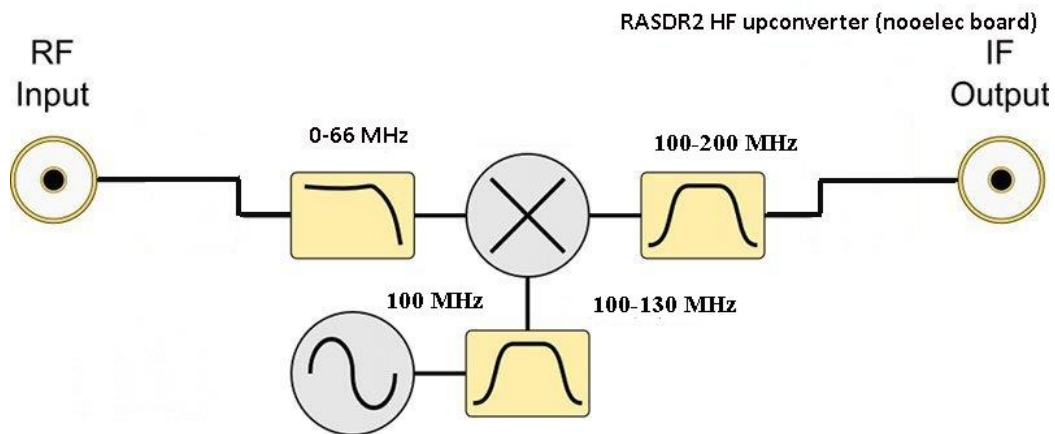**FIGURE 9 FUNCTIONALITY OF THE NOOELEC UPCONVERTER IS AS SHOWN. THE RF INPUT IS NOMINALLY SPECIFIED 0-65 MHZ AND THE MEAS-URED PERFORMANCE COVERS IN THE RANGE 2-66 MHZ. FILTER FUNCTIONS ARE AS DESCRIBED WITH REFERENCE TO FIGURE 4.**

For testing purposes, the HF upconverter was mounted as shown in Figure 10, where it is the PC board on the lower left. The VHF converter discussed earlier is shown on the upper right.
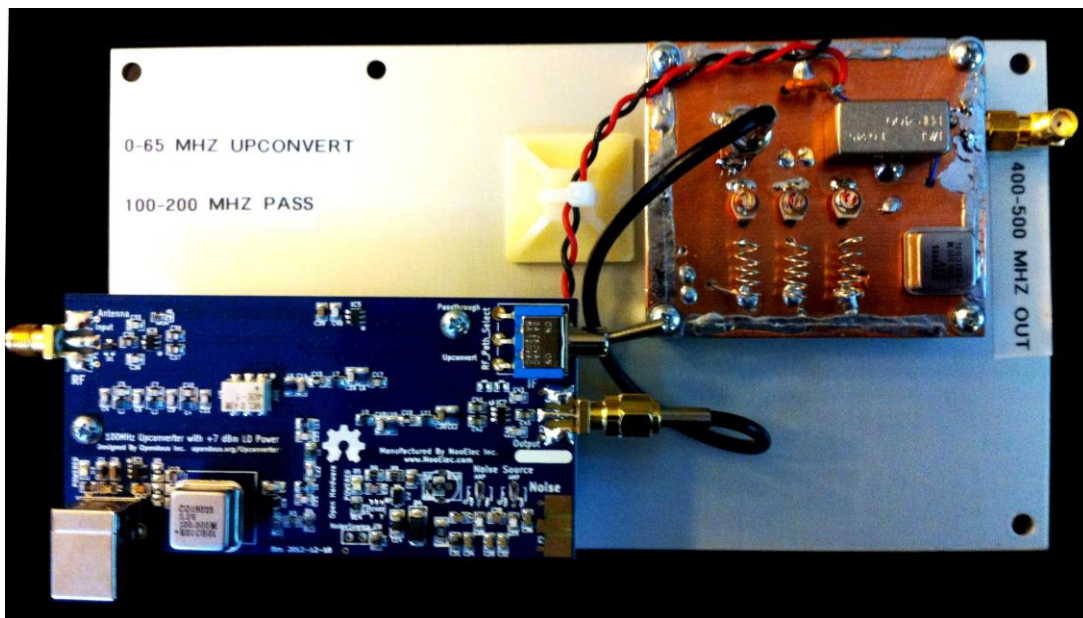
FIGURE 10 TWO UPCONVERSION STAGES ARE SHOWN HERE, WHICH PROVIDE FOR CONVERSION OF THE 2-66MHZ PORTION OF THE HF BAND TO THE 402-466 MHZ BAND PRIOR TO PROCESSING WITH RASDR2. THE NOOELEC CONVERTER IS ON THE LOWER LEFT WHILE THE VHF CONVERTER DESCRIBED EARLIER APPEARS AT THE UPPER RIGHT.

Results were as might be expected using an antenna very short (2m) compared to the frequency. Figure 12 shows a 5.5 MHz section of the HF band centered on 15 MHz. The plot contains signals, spurs, and noise, the lesson from this figure is that one must use a respectable antenna and preamplifier, possibly a preselection filter, and background subtraction for a noisy band.

FIGURE 11 NOISY 5.5 MHZ SECTION OF THE HF BAND CENTERED ON 15 MHZ. THIS MEASUREMENT WAS MADE WITH AN ELECTRICALLY SHORT ANTENNA AND NO PREAMPLIFIER. IT SHOWS VARIOUS SOURCES OF NOISE INCLUDING SO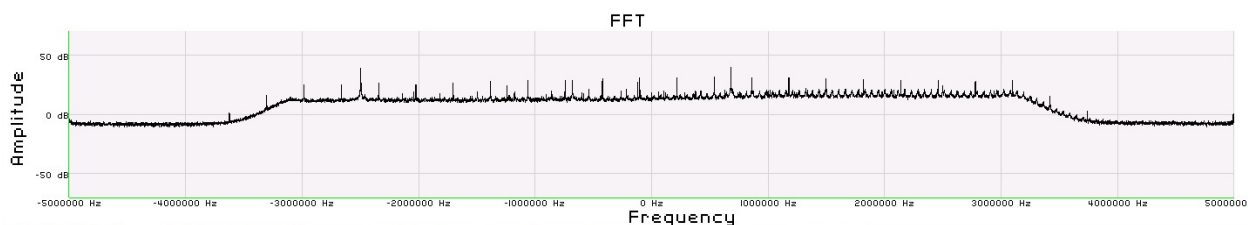ME FROM THE NOOELEC UPCONVERTER. THIS EXPERIMENT SUGGEST THE IMPORTANCE OF A DECENT ANTENNA, MORE PREAMPLIFICATION AND BACKGROUND SUBTRACTION.

Summary

Several initial applications and extensions of the RASDR2 device have been discussed. The unit is showing considerable potential, provided the user is willing to precondition the input and use software processing at the output.

CITATIONS

[1] RASDRgroup, "RASDR – Radio Astronomy Software Defined Radio," 2014. [Online]. Available: http://rasdr.org.

[2] P. Oxley, B. Vacaliuc, D. Fields, C. Lyster, S. Kurtz and Z. Tamosevicius, "RASDR update," *Radio Astronomy -- Journal of the Society of Amateur Radio Astronomers,* no. January-February, p. 72ff, 2014.

[3] LimeMicrosystems, "Field Programmable RF (FPRF) Tranceiver IC," Lime Microsystems, 2014. [Online]. Available: https://github.com/myriadrf/LMS6002D-docs.

[4] Myriadrf, "Home page of Myriadrf," [Online]. Available: http://myriadrf.org/. [Accessed 20 May 2013].

[5] Myriad, *Personal Communications to RASDR team,* March-June, 2013.

[6] B. Vacaliuc, D. Fields, P. Oxley, S. Kurtz, C. Lyster, R. Vadoklis and Z. Tamosevicius, "Production Manufacturing Plan for RASDR2 Appliance," in *Proceedings of the 2014 SARA Conference*, Green Bank, WV, 2014.

[7] P. Oxley, D. Fields and S. Kurtz, "RASDR2 Control and Analysis Software," in *Proceedings of the 2014 SARA Conference*, Green Bank, WV, 2014.

[8] Wikipedia, "Radio_spectrum," 2014. [Online]. Available: http://en.wikipedia.org/wiki/Radio_spectrum. [Accessed 11 May 2014].

[9] D. Fields and N. Tesla, "Detection of Jupiter Radio Emissions below the Plasma Cutoff Frequency: Implications for SID Monitoring," in *Proceedings of the Annual Meeting of the Society of Amateur Radio Astronomers*, Green Bank, WV., 2011.

[10] J. Avellone, "Detection of Jovian VLF Noise," *Radio Astronomy -- Journal of the Society of Amateur Radio Astronomers,* no. March - April, p. 48ff, 2014.

[11] D. Fields, R. Kennedy and K. Roy, "Interplanetary Radio Transmission through Serial Ionospheric and Material Barriers," in *Proceedings of the Seventh IAA Symposium on Realistic Near-Term Advanced Scientific Space*

Missions : Missions to the outer solar system and beyond. International Academy of Astronautics, Aosta, Italy, 2011.

[12] J. Bernard, "SpectraCyber I/II™ 1420 MHz Hydrogen Line Spectrometer Installation and Operation Manual No. SC1/2-2006," Carl Lyster through Radio Astronomy Supplies, [Online]. Available: http://www.ncra.tifr.res.in/rpl/facilities/4m-srt/SCI_IIManual.pdf.

[13] NRAO, "NATIONAL RADIO ASTRONOMY OBSERVATORY 40-FOOT RADIO TELESCOPE OPERATOR'S MANUAL," 2014. [Online]. Available: http://www.gb.nrao.edu/epo/manual.pdf.

[14] Ebay, "Raltron CO19025-100.000MHz," 2014. [Online]. Available: www.ebay.com.

[15] "Through hole clock oscillators – 3 state HCMOS compatible," Raltron, 2014. [Online]. Available: http://www.raltron.com/products/pdfspecs/clock_co15-co19.pdf.

[16] "LFCN-225," Mitron, 2014. [Online]. Available: http://www.mitron.cn/cxchanpin/Filters-n/LFCN-225.pdf.

[17] Hewlett-Packard, "Silicon Bipolar MMIC 5 GHz," 2014. [Online]. Available: http://www.qsl.net/n9zia/omnitracs/IAM81008.pdf.

[18] Minicircuits, "Plugin High Pass Filter," [Online]. Available: http://www.minicircuits.com/pdfs/PHP-100+.pdf.

[19] Nooelec, "Ham It Up v1.2 - RF Upconverter For Software Defined Radio," Nooelec, 2014. [Online]. Available: http://www.nooelec.com/store/ham-it-up-v1-0-rf-upconverter-for-software-defined-radio.html.

RASDRviewer

RASDR2 Control and Analysis Software

Paul Oxley, David Fields, Stan Kurtz

ABSTRACT

The Radio Astronomy Software Defined Receiver (RASDR) is a system that provides a versatile Software-Defined Receiver (SDR) that is optimized for Radio Astronomy. RASDR2 is the current hardware that is in testing with a planned general release at this conference. See multiple other presentations at this conference as well as previous SARA Journals and Proceedings publications for the history of this SARA project.

RASDRviewer is the software that controls RASDR2 and presents captured data to the user. It uses a Windows based GUI that is designed for portability to both the Linux and MAC platforms. This portability is mainly based on the use of the wxWidgets development tool that is available as open source freeware. wxWidgets abstracts most of the common graphical window objects to a common language that is applicable across all of the platforms. Thus the look and feel of the user experience is the same regardless of the platform being used. Loading and using RASDRviewer on a Windows operating system is straightforward.

This paper describes the RASDRviewer software and documents some of the experiences in its implementation. A brief discussion of the Windows Driver and FX3 firmware is also included.

RASDRviewer is an extension of the Lime Microsystems FFTviewer to optimize radio astronomy functionality. The original FFTviewer presented three charts, I & Q samples vs time, I vs Q for system verification and an output display showing results of a large Fast Fourier Transform (FFT) that operates in near real time. The FFT is capable of delivering up to 16,384 frequency bins multiple times per second. The control of the system required knowledge of the Lime chip architecture and RF engineering theory.

For RASDRviewer, modifications have been made to customize the software for Radio Astronomy use. This includes optimization of control functions for radio astronomy use, addition of a Power vs Time plot, file outputs and inclusion of a simplified selection of the user options. In addition, RASDRviewer makes full use of the receive capabilities of the Lime Chip including sample rates up to 32 M Samples/Second and 28 MHz of bandwidth. RASDRviewer is being demonstrated at this conference. The demonstration will include real-time control of RASDR2 to produce three dimensional FFT plots. A copy of the software executable is included in the CD for this meeting. The source code will be made available to anyone who requests a copy and is willing to be coached through the setup of the compiling environment.

SOFTWARE LANGUAGE

The system uses a combination of C, C++,wxWidgets, FFT-W and Open GL with the Code::Blocks Interactive Development Environment. The system uses a driver provided by Cypress the maker of the USB3 chip on the RASDR2–Digi-Red board. These development tools have created a powerful GUI and data processing capability. The GUI provides the user interface in a format that is familiar to the user of the chosen platform. However, the complexity of the compilation chain can prove difficult to establish. This complexity has limited the porting of the system to platforms beyond Windows at this time.

USER PLATFORMS

RASDRviewer currently operates on most Windows platforms that are in current use. This includes Windows 2000, Vista, XP, 7 and 8. It has been tested on Windows 7 and XP. Plans include the porting of the system to Linux and MAC platforms.

SOFTWARE ARCHITECTURE

The software is organized in classes, modules and files to allow maximum flexibility in the reuse of code. Threading, Call back and event timers are used to maximize the high speed processing of the data. To allow the slower machines or those with only a USB2 interface to operate, the user can set performance parameters to optimize the system for their platform. The high speed multiple core platforms will provide the maximum performance which includes data collection at 32 M Samples/Second and the full 28 MHz bandwidth of the RASDR2 board.

FIRMWARE

The system uses custom firmware that is loaded onto the FX3 chip in the Digi-Red board. This includes a unique SARA Vendor and Product ID (VID/PID) pair. This allows the user to connect to RASDR2 without concern of not finding the correct USB3 channel. The software uses this unique VID/PID together with a version register on the Lime Chip to verify that system connections are correct.

The firmware provides not only the high speed data interface, but also a capability of establishing a Serial Peripheral Interface (SPI) bus to perform the control of the chips on RASDR2. In addition, the firmware provides the use of the General Purpose Input Output (GPIO) pins on RASDR2. Thus there is no need for a separate micro-controller or FPGA on RASDR2. This has significantly reduced the cost of RASDR2.

GRAPHICAL USER INTERFACE (GUI)

When the user executes RASDRviewer, they are presented with a screen that provides charts of the collected data. Figure 1 shows this screen. Starting in the upper left side, the In Phase (I) and Quadrature (Q) samples are displayed against time. The range on the chart was set to display the quadrature relationship of the I & Q signals where I is leading Q by 90 degrees.
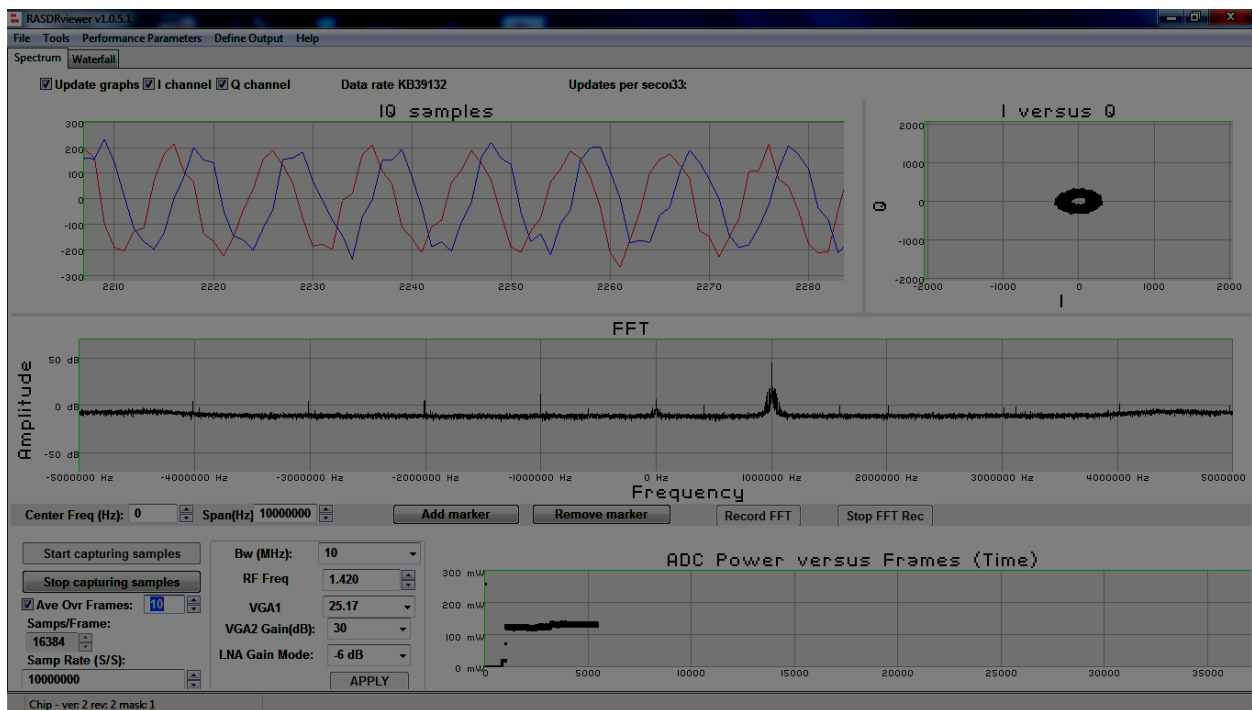

Figure 1 the main RASDRviewer Screen with an inserted CW signal

To the right, there is a chart that displays the phase relationship between the I and Q samples. Since a significant spectral line is present, the circle is present. The circle is created by the 90 degree relationship between the samples. This chart is used mainly to verify the system. However, it is a useful educational tool for students that are learning the phase relationship between I & Q signals and flags the existence of any possible imbalance between I and Q channels.

In the middle of the screen there is a display of the FFT output. The vertical axis is in dB. The horizontal axis is the frequency of the FFT bin at baseband. Zero frequency corresponds with the center RF frequency. The frequency bin bandwidth can be changed by using different sample rates and samples per frame that is set on the bottom left of the screen. Appendix A contains a spreadsheet that displays a few of the possible bin bandwidths. Figure 2 shows an enlarged portion of the screen where chip parameters can be set.
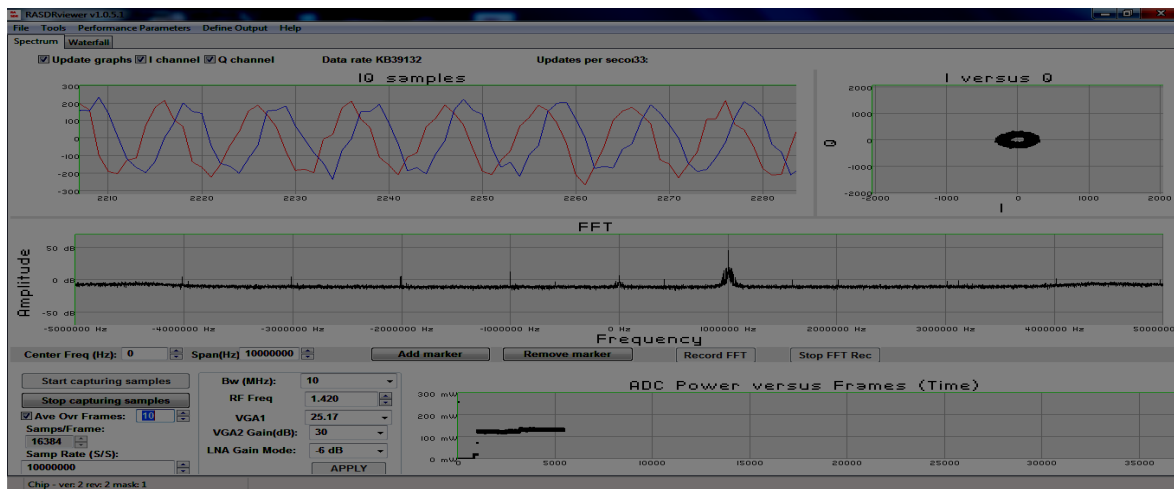
Figure 2 Enlargement of the bottom left portion of RASDRviewer Screen

In the bottom right corner is a display of power at the ADC input. Figure 3 shows this portion enlarged. The power is calculated over a frame of complex samples creating a display of the RMS power in the frame. Although the values are in milliwatts, to obtain the corresponding total power at the antenna would require calibration. The main purpose of the power chart is for use during drift scan experiments. The power will peak when the desired object is centered in the antenna beam width.

Figure 3 The ADC Power chart enlarged

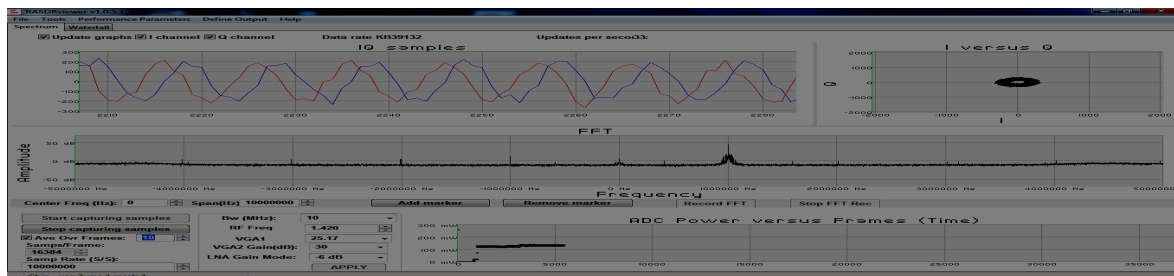All of the charts have the feature where the user can change the range of the chart by dragging a box around the section of the chart to enlarge. Clicking on the left side of the chart restores the default ranges.

The FFT chart has the ability to set markers to help identify the specific frequency and peak value of a spectral line. The marker controls are below the FFT chart enlarged in Figure 4. To add a marker, click the "Add Marker" button. Then move the cursor to the screen and click where the marker should be placed. The marker can be moved left or right by dragging it with the mouse. With a little bit of practice, the user can find the peak value.

The user can also set the span and center frequency of the display.
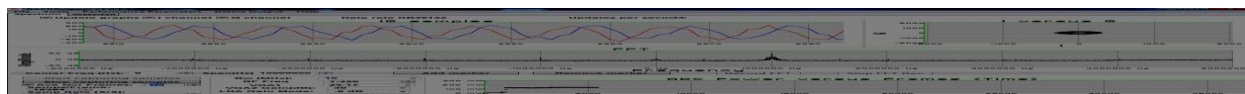

Figure 4 Enlarged showing the FFT display controls and record buttons

The charts are updated multiple times per second. The time between updates varies with different setup parameters. The frequency (updates / Second) is shown on the top of the screen.

The user can change the experiment parameters by using the controls in the bottom left section of the screen. See Figure 2 for enlargement. This is where one would set the frequency, bandwidth, sample rate, frame size and gain. The changes are not placed in effect until the user pushes the apply button. When the apply button is clicked, the system forwards the necessary commands via the SPI bus described above to the Lime chip on RASDR2.

The top left portion of the controls section on Figure 2 contains buttons which start and stop the capturing of the data. When the start button is clicked, the charts will show the results of the samples. The start button will also activate the "Apply" button which ensures that changes in parameters are included in the results.

Just below the "Start" and "Stop" buttons is where the user can establish averaging of the FFT output. This is done by clicking the check box and setting the number of FFTs to average. Averaging is useful to enhance spectral lines by reducing the baseline noise. Since the baseline noise is random, its average value is reduced to the mean of the noise. Since the Spectral line is not (or partially) random, it is enhanced.

Setup FFT Output to Disk

Recording data to a disk file or files can be accomplished by using the Define Output menu item on the second line of the screen. Clicking the button will bring up a sub-menu of the types of outputs available (only FFT output at present). Clicking the FFT output menu item will bring up

an overlaid screen for the setup of the parameters of the recording. Figure 2 is a screen shot of this window.

On the left of the top line the user can select the File type. Two options are available. The first is for use in MS-Excel where the number of frequency bins is reduced to a maximum of 128 to allow Excel to be able to process a 3D chart in a reasonable period of time.

The user can select the General Purpose output for use in other post processing programs. The output in this case uses whatever sample rate, samples per FFT and bandwidth is present in the controls on the bottom left of the main screen. The general purpose output produces a comma delimited data file with a .csv file extension.

The top center of the setup window is used to determine the behavior in the event multiple record sessions are desired. There are two options one to append the data to the previous file and one to create a new file with a suffix number in the file name.
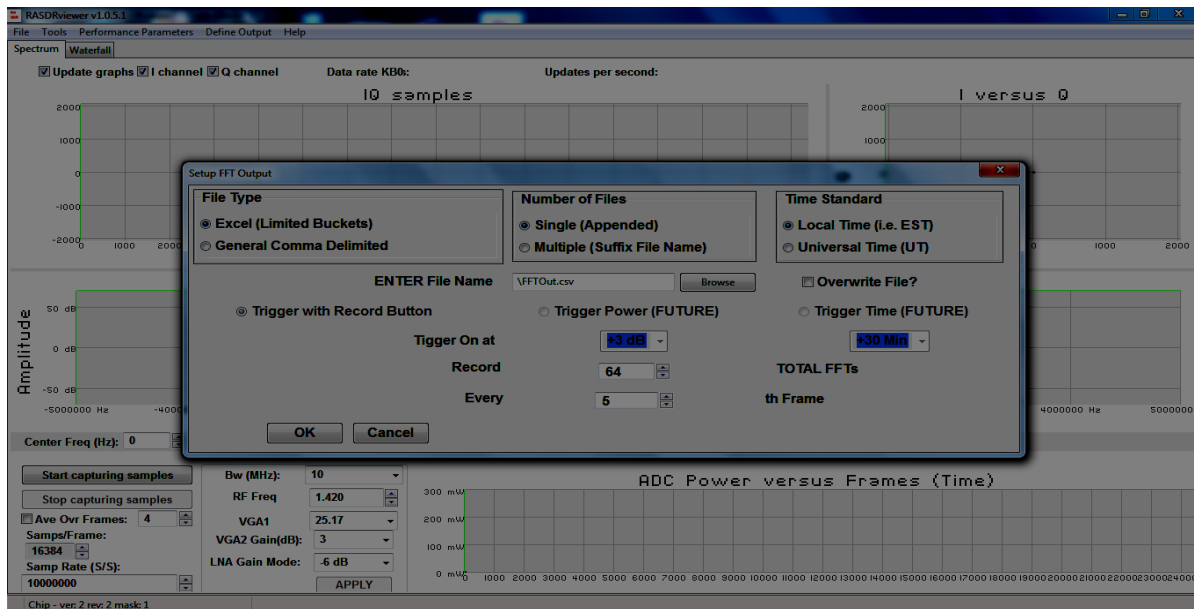
Figure 2 the FFT Output Setup Screen

The top right section of the setup screen is used to define the type of time stamp to be used. There are two options Universal Time and Local Time.

The second section of the Setup Window is used to define the file name. A browse button is included to allow the user to find the directory and file name for the data. If the file already exists, it is necessary to either select a different file name, or check the "Overwrite" box.

On the next line, in the future, the user will be able to define the condition which will trigger the recording to the disk. At present, only the manual trigger is operational.

Near the bottom of the screen is where the user can establish how many FFTs to record and how frequently.

The bottom section contains the "OK" and "Cancel" buttons. To abandon the setup, click the cancel button. To establish the selected parameters, click ok.

Recording FFT Output to Disk

The user clicks the "Record FFT" button which is located on the line below the FFT chart. See Figure 1 and 4. This button is only active when data is being captured by use of the "Start Capturing Samples" button on the left of the screen and an output is defined. The defined number of FFTs will be recorded on the disk. The "Stop FFT Rec" button can be used to stop recording data before the defined number of FFTs is recorded.

Once the recording is stopped, the "Record FFT" button can be clicked for additional data as defined (either appended or new file suffix).

RESULTS OUTPUT

The following chart shows an example of the capability to produce 3D charts using the Excel output option.

The chart was created by inserting a 1421 MHz CW signal on the input to RASDR2. The signal was manually pulsed. All data processing was done with RASDRviewer. Excel was used to produce the chart without any data processing.

The following chart was created using a Python Post processing program.

Collected between 2014-05-07T15:50:57 and 2014-05-07T15:54:32
Averaged over 998 frames
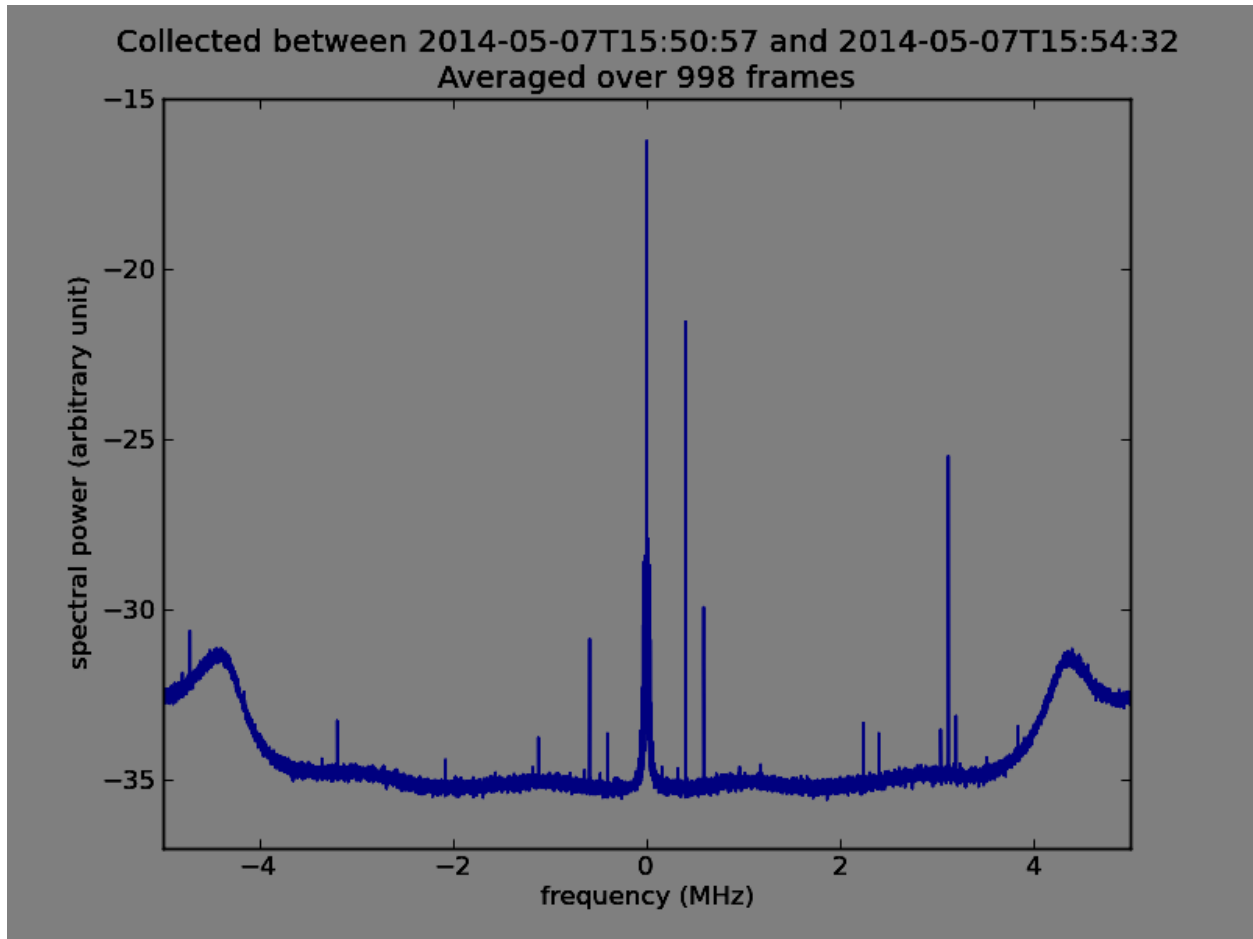
The data was collected using a center frequency of 1420 MHz, 10 MHz bandwidth, 10 M Samples/Second and default gain. A Pulsed CW signal was inserted at -100 dBM at 1420.4 MHz. This produced the spectral line that is closest to zero frequency at baseband. The peak at zero and the other peaks are system produced spurs.
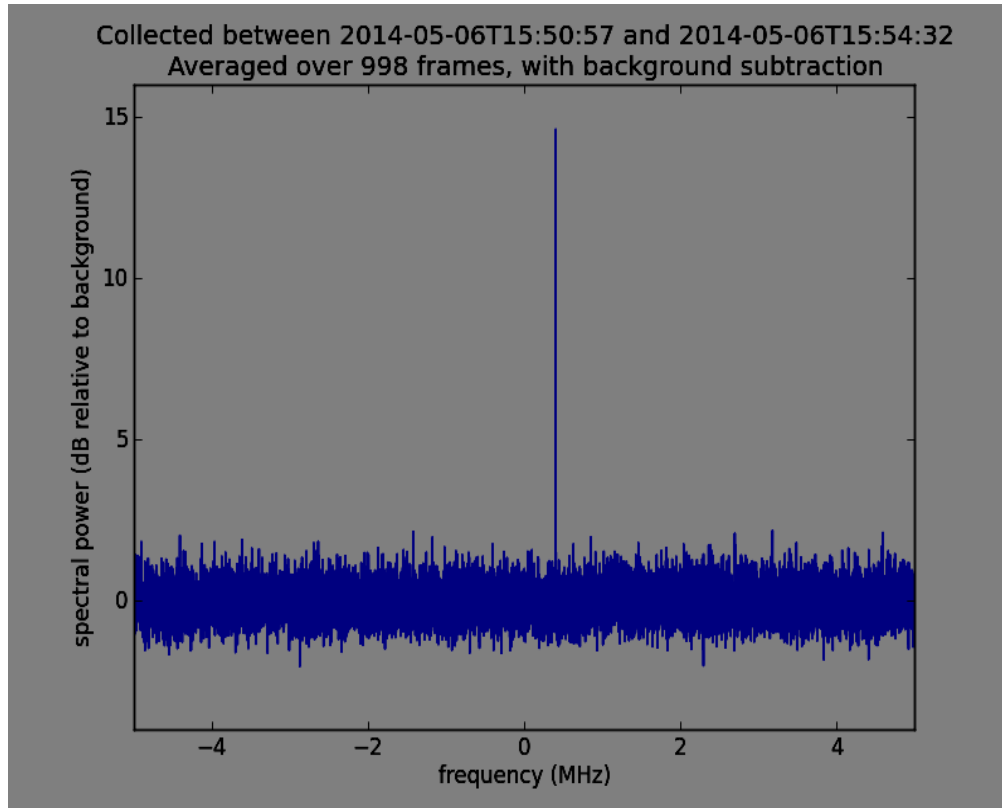
The chart shows how one can enhance spectral lines using a large amount (998 frames) of averaging. The pulsed nature of the input signal was averaged out of the data leaving only the single input spectral line at 0.4 MHz. It also shows that the system spurs can also be enhanced. Thus the user must be careful when interpreting the data to ignore the enhanced spurs.

The following chart was created by subtracting the background from 10 FFTs where the pulse wasn't present. This leaves just the spectral line from the pulsed CW signal and a residual noise floor.

Collected between 2014-05-06T15:50:57 and 2014-05-06T15:54:32
Averaged over 998 frames, with background subtraction

CONCLUSION

RASDRviewer has been proven to provide the necessary software support for RASDR2. The high degree of flexibility in setting parameters will allow the user to customize RASDR2's performance to meet their needs. The user has a choice for output post processing. The 3D Excel charting capability is useful. For other types of processing such as large amounts of FFT averaging or removing the background, the system supports external programs.

FUTURE ENHANCEMENTS

Work is in progress to add a configuration storage file. This will allow the user to pick up where they left off without reentering the configuration parameters. A binary source data file will be added for post processing the raw I & Q samples. If it proves possible, either a real time waterfall or 3D chart will be added on separate screen within the main notebook. Help is needed with the waterfall feature.

ACKNOWLEGEMENT

APPENDIX A

The following spreadsheet shows some examples of the ability to obtain multiple FFT bin widths with different RF bandwidths, samples/FFT and sample rates.

A.

Sample Rate	Samples / FFT (Bins)	Bin BW (Hz)
2.048E+07	16384	1250.00
	8192	2500.00
	4096	5000.00
	2048	10000.00
	1024	20000.00
	512	40000.00
	256	80000.00
	128	160000.00
	64	320000.00

B.

Sample Rate	Samples / FFT (Bins)	Bin BW (Hz)
2.800E+07	16384	1708.98
	8192	3417.97
	4096	6835.94
	2048	13671.88
	1024	27343.75
	512	54687.50
	256	109375.00
	128	218750.00
	64	437500.00

C.

Sample Rate	Samples / FFT (Bins)	Bin BW (Hz)
1.00E+07	16384	610.35
	8192	1220.70
	4096	2441.41
	2048	4882.81
	1024	9765.63
	512	19531.25
	256	39062.50
	128	78125.00
	64	156250.00

D.

Sample Rate	Samples / FFT (Bins)	Bin BW (Hz)
6.40E+05	16384	39.06
	8192	78.13
	4096	156.25
	2048	312.50
	1024	625.00
	512	1250.00
	256	2500.00
	128	5000.00
	64	10000.00

Section A shows a high sample rate that would produce similar results to SpecrtraCyber with the 5Kz bin bandwidth using 4096 samples per bin. Section B shows the bin widths with the maximum available RF bandwidth (28 MHz). Section C shows the bin bandwidths using the default sample rate of 10 MHz. Section D shows the bin bandwidth with the sample rate set low enough to provide a 5 KHz bin bandwidth when used with 128 Samples/FFT. This setup may be useful to produce Excel 3D charts where the number of bins must be limited to 128 or less.

The user can design their experiment to make use of any sample rate that is a power of 2 samples/FFT that best meets their needs. The Bin Bandwidth can be calculated by dividing the sample rate by the number of samples / FFT. Nyquist Criteria must be met when setting the RF bandwidth.

Measuring VLF Field Strengths

Tom Hagen

Introduction

This presentation is about an attempt to get calibrated measurements of the magnetic field strengths of the various VLF stations used by the SuperSID program as reference sources to detect sudden ionospheric disturbances (SID's).

Presently, data coming in from the various SuperSID stations around the world is uncalibrated in amplitude. When a SID is detected, there is a measurable change in relative signal strength, but actual field strengths are unknown. Also, different stations around the world report different SID levels for a given event. Are the causes of these differences different loop antennas, different preamp gains, sound card settings, sound card gain, and/or actual differences in field strength levels?

And from a system design standpoint, the range of field strengths typically encountered would be good to know for improving and standardizing the design of pre-amps and loop antennas.

If field strength at a given location can be measured, a recommendation can be made for the needed loop antenna for that location for a proposed SuperSID station.

Perhaps a standard loop antenna could be specified to improve the repeatability of results.

It may be desirable to measure signal strengths at different places around the world to see if a SuperSID station can actually work in a given location before sending it out to that location.

I have noticed that different rooms in a building give vastly different results in signal strengths. A station can be undetectable in one room in a building and comes in fine in a different room. A quick check with a calibrated system could verify a condition such as this.

Another outcome of the project could be a simple portable setup to test field strengths at different sites around the world. The setup would fit into carry-on luggage on a plane or could be mailed to the remote site. Perhaps a calibrated Arduino microcontroller could be used with the loop and a PC with COM port for field strength checks.

The setup will be a shielded loop calibrated with a Helmholtz coil. A preamp is used to get usable output levels for the recording system.

For portable use the output will be put into a sound card of a PC running Spec Lab or equivalent and the levels will be compared to those of the selective level meter.

Steps:

1. Build and test a setup according to best guess design, verify design as acceptable.
2. Verify that Helmholtz coil has a uniform field within the loop area.
3. Calibrate receive loop in Helmholtz coil using oscilloscope to measure open circuit voltage.
4. Compare calibrated values for loop to calculated values at different field levels and frequencies.
5. Make field strength measurements at my location on the VLF stations I can receive.

Test Setup Diagram

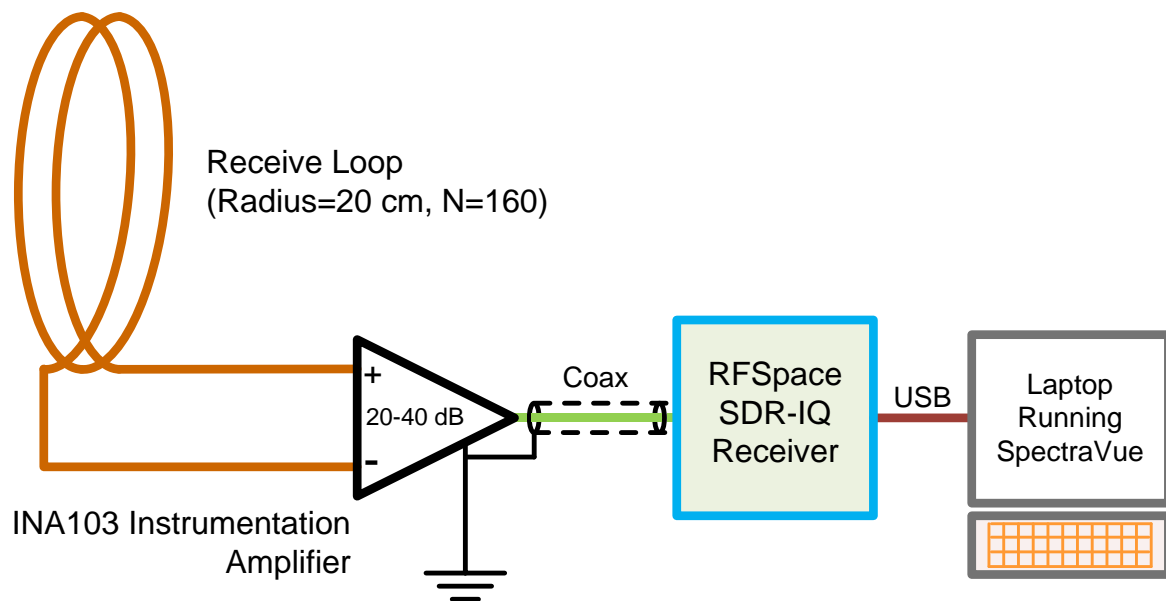The setup block diagram is as below.

Figure 1: Block Diagram of Measurement Setup

The setup for the VLF measurements is kept as simple as possible. The detected strength of a signal is shown in the laptop display. Settings on the SDR-IQ are adjusted for the minimum RF and IF gains to get a usable signal with acceptable signal-to-noise ratios. Bandwidth is set to 50 Hz.

Construction of Test Setup

The loop antenna used is 40 cm in diameter, is wound on a 2" thick polystyrene disc, and was cut from a piece of 2"x4'x8' rigid polystyrene foam insulation board with a hotwire cutter. The coil diameter and number of turns is selected from prior experience of measuring VLF signals.

Hotwire cutter with Variac and Current Meter

The variac current was monitored and set to approximately 8A$_{RMS}$ while monitoring the current with the meter. A 60 cm length of solid copper wire, 22 AWG, was used as the cutter and current was monitored to maintain the temperature of the cutting wire. Once cutting had started, the action of the cutter was monitored and used as feedback to control the current by varying the setting of the variac output voltage. Note that I did this job outside because of the smell of molten polystyrene!

An 60 cm square piece of foam was cut from the original 4'x8' piece of board and a 40 cm diameter circle was marked within this square as a cutting guide. The foam was turned against the hotwire cutter and the cut was made freehand style.

The loop was next wound on the form using 28 AWG enameled solid copper wire. About 160 turns were applied for a total length of approximately 200 m. Connections to the wire ends were made with female banana jacks. The wire was secured to the disc with electrical tape.

Cutting the Round Coil Form from a Square Piece of Rigid Foam Insulation

and banana jack connections made with hole from 1.25" hole saw

Finished Coil in the Field

For field measurements, the coil is affixed to a lightweight camera tripod with a brass bolt through the disc to attach to the custom made adapter. In this way the coil can be rotated through the azimuth axis well over 90° to cover stations from all possible directions.

For portable work, I fixed up an old briefcase with a dual battery supply and a breakout box to make banana plug connections. This is to avoid connecting long and heavy wires to the relatively delicate breadboard prototyping setup.


Briefcase Field Setup: Prototype pre-amp shown

INA103 Pre-Amplifier in Shielded Enclosure

Next I built up a more permanent preamp setup for the INA103 instrumentation amplifier. The enclosure is made of single sided printed circuit board material, soldered together at the seams. Dual voltages are supplied through the 3 banana jacks on the lower side of the box. Input from the loop antenna is connected to the 2 white banana jacks on the right side of the box and the output of the amp is supplied through the BNC connector on the left side of the box. The lid and retainer tabs for the box is on the right and is also fabricated from PCB material.
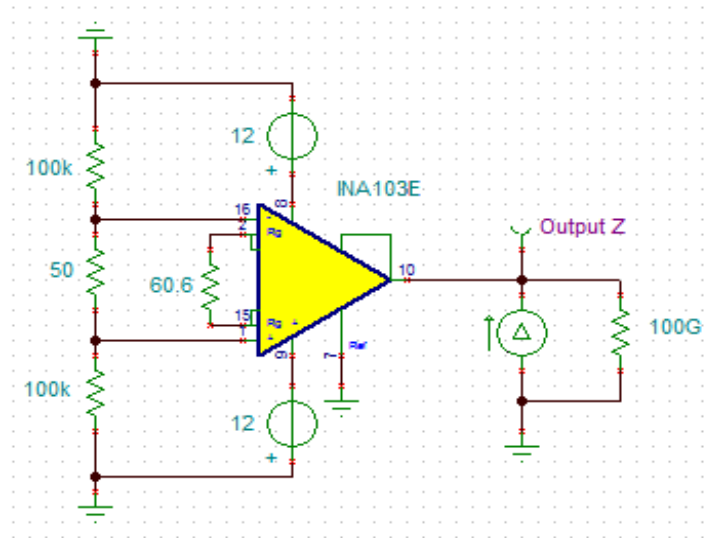
INA103 Instrumentation Amplifier Schematic

The IN103 is quite easy to set up. The gain is set by a resistor, in this case, the 60.6 Ohm resistor sets the gain to 40 dB. The 100k resistors were selected to supply input bias currents and incidentally set the input impedance to 200k Ohm as seen by the loop terminals.

Initial Test of Setup

The finished loop was tested at an RF quiet location at a state recreational area around 10 km from my home. I use an RFSpace SDR-IQ receiver with an INA103 preamplifier with adjustable gain. My first setup employed my 30 year old RYCOM 6040 selective level meter ($50 on eBay) to get an initial check of the loop and preamplifier.

Initial Field Setup

The first quick tests with the RYCOM showed promising results. (This setup with the INA103 preamp even works well in the AM broadcast range.) During the day, the 4 strongest VLF stations (NAA, Cutler ME; NML, LaMoure ND; NLK, Jim Creek WA; and NPM, Lualualei HI) that I monitor from my location were coming in well enough above the noise floor that steady strength readings were obtained.

The test was repeated with the SDR-IQ software defined radio receiver.
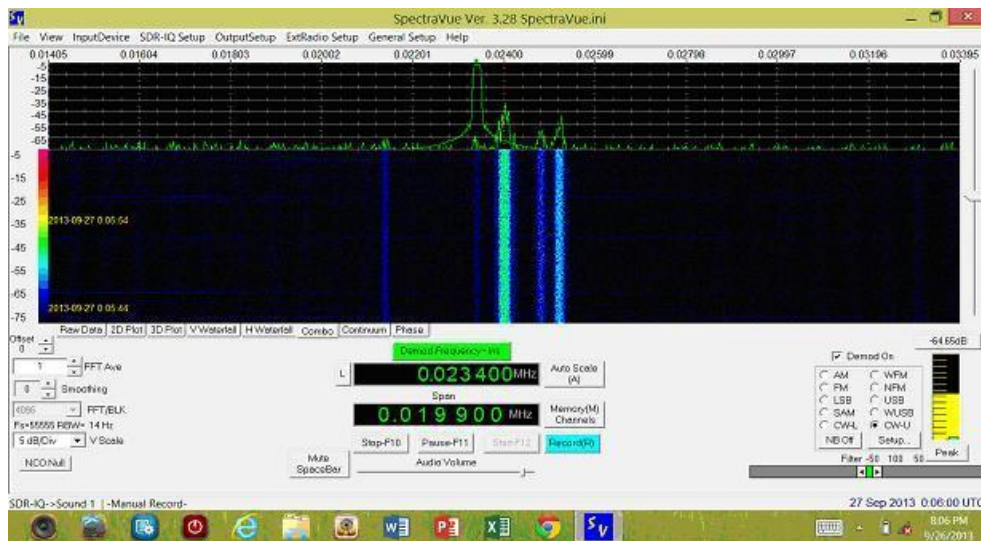
Screenshot of SDR-IQ Display

Figure 7 was taken after sunset in the early evening at my quiet location. Stations at 21.4, 23.4, 24.0, 24.8, and 25.2 kHz are seen. The weakest signal at 23.4 kHz is DHO38 from Germany. The 4 strongest signals are from the US North America and Hawaii stations.

Loop Antenna Theory[10]

The theory of a circular loop antenna is very straightforward and that is why it was chosen for this project.

The open circuit induced voltage for the electrically small loop of this project is given by Faraday's Law:

$$V_{oc} = -\frac{d\Phi}{dt}$$

Where V_{oc} is the open circuit voltage of the coil, Φ is the magnetic flux through the coil (normal to the coil plane), and t is time. In other words a time varying magnetic field through the coil induces a voltage at its terminals.

The magnetic flux through the coil is the integral of the magnetic flux density B over the area of the loop (again the field is normal to the loop):

$$V_{oc} = -\frac{dB}{dt}\pi r^2$$

Where B is the magnetic flux density and r is the radius of the loop. In the case of N turns on the loop, the open circuit voltage is simply:

$$V_{oc} = -N\frac{dB}{dt}\pi r^2$$

And for the case of a sinusoidal field as received by the loop, dB/dt simply becomes the rms value of the field multiplied by the radian frequency ω:

$$V_{oc,rms} = N\omega B_{rms}\pi r^2$$

or

$$V_{oc,rms} = N2\pi f B_{rms}\pi r^2$$

Where f is the frequency in Hz. This is intended to be a calibrated loop so it will not be resonated with a capacitor to maximize the output voltage. Keeping things simple simplifies predicted output voltage given a frequency and a planar uniform field as generated in the Helmholtz coil.

For the 40 cm loop antenna, the numbers work out to (N=160, r = 0.2 m):

[10] From Whitham Reeve's Loop Antenna Paper

$$V_{oc,rms} = 126.3\ f\ B_{rms}$$

or

$$B_{rms} = V_{oc,rms}/(126.3\ f)$$

Helmholtz Coil Theory[11]

The next step in this process is calibrating the loop antenna with a known constant and uniform magnetic field. One of the easiest ways to create such a field is to us a Helmholtz coil. The Helmholtz coil provides a uniform field inside the volume between the two coils that are spaced one coil radius distance apart. I have a Helmholtz coil available at my place of employment that I used to create a known field to calibrate my 40 cm loop.

ρ↑   z→
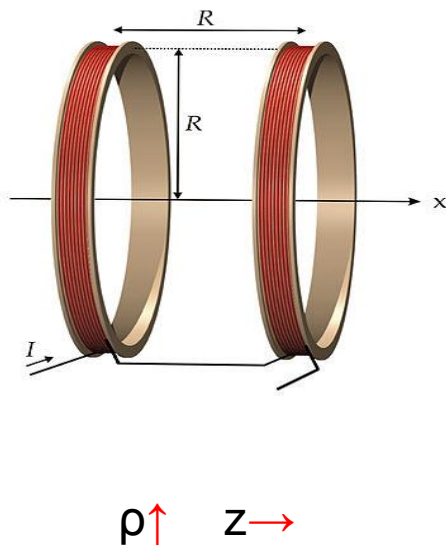
Standard Helmholtz Configuration
Permission: Ansgar Hellwig CC-BY-SA-2.0 and GFDL

My 20 in. "Sonotube" Helmholtz Coil

The two papers by Kuns and Detroye/Chase referenced in the Wikipedia article give detailed derivations and techniques on how to calculate and measure the fields generated in the space between the coils. I followed their methods for the following work.

---

[11] Wikipedia article on Helmholtz Coil; see excellent references for the article itself

The problem to be solved is to get a good understanding of the field passing through the loop antenna when it is placed in the center of the Helmholtz coil and a known current is driven through the Helmholtz coil. One could simply measure the field across the diameter at the center of the coil with a small (~2 to 4 cm dia.) loop and use this information to calibrate the loop antenna, but I decided to go a step further and attempt to compare calculated and measured values of the field to see how my particular coil compares to reality.

So I developed a mathematical model of the Helmholtz coil and simulated it using computer algebra system (CAS) software, in point, Mathcad and compared to measured results. I would have used a finite element analysis (FEA) program had I had such a program available, but fortunately the calculations for the Helmholtz coil are "simple" enough that they can be simulated using CAS software.

After an extensive derivation starting with the definition of magnetic vector potential, Kuns does a thorough job (over a half dozen pages or so) deriving the equations that describe the magnetic flux densities in the Helmholtz coil in the ρ and z directions.

The equations as entered in Mathcad are seen below.

I is current through the coil in Ampere, a is the radius in meters and d is the spacing between the coils in meters.

$$I := 0.01 \quad \mu_O := 4 \cdot \pi \cdot 10^{-7} \quad a := 0.265 \quad d := 0.125$$

K(k) and E(k) are elliptic integrals of the first and second kind respectively with k(ρ,z) being a function that is derived to make the elliptic integrals function as desired.

$$k(\rho, z) := \sqrt{\frac{(4a \cdot \rho)}{(\rho + a)^2 + (z)^2}}$$

$$K(k) := \int_0^{\frac{\pi}{2}} \frac{1}{\sqrt{1 - k^2 (\sin(\phi))^2}} \, d\phi$$

$$E(k) := \int_0^{\frac{\pi}{2}} \sqrt{1 - k^2 \cdot (\sin(\phi))^2} \, d\phi$$

The expressions for the magnetic flux density in Tesla for the field in the p and z directions then become:

$$B_\rho(\rho,z) := 0 \quad \text{on error}\left(\left(\frac{\mu_o \cdot I}{2 \cdot \pi}\right)\right) \cdot \left[\frac{z}{\rho \sqrt{(\rho + a)^2 + (z)^2}}\right] \cdot \left[\frac{\left[\rho^2 + a^2 + (z)^2\right] \cdot E(k(\rho,z))}{(a - \rho)^2 + (z)^2} - K(k(\rho,z))\right]$$

$$B_z(\rho,z) := 0 \quad \text{on error}\left(\left(\frac{\mu_o \cdot I}{2 \cdot \pi}\right)\right) \cdot \left[\frac{1}{\sqrt{(\rho + a)^2 + (z)^2}}\right] \cdot \left[\frac{\left[a^2 - \rho^2 - (z)^2\right] \cdot E(k(\rho,z))}{(a - \rho)^2 + (z)^2} + K(k(\rho,z))\right]$$

The output of the calculations for 1 current loop can be displayed as a vector or surface plot showing B_z in the ρ and z directions.

The calculated values of B_ρ and B_z are stored in a 2-dimensional matrix and are plotted in either vector or surface plot forms as desired.

The following plots show the field represented graphically. For all plots, a 20x20 matrix was used for a total of 400 points in all the plots.

Mathcad allows one to make plots in various forms. I used vector plotting and surface plotting for the different graphs in this paper.
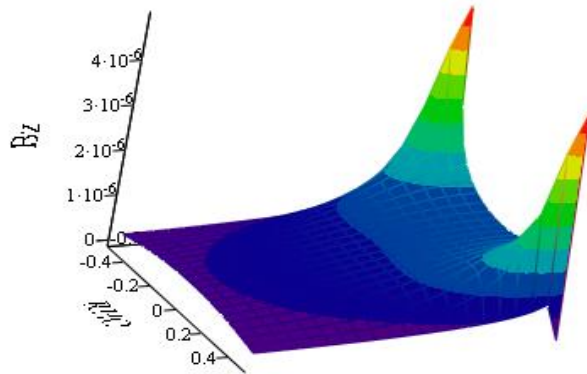

(L , M)
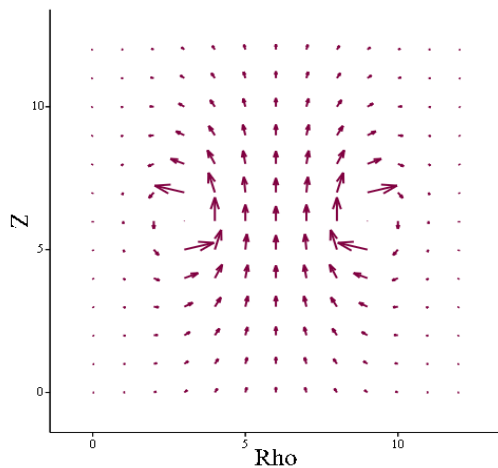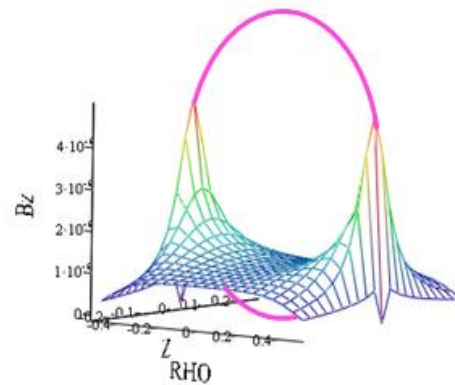
(ρ , z , M)

Mathcad Plots showing magnetic flux density of a single current loop. The left plot shows the vector view of the field and the right plot shows the amplitude of the Bz field with the loop shown for reference.

47

(ρ, z, M)

Mathcad plot showing a single loop offset from the 0 position
along the z-axis to z=d. B_z amplitude plot is shown.

The field of the Helmholtz coil is simply the summation of the fields from two single current loops spaced at ±1/2 coil radius from the z=0 position. See the figure below.
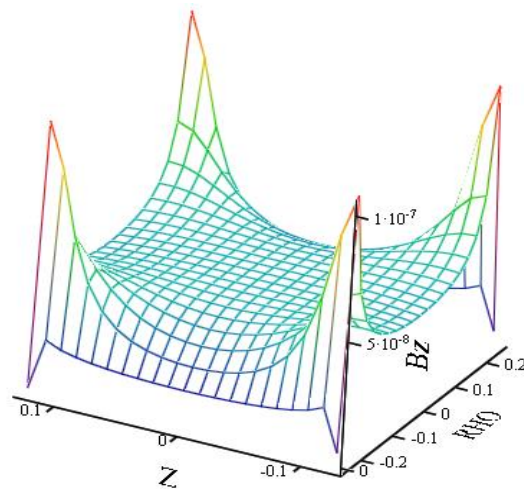
Bz Field of the Helmholtz Coil, a=0.5m, ±d=0.25 m, i=1 A

(ρ, z, M)

(L, M)

Mathcad Plots of Bz; Contour Plot on Left, Vector Plot on Right;
50 Contours shown, or 2% Difference Between Contour Lines

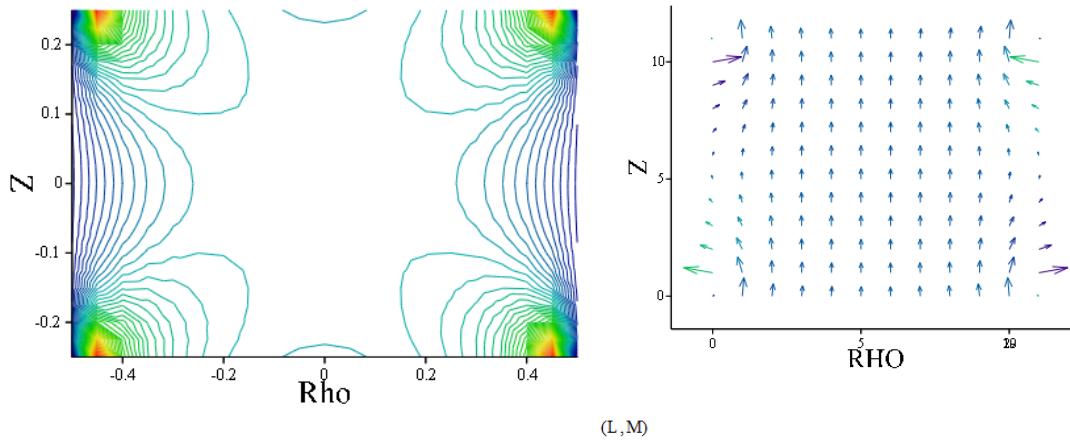Now the preceding plots are based on a theoretical Helmholtz Coil comprising 2 infinitely thin current loops. The Helmholtz Coil that I use is made up of 2 solenoidal coils as follows:

53 cm

13.7 cm

14.2 cm

25 cm

N=50 (each winding)

Wire: AWG 10;
D= 2.6 mm
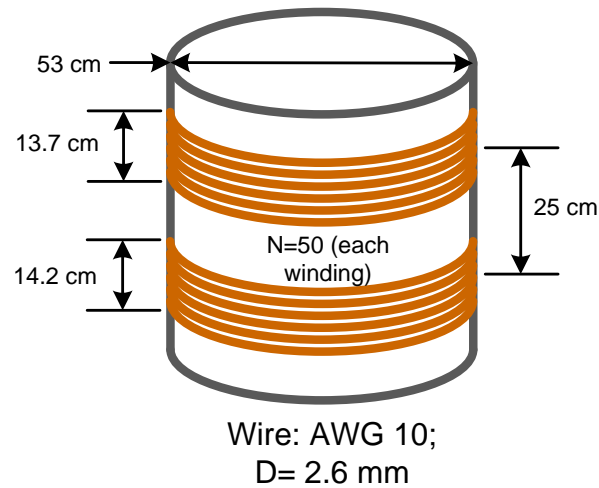
Mathcad can easily simulate this configuration as the summation of the magnetic fields from 50 current loops instead of only 2.

49
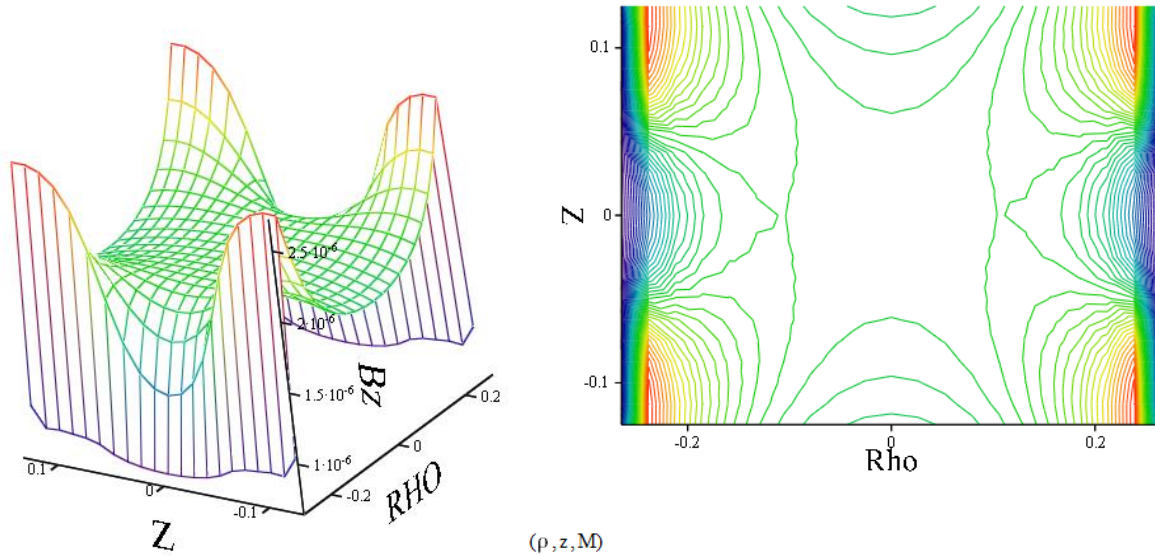
Helmholtz Coil with 2 50-turn Solenoidal Windings: Equivalent Plots

Note the difference between the simulations of the 2 turn versus the 50 turn Helmholtz coils. The constant field region in the center of the coils is noticeably different too. The field inside the Helmholtz Coil is getting longer and thinner, approaching that of an infinite solenoid.

Testing the Helmholtz Coil

The careful workman has a good understanding of the appropriate use of his tools! Some assumptions on the behavior of an ideal Helmholtz coil may be:
   ● The magnetic field strength is uniform over the entire volume inside the coil.
   ● The magnetic field strength is exactly proportional only to the frequency of the current and nothing else.
   ● The Helmholtz coil has no resistance or capacitance associated with it.

As a rule, the above ideal assumptions have to be modified in the real world.

Since we're only going to be using the middle of the coil to calibrate the essentially flat sense coil, the important part of the coil to check is a narrow slice of the Helmholtz coil its center. A setup as seen below would be appropriate. The sense coil is a commercial ETS Lindgren 7604 loop antenna. A 10Ω resistor inserted in series with the function generator and the Helmholtz coil. The voltage drop across the resistor is measured to fix the current through the Helmholtz coil at a set value across the frequency range of the test. Remember that the inductive reactance of the Helmholtz coil requires a higher and higher drive voltage as frequency is increased to maintain a constant current.
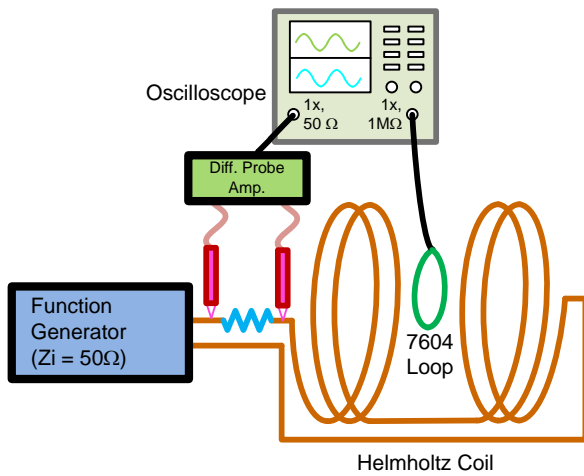
Helmholtz Coil Resonance Test Setup

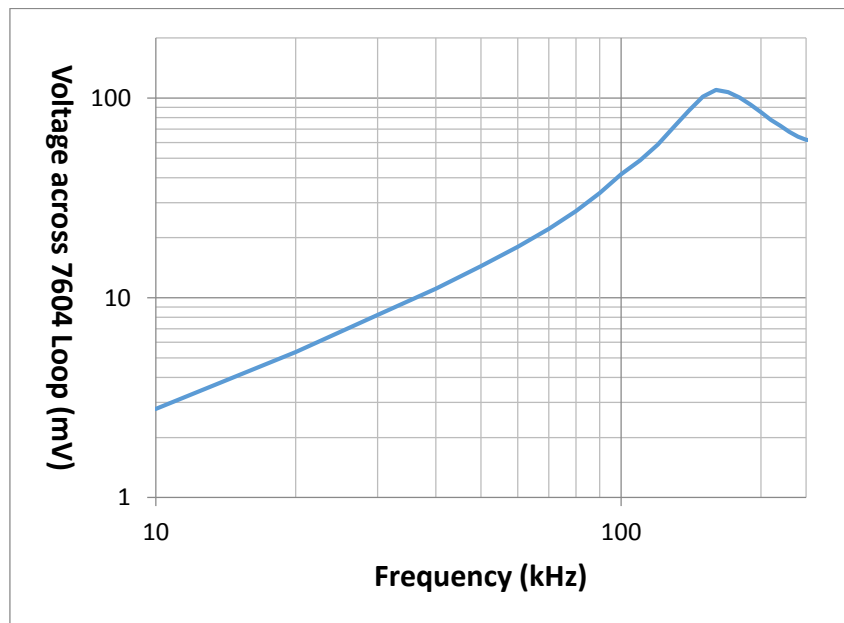

ETS Lindgren 7604 Loop
Antenna Inside Helmholtz Coil

Helmholtz Coil Parameters:
- Inductance = 4.38 mH
- R_{DC} = 0.556 mΩ

The result of the above setup is seen as:

The Helmholtz coil has a resonant frequency of about 160 kHz. This is caused by the unavoidable

interwinding capacitance. The asymmetrical appearance of the hump is caused by the approaching resonance of the sense coil. Its resonant frequency is at around 400-500 kHz.

This coil is usable to maybe 60 kHz frequency as evidenced by the mostly linear slope of the characteristic up to that frequency:
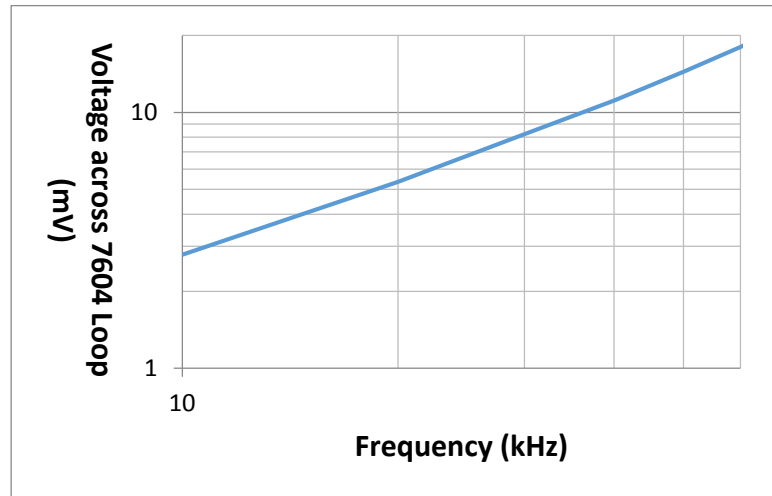
Upon closer inspection of the figures above, you can see that the line does deviate somewhat from linearity and this indicates that perhaps interwinding capacitance does have a noticeable effect, even at the lower frequencies. For now, we'll neglect the effect and forge ahead.

Next the uniformity of the field across the diameter of the coil is checked, as the 40 cm loop antenna will be placed at the center of the Helmholtz coil (z=0) and normal to the z-axis. The setup below was used to map the field across the diameter of the Helmholtz coil. A 4 cm shielded loop antenna was used and it was mounted on a Plexiglas fixture that spans the diameter inside the Helmholtz coil. The sense coil is based on the MIL-STD 461 military EMC test specification, RS101 test for magnetic immunity testing.
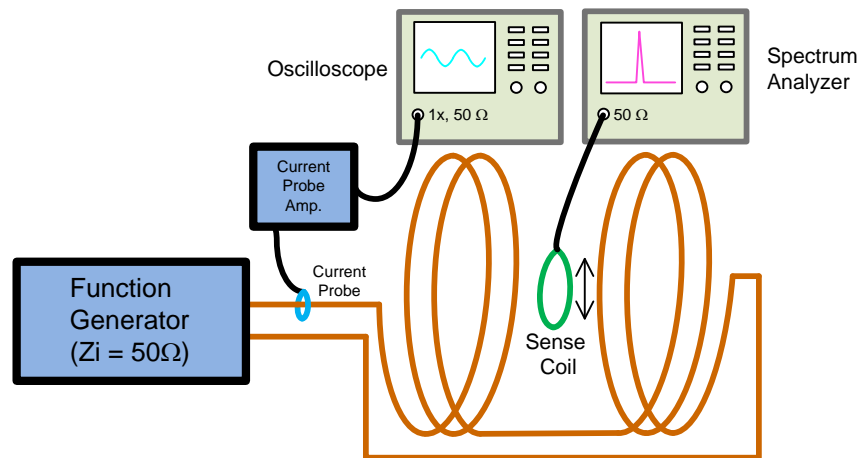
Sense Coil: MIL-STD 461, RS101

Sense Coil Mounted to Fixture Inside Helm-holtz Coil (20 cm position)

Measurements of the field were made at the center of the Helmholtz coil and the sense coil was moved in 5 cm steps out to the edge of the cardboard coil form. The last step was only 2.8 cm, since the coil hit the edge of the form. Frequency was set to 1 kHz, and current was set to 10 mA$_{RMS}$. The blue line is the calculated field for these conditions and the red markers were the measured field. Agreement between calculated and measurements is around 1% or less.
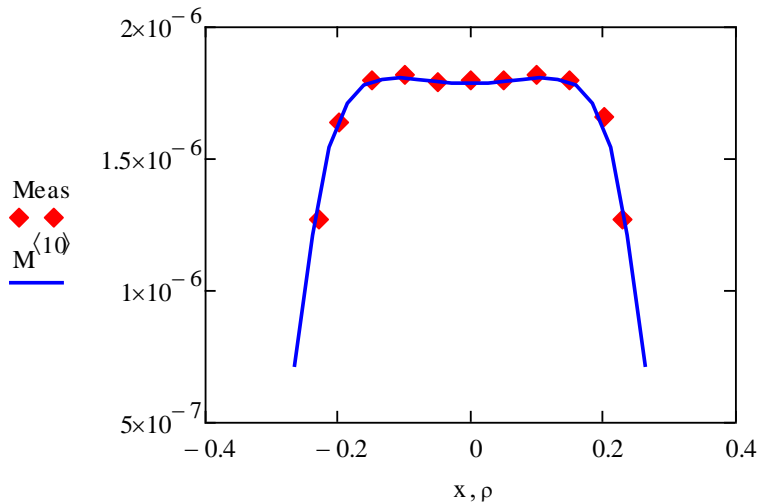
Helmholtz Coil Measured vs. Calculated: Magnetic Flux Density, 1 kHz

At 24 kHz, measured and calculated don't agree so well. This difference is under study. Part of the disa-greement could be due to interwinding capacitance. A correction factor of around 0.9 dB brings things back into agreement, and the work proceeded with this factor assumed.
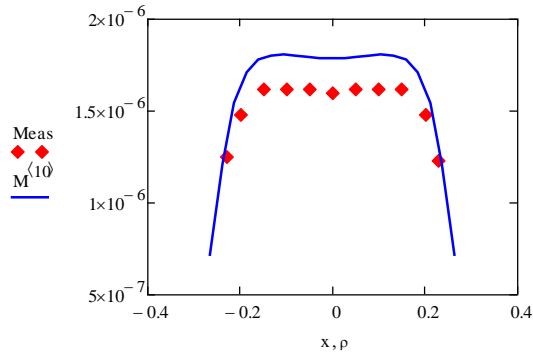
Original Measurements	Corrected Measurements
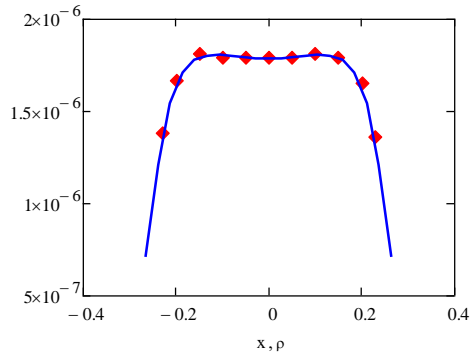
Helmholtz Coil Measured vs. Calculated: Magnetic Flux Density, 24 kHz

Calibration of Loop Antenna

Once the modeling and behavior of the Helmholtz coil is understood, the loop antenna can be calibrated.
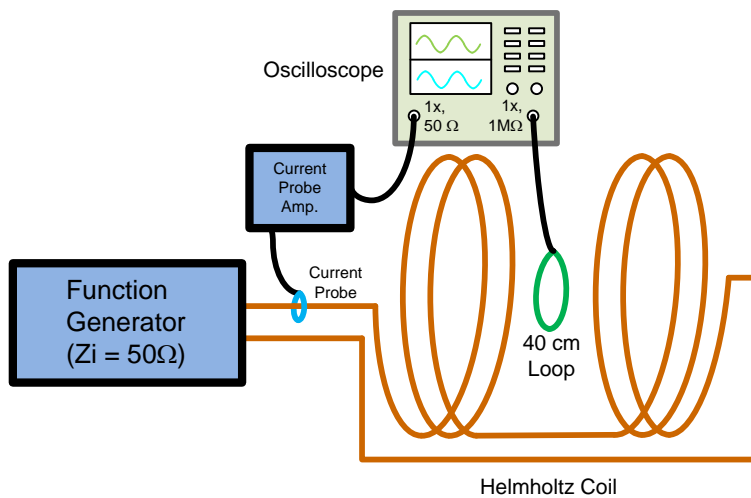
40 cm Loop Antenna Calibration Setup
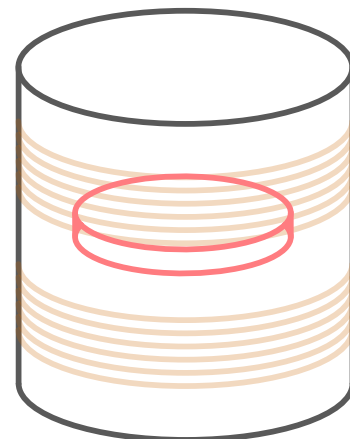
Test Position of 40 cm
Loop Inside Helmholtz Coil

The first consideration in calibrating the 40 cm loop antenna is the non-uniform cross-section of the field across the ρ axis in the center of the Helmholtz coil (z = 0). The 10 mA field has the approximate shape:
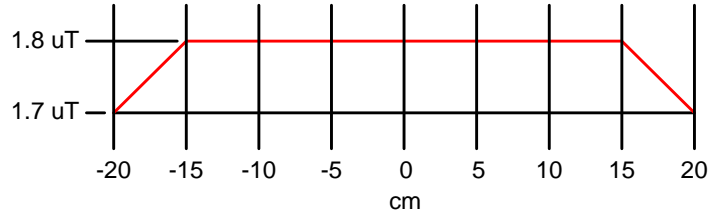
To 2 significant figures, the average field across the area of the loop antenna is 1.8 μT. This is accurate enough for our purposes.

The second consideration in calibrating the loop is the determination of the correction factor of the receive loop for the VLF frequency range. This is found the same way it was found for the same for the Helmholtz Coil. The calibration was done by applying 10 mA to the Helmholtz coil and then applying the 0.9 dB factor to increase the current to 11.1 mA. The open circuit voltage of the loop antenna is measured and compared to calculated. This was done and the correction factor for the 40 cm loop antenna was found to be around 1.7 dB for the 40 cm loop antenna.

Recalling the setup block diagram:
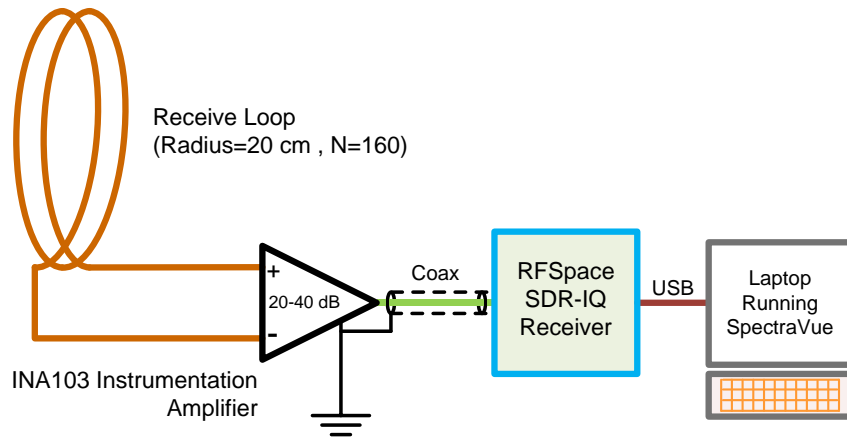
The gain budget for the system then comes out to:
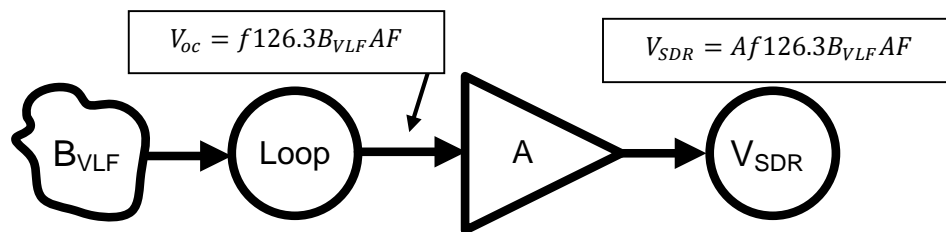
Or:

$$B_{VLF} = \frac{V_{SDR}}{Af126.3AF}$$

Or in dB notation:

$$dBT = V_{SDR_{dB}} - A_{dB} - f_{dB} - AF_{dB} - 42.0$$

So the magnetic flux density of the received signal from a VLF station at 24 kHz using the 40 cm loop antenna with its corresponding antenna factor would be:

$$dBT = V_{SDR_{dB}} - A_{dB} - 87.6 - 1.7 - 42.0$$

$$dBT = V_{SDR_{dB}} - A_{dB} - 131.3$$

$$dBpT = V_{SDR_{dB}} - A_{dB} + 128.7$$

Where dBpT is the magnetic flux density in decibels above 1 picoTesla.

Calibrated B-Field Measurements

The setup was built and data was taken on 3/4 & 3/5/2014 with the loop set up on my patio. (Thankfully it's almost spring in Michigan and the weather's quite balmy!)

The 25 hour plot below shows the SDR reading on the left scale and the corresponding magnetic field strength on the right scale. Preamp gain was set to 40 dB. Spectraview was used in the

"Continuum" data logging mode. Data points were individually time-stamped and stored in a CSV file. Points were taken at 20 s intervals and no data averaging was done. There is a bit of electrical noise present and this is probably limiting the measurement of the lower amplitude of the signal to maybe 45 dBpT or so.
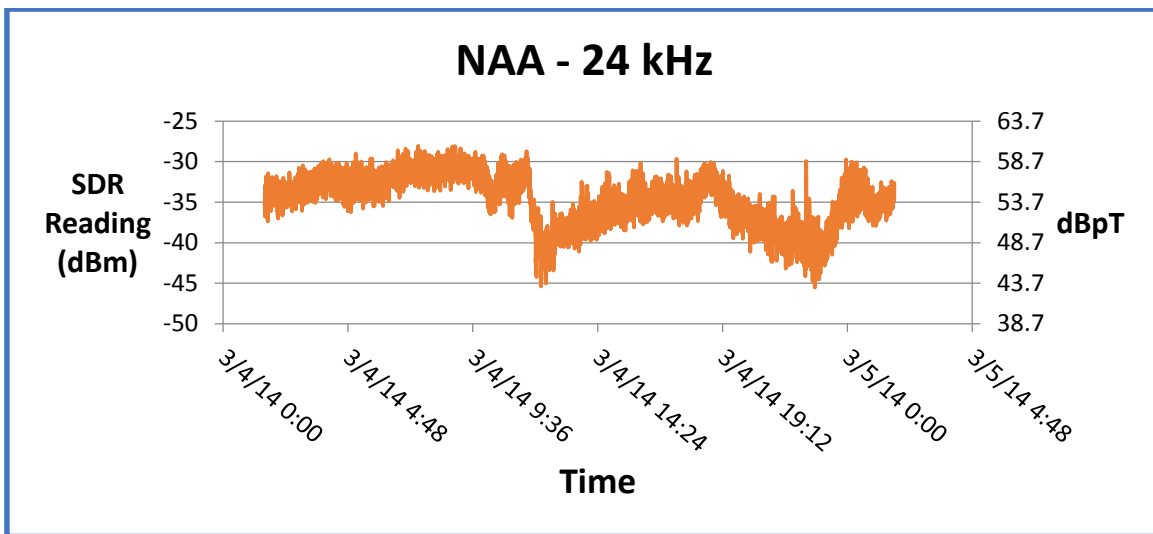
Conclusion

A VLF field strength setup was developed, tested and found to be acceptable for purposes of this project. The Helmholtz coil that was used for the loop antenna calibration was characterized and a Mathcad model for the coil was developed which agreed well with verification measurements. The loop antenna was calibrated with the Helmholtz coil. A conversion factor for the loop antenna was found and the setup was used to measure the field strength of US Navy station NAA on 24 kHz. (NAA is around 1300 km from my house.)

Further Work

1. The setup was not tested end-to-end with the loop antenna placed in the Helmholtz coil. The setup should be verified this way to ensure that no other errors have sneaked into the setup.
2. The receiving loop was not shielded against electrostatic field coupling. This should be done and the differences in performance should be noted.
3. A portable setup could be developed that could be mailed to any location in the world for checking VLF field strengths at that location. The setup might look like that below. It would be desirable to use SuperSID software for recording and measuring field strengths, since it is easy to use and has the built-in data recording feature.
4. It would be desirable to model the Helmholtz Coil using freeware such as the Python-based

SageMath. This would make modeling more accessible for amateur investigators.
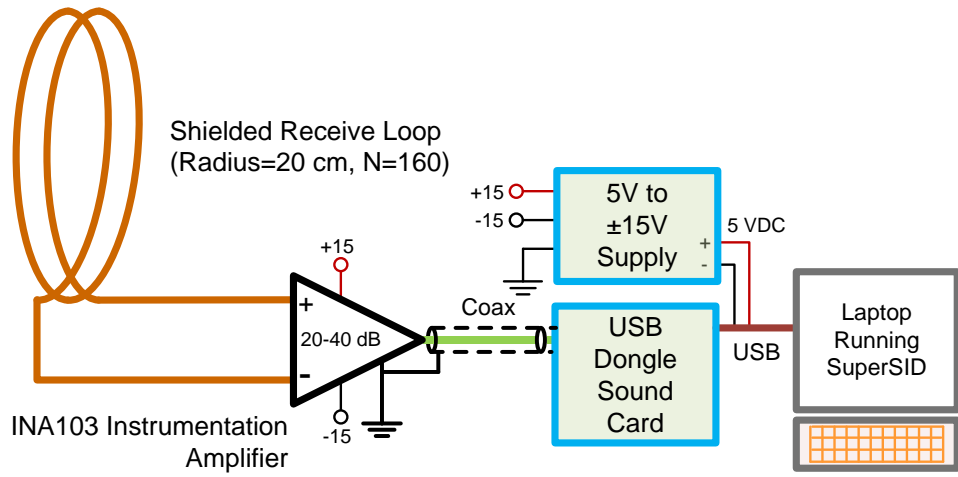
Portable Setup for Measuring VLF Station Field Strengths

SETI's New Horizons

by H. Paul Shuch, N6TX (paul@setileague.org)

Executive Director Emeritus, The SETI League, Inc.

Abstract

The author and his colleagues have proposed to NASA the creation and uploading of a message into the New Horizons spacecraft's memory, following a successful Pluto encounter in 2015. In the tradition of the Voyager Records now traveling through interstellar space, this message will be a self-portrait of our planet and species, to be shared with all humanity, and potentially with intelligent species elsewhere. The message contents are being crowd-sourced by people worldwide, and thus represent our planet as a whole. An international board of expert space scientists and engineers has determined this proposal to be technically feasible, and is currently managing all technical details. Programs for K-12 students will also increase interest in the New Horizons interplanetary probe mission, as well as showing students how they may share in this rare chance to help make a message that will soar among the stars.

Introduction

In September of 2006, even as astronomers were in the process of demoting Pluto to dwarf status, a half-ton robotic spacecraft was already enroute to a close encounter with the former planet. Engineered by the Applied Physics Lab at Johns Hopkins University, NASA's New Horizons mission had been launched from Cape Canaveral in January 2006, into an Earth and solar system escape trajectory. It would slingshot around Jupiter a year later, the giant planet's gravity accelerating it to become the fastest object ever launched by humans. After flying within 10,000 km of Pluto in 2015, it is expected that New Horizons will survey several Kuiper Belt objects, before exiting our solar system and drifting into interstellar space.

Seven years after launch, the spacecraft is already more than 26 Astronomical Units from Earth, and within less than 6 AU of its primary target. At that distance, radio commands from Earth take nearly four hours to reach its receivers. And now, with New Horizons far from our local neighborhood, my colleague Jon Lomberg has come up with an ambitious plan to turn the planetary probe into an interstellar ambassador.

Lomberg is no stranger to galactic greetings. In the 1970s, he was the Design Director of the famous Voyager Golden Records, later a plot element in many a good science fiction film. So, it was no surprise that he proposed attaching a similar message from humanity to the rapidly receding spacecraft. But, how does one saddle a horse that has already long left the barn? Jon, a staunch SETI supporter, adopted a

strategy quite familiar to those of us who spend our days searching for signals from the stars. He would employ photons, the fastest spaceships known to man.

The plan, after crafting a suitable *Encyclopaedia Terrestria*, is to beam it via microwave from NASA's Deep Space Communications Network, directly into New Horizon's onboard computer memory, from which extraterrestrial computer scientists may attempt, some eons hence, to extract it. All of which is highly speculative (but no more so than the SETI enterprise itself). A number of SETI League members (including myself) have joined a team to try to pull off this newest *Hello from the Children of Planet Earth*. What remains to us is to answer a plethora of questions, to be addressed below.

Who Speaks for Earth?

The short answer is: *you do*.

When NASA launched the two Pioneer space probes toward the outer planets in 1972 and 1973 respectively, the plaques affixed to them were very much an afterthought. The plan, as initially suggested by Eric Burgess at JPL, was quickly implemented by Carl Sagan and Frank Drake, and the artwork hastily sketched by Sagan's then-wife Linda Saltzman, just weeks before the first of the Pioneer spacecraft departed planet Earth. It was only later that the public became aware of the existence of the plaques, which boldly depicted two naked humans. Great controversy resulted, possibly because in those dark ages before Al Gore invented the Internet, few Americans had ever actually seen a naked human being. The resulting public outcry reverberated through the cubicles of NASA, nearly spelling an end to the inclusion of such ad-hoc expressions of human aspirations in future space missions.

The next major effort at interstellar messaging was probably the Voyager Golden Records, launched on a Grand Tour of the Solar System in 1977. Under considerable NASA scrutiny, Carl Sagan and a somewhat larger committee assembled a collection of 116 images, various musical selections, and spoken greetings in 55 different Earth languages, including an innocent and childlike "hello from the children of Planet Earth," spoken in English by Sagan's young son. NASA took great pains to ensure that the records contained nothing that might incite controversy.

This time around, the committee crafting the message will be much larger still. At this writing, a petition to NASA seeking project approval has gathered over 10,500 signatures. Contributions of content are solicited from all inhabitants of this planet, to be reviewed and complied by an international advisory board of 81 individuals from 25 countries. The resulting message will thus be crowd-sourced from people around the world, creating a self-portrait of Earth in the second decade of the 21st Century. (Since New Horizons is a NASA mission, we anticipate that NASA will still maintain some editorial control, and possibly exercise veto power over any message content that its managers deem objectionable.)

How Much Can We Say?

It's sadly ironic that our message, meant to hurdle through limitless space, will in fact be space-limited. The digital memory potentially available to house the New Horizons Message is a scant 100 MBytes. Terrestrial computer scientists are very adept at data compression, fitting a huge volume of text, sound, and images into a comparable closet. However, lacking a mutually agreed upon compression and expansion algorithm, any attempt to cram ten pounds of bits into a five pound bag will result in incomprehensible gibberish.

So, how much meaningful information can we convey in a billion uncompressed ones and zeros? Quite a bit, actually, if past experience is any indication. In 1974, for example, Frank Drake crafted a clever message just 1679 bits in length, and beamed it to the stars from the Arecibo radar telescope. In 73 rows by 23 columns (both being prime numbers, a concept doubtless familiar to intelligent extraterrestrials), the Arecibo Message conveyed a primer on binary arithmetic, depictions of those molecules most critical to life as we know it, the double helix structure of DNA, a sketch of our solar system (including the subsequently demoted Pluto) indicating the relative size of the planets and locating our home planet as the third orbit from its star, a stick figure of a human with an indication of our physical size, a rough count of Earth's human population, and a crude schematic diagram of the antenna sending the message (complete with a measure of its diameter). All in a mere 1679 bits. Presumably, the New Horizons digital memory could accommodate about 600,000 such images of similar information density.

What we choose to say in those 600,000 images (or a lesser number of higher resolution ones) is another question altogether.

Can ETI Even Understand It?

One of the great challenges of interstellar message construction is to devise content that is comprehensible to members of a civilization with which we have no historical, social, cultural, or biological commonality. Crafting such a message requires an inverse to encryption; instead of disguising content, it must be made self-evident.

Fortunately, the New Horizons Message team enjoys participation from a number of social scientists and linguists who specialize in this very form of communications. It is hoped that a combination of pictures and sounds can be uploaded into the spacecraft's memory in such a way as to make their significance and information content obvious to the intelligent extraterrestrial observer. In considering this challenge, SETI scientists are given the opportunity to contemplate its converse: how would *we* go about decoding and interpreting a message from *them*?

How Long Will It Last?

Nobody really knows. The spacecraft memory is similar to a flash drive storage device, very different from the gold records on the twin *Voyager* spacecraft. The extreme cold might *lengthen* the time it takes the message to degrade, or the radiation environment might *shorten* it. The most conservative estimates are a lifetime of a few decades. Other physicists and engineers believe the message might remain for centuries or even millennia.

Another unknown is the advanced technology possessed by any ETs who find the spacecraft. They might have ways of reading the faded memory we cannot yet imagine.

What Are The Chances of Detection?

Most admit that the chances of the New Horizons spacecraft ever being intercepted by intelligent extraterrestrials are slim. Pessimists say the chance of detection is zero. But, even if the spacecraft is never recovered, or even if the contents of the spacecraft's digital memory do not last long enough for

them to be examined by our cosmic companions, the project still has inestimable merit. This is a message to Earth as well as a message to ETI.

For 40 years people have been inspired by the symbolism of making the *Voyager* Record, of describing ourselves to a hypothetical cosmic audience. Carl Sagan and Frank Drake brilliantly led a small team to make that message. Now, thanks to the world wide web, we can invite millions of Earthlings to join together to speak for Earth! The act of creating the message has great educational, cultural and even spiritual value, whether the message is ever found by other beings or not.

Why Does This Even Matter?

Like all messages in a bottle, the proposed New Horizons Message presents its creators with an opportunity to grapple with fundamental questions long haunting humanity: how do we wish to present ourselves to others? In this respect, the proposed project is more a message to *us* than it is directed to *them*. It forces us to contemplate our place in the cosmos, it inspires wonder, and it enables us to ask *what if*? Any actual detection by others, no matter how unlikely, must be considered merely a fortunate and exciting bonus.

You can be a part of the adventure, by browsing to www.newhorizonsmessage.com. Together, we inhabitants of Planet Earth are being given an opportunity to define ourselves --   paraphrasing Robert Burns, "to see ourselves as *we would have others* see us."
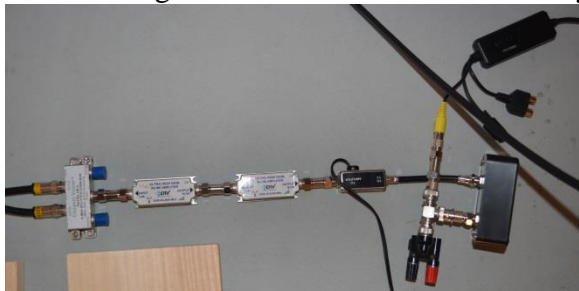
VSRT Radio Demonstration – Jon Wallace

Abstract: After working with the new radio astronomer at Wesleyan University, Meredith Hughes, building the SRT and VSRT, the presenter experimented with the VSRT himself. The VSRT was designed primarily by Alan Rogers of Haystack Observatory in Massachusetts. We visited him and tested equipment and were able to come away with some real insight into the Haystack teaching radio telescopes. The presenter hopes to demonstrate the VSRT and show some of the activities it can do. It is a wonderful way to explore interferometry in a classroom and perhaps beyond.

Much of the material presented below comes from two sites: Haystack's VSRT site (www.haystack.edu/edu/pcr/vsrt-ret/index.html) and a site at Union College maintained by Jonathan Marr (www1.union.edu/marrj/radioastro/labfiles.html).

Introduction: With more and more of radio astronomy research relying on large arrays instead of single antenna telescopes, it is necessary to learn a more about interferometry. Trying to read about aperture synthesis, the process which produces the high resolution images from interferometer arrays, can be difficult, especially with no background in Fourier analysis. Learning by doing seemed the most productive way to develop at least a basic understanding of the subject. Luckily, Alan Rogers of Haystack Observatory and Jonathan Marr of Union College (along with others), developed the Very Small Radio Telescope (VSRT) system for just this purpose. Originally developed as a way to introduce undergraduate students to the subject, it seems a perfect level for many of us as well. Having helped build one last year for Dr. Meredith Hughes of Wesleyan University, I decided to make one for myself. The construction is relatively simple, attaching off-the-shelf components together and feeding the output into the computer. Details about the equipment used in the VSRT can be found at the VSRT website listed above. Unfortunately, many of the components listed have changed in just a short time so you may have to look around to find comparable parts.

In aperture synthesis the calibrated signal from the antennas, called the "visibility" is related to the baseline length of the antennas. The visibility of an antenna pair is most sensitive to a source of wavelength / baseline (λ/B). This is like the λ/Diameter of optical astronomy's diffraction limited angular resolution. Using an array with a variety of baseline lengths provides a range of resolutions to evaluate the source under study.

The VSRT was designed to simplify studying interferometry by measuring the amplitude but not the phase of the visibility function. The labs were also designed to be all in one plane so the analysis is one-dimensional.

Lab Exercises: The lab exercises were designed to explain various aspects of aperture synthesis. The program developed by Union College and Haystack allows users to measure the output from the pair of antennas in Kelvin (for more on temperature and radio astronomy see the article on blackbody radiation in the June edition of the SARA Journal).The program requires that the data point for each measurement is recorded into its own file with the independent variable in single quotes (i.e.: Lab 1'10'). When the lab is completed, all the files are dragged into the analysis program (VSRTI_Plotter) and a graph is produced. Data can be 'saved' and imported into Excel or turned into a JPG by right clicking the graph and selecting JPG.

Lab 1 – The Primary Beam – As was mentioned, resolution is related to λ/B. Since B can change, we need to get an idea of the upper limit for resolution, which is the beam width of a single telescope. By placing the feeds one on top of the other, so they have the same horizontal location, the pattern for a single antenna can be obtained. Placing the CFL source at varying angles to the Low Noise Block Feed horns (LNBFs) (from -40º to +40º in 5º increments) and using a protractor and string, the CFL is moved around the LNBFs. Remember that each point measurement gets its own file and is plotted using the Beam Plotter part of the VSRTI_Plotter program. My results are shown at the right with the detected power as a function of CFL angular position.

Beam (pba)
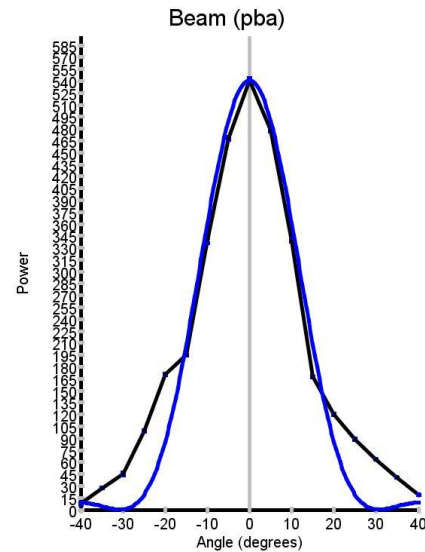
Lab 2 – One Source – As the baseline is increased, you gain more resolution but the energy from the source is spread over a larger area, so the detected power falls off. This rate of falloff of power can be used to determine the angular size of the source.

For this lab a single CFL source is placed directly in front of the two LNBFs. The baseline is then increased (I chose increments of 2 cm for a total of 40cm) and each measurement again gets its own file name. When completed, the lab is repeated with a metal sheet covering half of the CFL. Data is dragged into the Visibility Plotter part of the VSRTI_Plotter program and it is seen that the larger source power falls off faster than a smaller source.
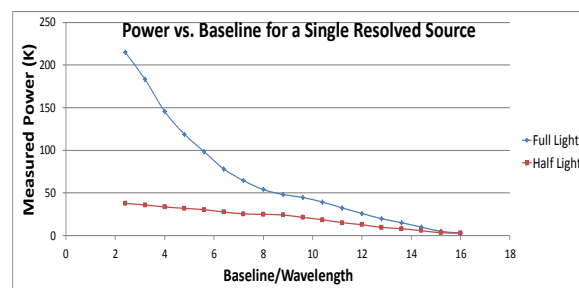
Power vs. Baseline for a Single Resolved Source

Lab 3 – Two Sources – The CFLs are placed at fixed points of separation and the baseline of the LNBFs are increased as in Lab 2. When this lab is completed it is repeated again using a different separation (I chose 30 and 40 cm). Then data is again dragged into the Visibility Plotter. It is shown that the spacing between minimum values on the graph is related inversely to the angular distance between the CFL sources.

Observed Visibility Function for Two Sources of Different Separations
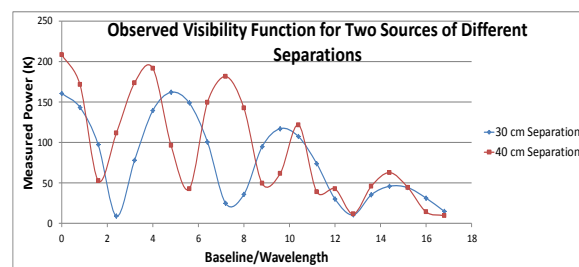
The "TIFT" Program – The "Tool for Interactive Fourier Transforms" (TIFT) is a program designed to allow students to experiment with various values of the Visibility function and see the consequences

of changes in those values. It is strictly a computer program but relates directly to the Labs done above and helps to cement the knowledge obtained in the labs above. The program is available at the Union College site: www1.union.edu/marrj/radioastro/labfiles.html. It provides a good document for understanding the program and questions (without answers!) that were developed to get students thinking about aperture   synthesis.
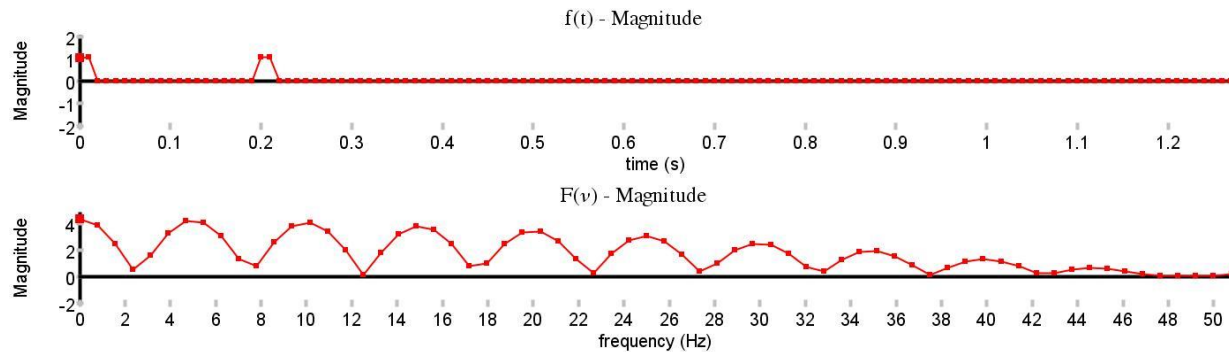
<u>Solar Exploration with the VSRT</u> – There are some activities that Haystack and Union College have developed around using the Sun as a source. I have not had time (due to extremely poor weather!) to try these, but hope to be able to report on them by the time of the SARA Conference in July. The link for these activities can be found at: www.haystack.edu/edu/undergrad/VSRT/VSRT_Memos/030.pdf.

It is hoped that participants will gain a better understanding of aperture synthesis and the use of this equipment to continue their exploration of this important topic.

12.2 – 12.7 GHZ RADIO TELESCOPE

By Curt Kinghorn

Introduction

Although man has been looking at the visible light of stars for as long as there has been man, looking at the stars with "radio eyes" occurred relatively recently. Finally, in the 1860s, James Clerk Maxwell[i] developed a set of equations[ii] showing in part that electromagnetic radiation is associated with electricity and magnetism and could exist at any wavelength, not just those of visible light.. This led several experimenters including Nikola Tesla[iii] to try to detect radio emission from the Sun. But those attempts were unsuccessful due to the technical limitations of their instruments.

Karl Jansky was the first person to "discover" radio waves from space when trying, in 1932, to figure out where some unaccounted-for-noise in long distance radio communications was coming from. Although Jansky had made a phenomenal discovery that was widely publicized[iv] and although Jansky himself wanted to conduct further research into this new discovery, Bell Labs, for whom Jansky worked, was not interested and assigned Jansky to other projects. Although Bell Labs was not interested in doing further research, it is surprising that despite Jansky's discovery being made during the Great Depression when money for research was limited[v], this discovery did not create a furor in the scientific community. It took an amateur, Grote Reber to continue researching these radio waves from space. Reber contributions include doing the first systematic survey of radio waves from space with a very large radio telescope built in his suburban Chicago backyard![vi] Eventually, in 1942 (ten years after Jansky's discovery!) radio waves from the sun (the brightest radio object in the sky!) were discovered.[vii]

FIGURE 1

(Image courtesy of NRAO/AUI)

Eventually, technology developed to the point where information is now beamed from the earth to satellites circling the earth in geosynchronous orbit. These satellites rebroadcast the uploaded information back to earth where it is received. In particular, radio and television communications are being broadcast from these satellites to the earth at frequencies in the so-called Ku band (12 – 18 GHz) where they are received, among other devices, by ubiquitous Ku band satellite dishes. Discarded Ku band satellite dishes have been converted into an "Itty-Bitty"viii (Figure 1), a fun device that is very useful in demonstrating the fundamental principles of radio astronomy. But, the Itty-Bitty lacks the discrimination and amplification power to be a serious radio telescope.

Why a 12.2 – 12.7 GHz Radio Telescope?

When I first decided to seriously try amateur radio astronomy, I struggled to figure out what projects I could do. While attending the SARA Western Conference in 2010, Shad Nygren gave a brief presentation on the concept of building a 611 MHz total power radio telescope using well-developed UHF technology instead of having to design and build many of the components himself. In particular, he presented the idea of using RadioShack's U8000 UHF antenna as the radio telescope's antenna. UHF channel 37 is allocated the frequency block from 608 to 611 MHz and is right in the middle of the entire UHF spectrum.ix Further, the FCC has reserved channel 37 for radio astronomy. As a result, there should be no stations operating within these frequencies.
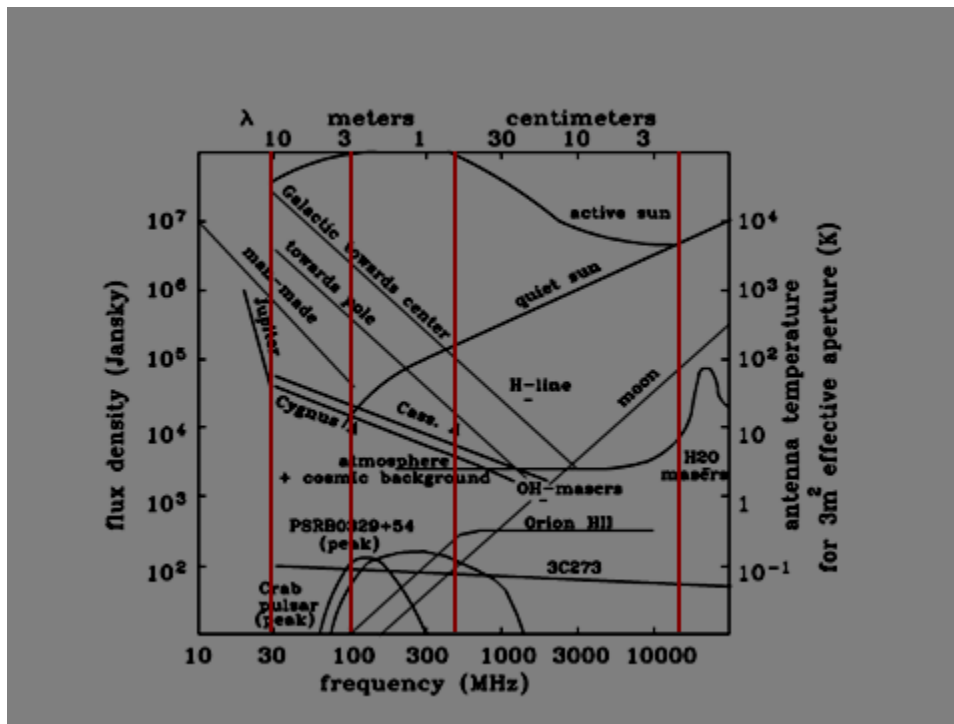
FIGURE 2

Shad's idea appealed to me and I began researching the possibility of building such a telescope. First, I had to determine what, from a radio astronomy perspective, is going on at about 611 MHz. As shown in the Figure 2, many radio sources including the sun, Sagittarius A (our Milky-Way galaxy's super-massive black hole), super nova remnants Cassiopeia A and Taurus A and Cygnus A (two colliding galaxies about 700 million light years away!) all emit fairly strongly at 611 MHz (see third red line from the left). As a result, there was a good chance I would be able to see interesting things at 611 MHz.

Investigating further, I quickly discovered that UHF antennas have to pick up stations in the entire UHF range. Because channel 37 lies right in the middle of the UHF range, the antenna is optimized for the channel 37 frequencies. In addition, the UHF preamps that are attached to the UHF antennas to amplify signals picked up by the UHF antenna are also optimized for channel 37. So, I decided to put together a 611 MHz radio telescope with the design constraint that, wherever possible, I would "piggyback" off of the already existing UHF technology. Eventually, I put together a system using a RadioShack U8000 UHF antenna, Channel Master 7700 preamp, ICOM R7000 receiver and a standard PC running Radio Sky-Pipe II strip recording software. Figure 3 shows a parts list and their associated costs for this telescope. This telescope works well and has at least sufficient sensitivity to see Cygnus A.

611 MHz Telescope Costs

	Already Have Computer	Need to Acquire Computer
RadioShack U8000 Stacked Array UHF Antenna	$76 from RadioShack.com	$76 from RadioShack.com
Channel Master Model CM-777 PreAmp	$63 on Amazon	$63 on Amazon
Cables – RG6 Coax Cable – 100'	$82 from DigiKey	$82 from DigiKey
ICOM R7000 Receiver	$325 on Ebay	$325 on Ebay
Computer	N/A	$300
Radio-Sky Pipe II Software Strip Recorder	$50 from RadioSky.com	$50 from RadioSky.com
Miscellaneous Parts	$50	$50
Total	**$646**	**$946**

FIGURE 3

Because of the success I had with the 611 MHz radio telescope by piggybacking off of already well-developed UHF communications technology, I decided to consider what other well-developed communications technology I could piggyback off of. I didn't have to look far, literally, to see the ubiquitous Ku band satellite dishes. It occurred to me that I might be able to piggyback off of this technology as well. I investigated making an Itty-Bitty. But, it became clear that the Itty-Bitty's signal detector, which is typically used to aim the Itty-Bitty's dish to pick up commercial satellites, was not powerful enough to pick up weak radio signals generated by naturally occurring phenomena in space. So, I decided to look at what it would take to "convert" an Itty-Bitty to a serious radio telescope, essentially putting the Itty-Bitty on steroids!

The Ku band technically extends from 12 – 18 GHz. But, the frequencies used for satellite communications are 12.2 to 12.7 GHz. Looking again at Figure 2, many of the interesting radio objects that are so bright from about 30 MHz up through about 1000 MHz, essentially the VHF and UHF bands, do not strongly emit at frequencies higher than about 1000 MHz. In particular, such interesting radio objects as Sagittarius A, Cassiopeia A and Cygnus A essentially drop away in the Ku band (red line farthest to the right). But, the sun, both quiet and disturbed, strongly emits at this frequency. So, in addition to seeing whether I could design and build a Ku band radio telescope, piggybacking off of the commercial satellite technology at these frequencies, I also wanted to see what radio objects I could see including at least the sun. (Remember that Nikola Tesla among others had been unable to detect radio emissions from the sun with the technology of their day.) Also, the Milky Way itself has fairly strong emissions at this frequency range and I thought I might be able to see this as well.

Total Power Radio Telescope

To understand some of the issues specific to a Ku band total power radio telescope, it is worthwhile to understand what a total power telescope is. A total power telescope measures the power of a radio signal impinging on the telescope within a frequency band. In the case of my 611 MHz telescope, ideally I would like to collect and measure the power of the radio signal impinging on its antenna between 608 and 614 MHz. With respect to the Ku band radio telescope, ideally I would like to collect and measure the power of the radio signal that impinges on its antenna between 12.2 and 12.7 GHz. Put another way, a large bandwidth is essentially a large photon bucket whereas a narrower bandwidth is a smaller photon bucket. Since radio astronomy signals are inherently weak, it is desirable to use as big of a "bucket" as possible to capture the radio signal. I say "ideally" because the practical limitations of my choices of "off-the-shelf" components, particularly the receiver, limit the bandwidth that I actually am able to capture (about 175 KHz!) from these desired bandwidths (6 MHz and 500 MHz, respectively).

Note that a total power radio telescope attempts to measure only the signal strength of the signal impinging on it. A total power radio telescope <u>does not</u> attempt to de-modulate any underlying signal that might be superimposed on, for example, a carrier frequency such as is done with radio and TV communications signals. Unless the signal coming from outer space is coming from extraterrestrial intelligence, and thus falls within the purview of SETI, the radio signals coming from outer space are the result of naturally occurring phenomenon and thus carry no underlying or modulated message.

An analogy for a total power radio telescope is the so-called "S meter" on virtually every ham radio receiver. The S meter indicates the strength of the signal that the receiver is currently receiving. When the receiver is receiving a strong signal, the S meter indicates a higher reading. Conversely, when the receiver is receiving a weak signal, the S meter indicates a low reading. If you were to listen to a typical radio signal coming from space at a particular frequency as received by a ham radio receiver and converted into an audio signal, all that you would hear is a hiss. A strong signal produces a loud hiss whereas a weak signal produces a soft hiss.
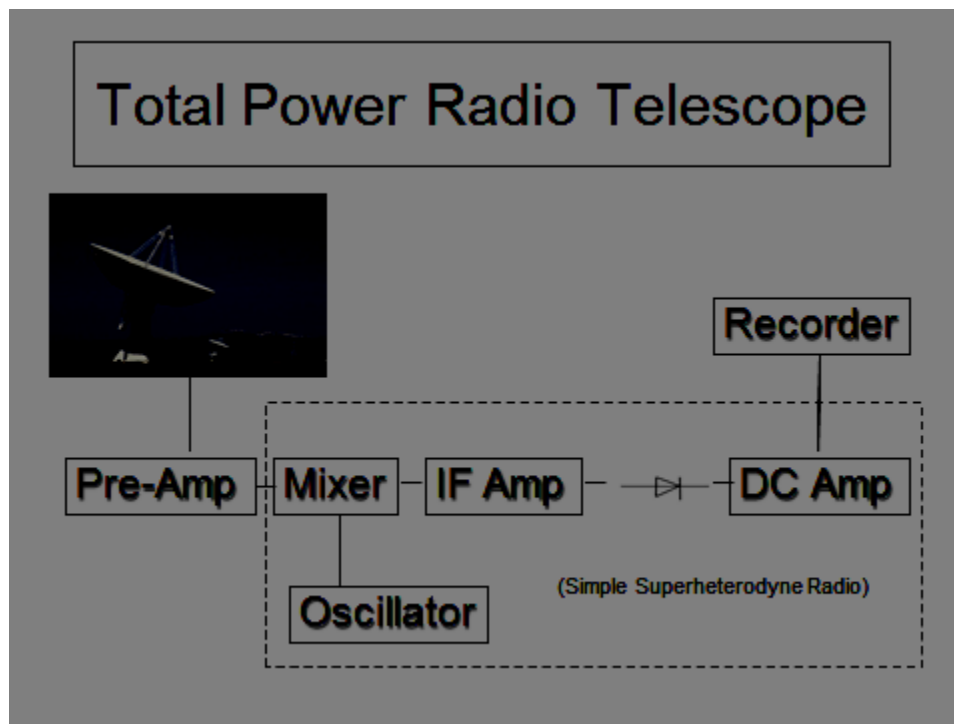
FIGURE 4

A typical total power radio telescope is shown schematically in Figure 4. The total power telescope includes an antenna, a preamp in close association with the antenna, a receiver, cabling connecting the antenna and preamp to the receiver and some sort of a recording device such as a strip recorder.

The antenna needs to be of a type capable of picking up signals of the frequency of interest. There are many possible types of antennas, including but not limited to, dipole, Yagi, helical, stacked array and parabolic dish. Each of these antennas has desirable and undesirable characteristics which characteristics depend dramatically on the frequency for which they are used. For example, as I will show shortly, parabolic dishes work very well at frequencies of about 1 GHz and above but work poorly at VHF and UHF frequencies. Conversely, Yagi's work well at VHF and UHF frequencies but typically don't work as well as, for example, parabolic dish antennas, at frequencies above these.

Parabolic Dish Issues

As mentioned, parabolic dishes work well at frequencies above about 1 GHz. The reason parabolic dishes do not work well at VHF and UHF frequencies is that the amount of gain a parabolic dish produces is inversely proportional to the wavelength of the signal it is trying to pick. Gain is a dimensionless parameter that is the ratio of the power received by the antenna from a source along its beam axis compared to a hypothetical isotropic antenna. The formula for the gain of a parabolic dish is given according to the formula:

71

$$\text{Gain}_{dBi} = 10\log_{10}(4\pi A/\lambda^2)\varepsilon_A = 10\log_{10}(\pi^2 d^2/\lambda^2)\varepsilon_A x$$

Where:

A is the area of the antenna.

d is the diameter of a circular parabolic reflector.

λ is the wavelength of radio wave (~ 0.5 m for 611 MHz and ~ 2.6 cm for 12.2 GHz).

ε_A is a dimensionless parameter between 0 and 1 called the *aperture efficiency*. The aperture efficiency of typical parabolic antennas is about 0.55 – 0.70.

0.46m Parabolic Dish Antenna Comparison at 100MHz, 408 MHz, 611 MHz, 1.420, 12.2 GHz and 42 GHz*

	100 MHz	408 MHz	611 MHz	1.420 GHz	12.2 GHz	42 GHz
Wavelength	3.0 m	.74 m	.5 m	.21 m	.026 m	.007 m (.7mm)
Beamwidth (Half Power)	N/A	113°	76°	32°	3.9°	1.1°
Gain	-8.9 dBi	3.2 dBi	6.6 dBi	14.2 dBi	32.3 dBi	43.7 dBi

*Aperture Efficiency (ε_A) = 0.55
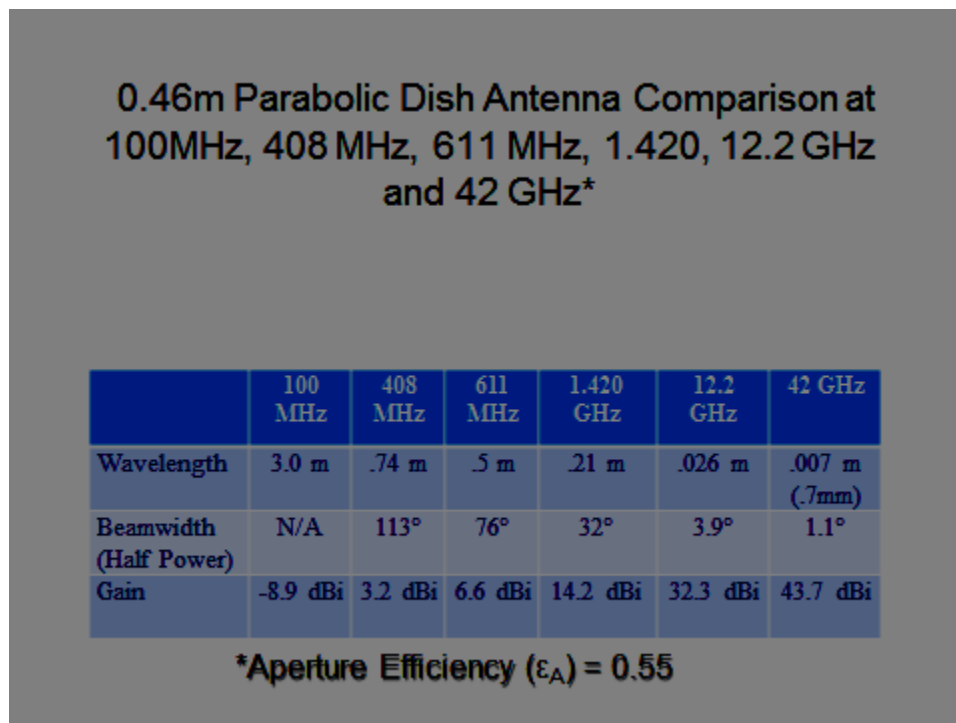
FIGURE 5

A as shown in Figure 5, at relatively low frequencies, for example 100 MHz, a small parabolic dish of the size of a typical Ku band antenna (0.46 m) produces negligible gain. Moving up in frequency to 408 MHz and 611 MHz (good radio astronomy research frequencies) produces only modest gains of 3.2 dBi and 6.6 dBi, respectively. Continuing up in frequency to the hydrogen alpha line at 1420 MHz, the 0.46 dish gives a modest 14.2 dBi gain. But, in moving to 12.2 GHz, we get a fairly large gain of 32.3 dBi which is pretty good considering how small the dish is! Moving even further up in frequency to 42 GHz yields 43.7 dBi of gain.

Parabolic Dish Antenna Comparison at 12.2 GHz

	Arecibo (305 m)	VLA (25 m)	2 m (78 in)	.46 m (18 in)
Beamwidth (Half Power)	0.006°	0.07°	0.9°	3.9°
Gain	88.7 dBi	67.0 dBi	45.1 dBi	32.3 dBi

*Aperture Efficiency (ε_A) = 0.55

FIGURE 6

Figure 6 shows what happens at 12.2 GHz as you move up in parabolic dish size. As noted above, a .46 m parabolic dish produces a gain of about 32 dBi. Increasing the size of the dish to 2 m increases the gain to about 45 dBi. Each 25 m dish of the Very Large Array produces about 67 dBi while the enormous 305 m dish at Arecibo produces a hefty 88.7 dBi!

Although the gain of parabolic dish antennas rises rapidly with frequency, the beam width of a parabolic dish decreases rapidly with frequency. The ½ power beam width of a parabolic dish antenna can be approximated by the formula:

$$\text{Beam Width}_{degrees} = 70\, \lambda/d$$

Where:

d is the diameter of a circular parabolic reflector.

λ is the wavelength of radio wave (~ 0.5 m for 611 MHz and ~ 2.6 cm for 12.2 GHz).

Antenna Comparisons at 408 and 600 MHz and 12.2 GHz

	408 MHz	600 MHz	12.2 GHz	600 MHz	408 MHz	600 MHz	408 MHz	600 MHz
	0.46 m Parabolic Dish	0.46 m Parabolic Dish	0.46 m Parabolic Dish	Radio Shack U8000 Stacked Array	Helical Antenna −10 Turns	Helical Antenna −10 Turns	Yagi−5 Elements	Yagi−5 Elements
Width/ Length	0.46 m (18.1 in)	0.46 m (18.1 in)	0.46 m (18.1 in)	1.0 m (40.5 in)	1.84 m (72.44 in)	1.25 m (49.21 in)	.74 m (29.1 in)	.52 m (20.5 in)
Depth/ Diameter				.91 m (36 in)	23.4 cm (9.21 in)	15.9 cm (6.26 in)	.38 m (15.0 in)	.26 m (10.2 in)
Beamwidth (Half Power)	113°	76°	3.9°	~30°	60.0°	32.9°	~55°	~55°
Gain	3.2 dBi	6.6 dBi	32.3 dBi	12.0 dBi	9.55 dBi	14.8 dBi	9.2 dB	9.3 dB

*Aperture Efficiency (ε_A) = 0.55

FIGURE 7

A comparison of the beam width of several antenna types at various frequencies is given in the chart of Figure 7. Depending on the type of project you are doing, you may want to have a wide or narrow beam width. The advantage of having a wide beam width is that you are gathering signal from a larger portion of the sky. As a result, the amount of signal you receive should be relatively larger than if you were looking at the sky with a narrower beam width. However, the resolution you are able to obtain using a larger beam width (i.e., the ability to discern that two point sources are discrete rather than a single object) is less than you would get if you were to use a narrower beam width. Conversely, the amount of signal you receive with a narrow beam width antenna is less than you would get with a larger beam width antenna. However, your resolution should be better. At frequencies above about a gigahertz, when using a parabolic dish antenna, the high gain that the parabolic dish itself produces in large part counteracts the fact that you're looking at a smaller portion of the sky. So, the signal received by a parabolic dish antenna at these frequencies should be "relatively" strong.

For an ideal parabolic antenna, the ½ power beam width is also the resolution. As a result, the equation for the resolution of a parabolic dish is exactly the same as the equation for calculating the ½ power beam width:

$$R_{degrees} = \text{Beam Width}_{degrees} = 70\,\lambda/D$$

Where:

       d= diameter of the dish

       λ= wavelength of radiation being observed.

For diameter "d" of 0.46 m and λ of 2.46 cm (corresponding to a frequency of 12.2 GHz), the resolution "R" is 3.9° which is about equal to the beam width of the antenna!

"Noise" from Commercial Satellites

Since a 12.2-12.7 GHz telescope is receiving signals in the frequency range that also correspond to those used by Ku band communications satellites, it is possible to inadvertently pick up the relatively strong satellite signals. To radio astronomers, such man-made signals are "noise" and to be avoided.

Often when doing radio astronomy, it is desirable to take so-called "drift scans" to collect data. Most often, these drift scans occur by aiming the antenna along the north/south axis, moving the antenna up or down to the desired elevation and then taking data as the earth rotates. The earth's rotation causes the antenna to scan a band across the sky as various objects "drift" past the antenna (hence the name "drift scan").

If a Ku band radio telescope were aimed directly south, would it see any commercial satellites? Commercial satellites are placed at geosynchronous orbit so that they stay in a fixed position relative to the earth as they orbit the earth. To stay in geosynchronous orbit, the position they must occupy is above the earth's equator. Consequently, they are always in a fixed position with respect to the earth. There are currently over 300 such satellites in geosynchronous orbit spaced a couple of degrees apart.

To determine what satellites are directly or nearly directly south of your location (and thus those that you might see if you aimed your telescope directly south), you have to determine what right-ascension "south" is from your location. This is simply done by determining your longitude using a GPS system or an on-line mapping program such as Google Earth. For me in San Diego, "south" is about 117° west. Further, for me, these geosynchronous satellites are about 51° of elevation. Figure 8 below sets out 11 satellites that are located within 4° east and west of "south" for my location and at elevations around 51°.xi

OFFICIAL SPACECRAFT DESIGNATION	COMMON NAME	RIGHT ASCENSION
03034A	GALAXY 23	-121.0
13058A	SIRIUS FM-6	-120.4
04016A	DIRECTV 7S	-119.0
10010A	ECHOSTAR 14	-118.9
02006A	ECHOSTAR 7	-118.8
07009A	ANIK F3	-118.7
13012A	SATMEX 8	-116.8
06049A	XM-4 (BLUES)	-116.8
01018A	XM-1 (ROLL)	-115.2
01012A	XM-2 (ROCK)	-115.2
11059A	VIASAT-1	-115.0
98070A	SATMEX 5	-114.9
12075B	MEXSAT 3	-114.8
06020A	SATMEX 6	-113.0

FIGURE 8

One interesting object to observe with the Ku band radio telescope is the sun. For two annual periods surrounding the vernal and autumnal equinoxes, the sun's elevation in the sky when it is directly south will be approximately the same as the celestial equator. As already mentioned, this is approximately the same location as many of the geosynchronous satellites. Because the sun and satellites are approximately in the same location in the sky at the same time at these times, from the perspective of an observer on the earth, the sun and one or more satellites will appear to be virtually on top of each other. This results in a condition that is called by a variety of names such as sun or solar fade, sun interference, solar transit or solar outage. This condition is shown in Figure 9 xii. From the perspective of trying to receive signals from these geosynchronous satellites, when this condition occurs, the sun overwhelms the satellite signal. Consequently, satellite reception is poor until the sun moves away from the satellite of interest. From the perspective of trying to observe the sun with the Ku band radio telescope, as is discussed later in this paper, the satellites produce "noise" that can be and is detected.
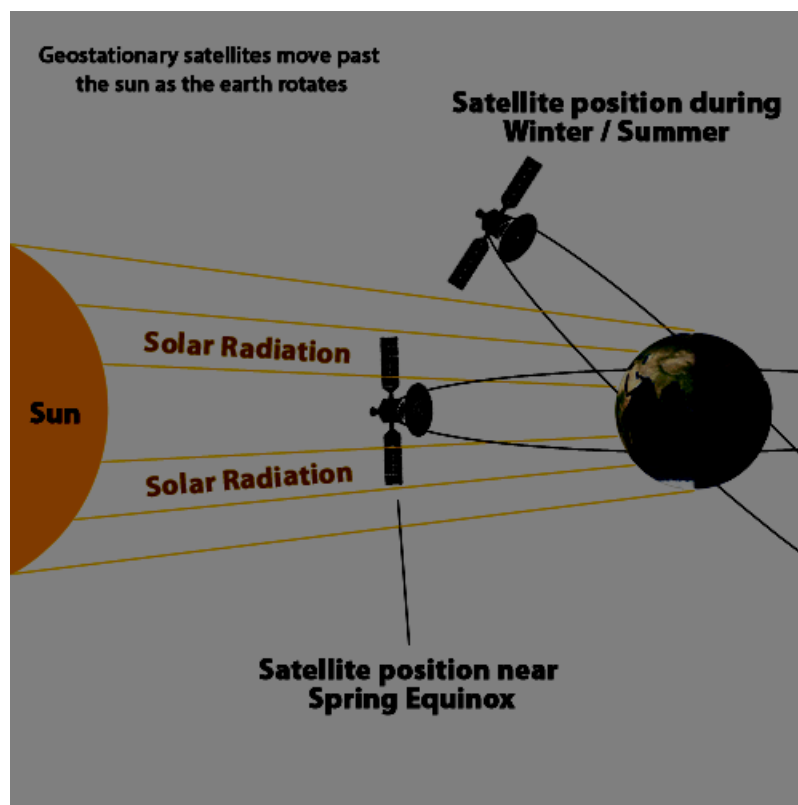
FIGURE 9

As the days pass moving away from the vernal equinox, at noon (i.e., when the sun is directly south) the sun will be higher and higher in the sky, moving away from the celestial equator and the geosynchronous satellites positioned there. This trend will continue until Summer Solstice when at noon each day, the sun will be located lower and lower until the autumnal equinox when the sun will again be located on the celestial equator. Thereafter, at noon each day the sun will be located lower and lower until it reaches its lowest

point at the Winter Solstice. After the Winter Solstice, the sun moves upward each day until the vernal equinox is reached and the cycle repeats. Of course, for the several days before and after the vernal and autumnal equinoxes, this problem of the sun and satellites overlapping each other, and consequently detecting "noise" from the satellites, will be manifest. In view of the foregoing, the problem of satellites interfering with the sun changes throughout the year depending on where the sun is when you are trying to record it.

Ku Band Radio Telescope

The Ku Band Radio Telescope of this project is a total power radio telescope. As a result, it has the same components of a total power telescope described above, namely: antenna, a receiver, cabling connecting the antenna to the receiver and some sort of a recording device such as a strip recorder. All of these will be discussed below.

Antenna

I have two different antennae that I have used in the Ku Band Radio Telescope: a .46 m dish from Dish Network and a slightly larger dish from Direct TV (Figure 10). These dishes were either left behind by previous inhabitants as we moved into our house or were collected from friends. As I discovered, besides these sources, the companies that install satellite systems often have discarded dishes that they will gladly give to you.

FIGURE 10

Mount

For my Ku band radio telescope, I used the mount originally produced by Direct TV to attach the corresponding satellite dish to the house where it was installed. One nice feature of the Direct TV mounting system is that it has several alignment bolts that can be turned to more precisely aim the antenna, in both right ascension and declination, than can be obtained by simply "eyeballing" the aim. I removed the original metal mounting bar from the mount. This mounting bar had about a 30° bend in it to facilitate the mounting of the dish to the house and to make it easier for the installers to aim the dish at the desired commercial satellite of interest. I replaced the metal mounting bar with a piece of PVC pipe that I mounted to an optical telescope tripod that I bought off of Craigslist for $20.

This particular tripod had a 5 inch "well" that was originally intended to hold an equatorial telescope mount. From Home Depot, I bought a flange for mounting 2" plumbing pipe. The flange was slightly larger in diameter than 5 inches. So, using a grinder, I removed sufficient diameter from around the outer edge of flange to bring it to the desired dimension to fit within the bottom of the well of the telescope mount. The flange has four mounting holes. Once the flange was set in place in the bottom of the well, I drilled holes through the mounting holes and through the bottom of the well to allow me to place threaded bolts to which nuts were attached to secure the flange and well together. Because the mounting being used to attach the aiming mechanism was intended to house a tube having outside diameter of 2 inches, and because the 2 inch flange actually mounts a threaded pipe having an outside diameter of about 2.4", I had to get an adapter from Home Depot that converted a 2" metal pipe with its 2.4 inch outer diameter to a PVC pipe with a 2" outer diameter. The resulting mechanism is shown in Figure 11.

FIGURE 11

Pickup and LNB

Signals in the Ku band are microwave signals. Although microwaves are electromagnetic signals, they behave differently from radio waves. Consequently, microwaves require their own "special" ways of detecting and moving the microwave signals around. The technologies needed to do these things are beyond the skills of most amateur radio astronomers. However, because this Ku band radio telescope piggybacks off of the work done by the satellite communications industry, this problem has largely been solved for us.

The way this problem has been solved is by the introduction of a low noise block (LNB) into the system. The purpose of a LNB is twofold: (a) amplify the signal produced by the antenna and (b) down convert the microwave signal to a frequency where traditional UHF signal transportation schemes can be used. The satellite communications industry has produced very low noise and high gain LNBs that even highly skilled amateur radio astronomers would have difficulty replicating.

With respect to down converting the microwave signals to a UHF frequency, the LNB uses super heterodyning principles. In particular, a local oscillator (LO) frequency is mixed with the received microwave signal to produce a signal at frequencies representing the difference and addition frequencies of the LO and signal of interest. In the case of Ku band for commercial satellite communications, a local oscillator frequency of 11.250 GHz is used. Since one purpose of the LNB is to down convert the received signal, the signal produced by adding the LO frequency and the frequency of the received signal would produce a higher frequency signal that would be even more difficult to work with. Consequently, for this practical reason, the additive frequencies are filtered leaving only the difference frequencies. In a commercial satellite Ku band LNB, because the band stretches from 12.2 to 12.7 GHz, the difference frequency ranges from 950 to 1450 MHz (12.2 GHz − 11.250 GHz = 950 MHz, 12.7 GHz − 11.250 GHz = 1450 MHz). So, the LNB takes the received signal of 12.2 - 12.7 GHz and down converts it to the much more manageable 950 to 1450 MHz.

Because the LNB is an active electronic system, it needs to be powered. In a satellite Ku band LNB, the power is sent from the system's receiver through the coax cable that connects the receiver to the LNB. However, in a Ku band radio telescope, since the receiver is a typical amateur radio receiver, this ability to send the power necessary to operate the LNB from the receiver does not exist. But, power can still be sent through the coax cable connecting the LNB to the receiver via an in-line power supply. In my case, I use the Channel Master Model 0747 Antenna Amplifier Power Supply shown in Figure 12. This power supply sends 18 volts DC down the coax cable to power the LNB.

FIGURE 12

The down converted signal is sent from the LNB to the receiver. Typically this is done using coaxial cable. But, the dissipation of a signal passing through coax cable is dependent on the frequency of the signal. At the 950 to 1450 MHz range, low cost coaxial cable such as RG 59 will not work well because of the rapid dissipation of signals in the RG 59 coax cable at this frequency. At a minimum, better quality coax cable such as RG 6 must be used. Although higher-quality coax cable such as RG 6 is used, it is good practice to keep your lines as short as possible to minimize the amount of signal loss due to just passing the signal through long, unnecessary lengths of cable.

Receiver

The receiver used for the Ku band radio telescope is an ICOM R7000 receiver (Figure 13) although any good quality receiver capable of receiving signals in the range of 950 – 1450 MHz will work. The ICOM R7000 receiver has gained a reputation for being a workhorse receiver for many radio astronomy projects. The R7000 receiver is a three stage super heterodyning receiver having a gain of 80 to 90 DB and is able to tune frequencies from 25 – 999 and 1025-2000 MHz. Note that there is a gap between 1000 and 1025 MHz where the receiver cannot receive. As explained above, this means that the receiver cannot tune a signal that corresponds to the band of 12.250 – 12.500 GHz.

FIGURE 13

The amplifiers in the receiver themselves add noise to the signal!xiii This can be seen in Figure 14. On the plotted signal where I have labeled "System Noise," I disconnected the coax cable connecting the receiver to the LNB. Although it appears on the chart recording that the signal level is zero, a look at the vertical scale indicates that there is still quite a bit of a noise signal (on this arbitrary scale, the system noise has a level of

above 8900 while the sun itself has a value of 16000).   This noise level depends on the gain setting of the receiver. So, as the gain is turned up, this noise signal level goes up. Consequently, it is desirable to have amplifiers in the receiver that produce as little noise as possible.
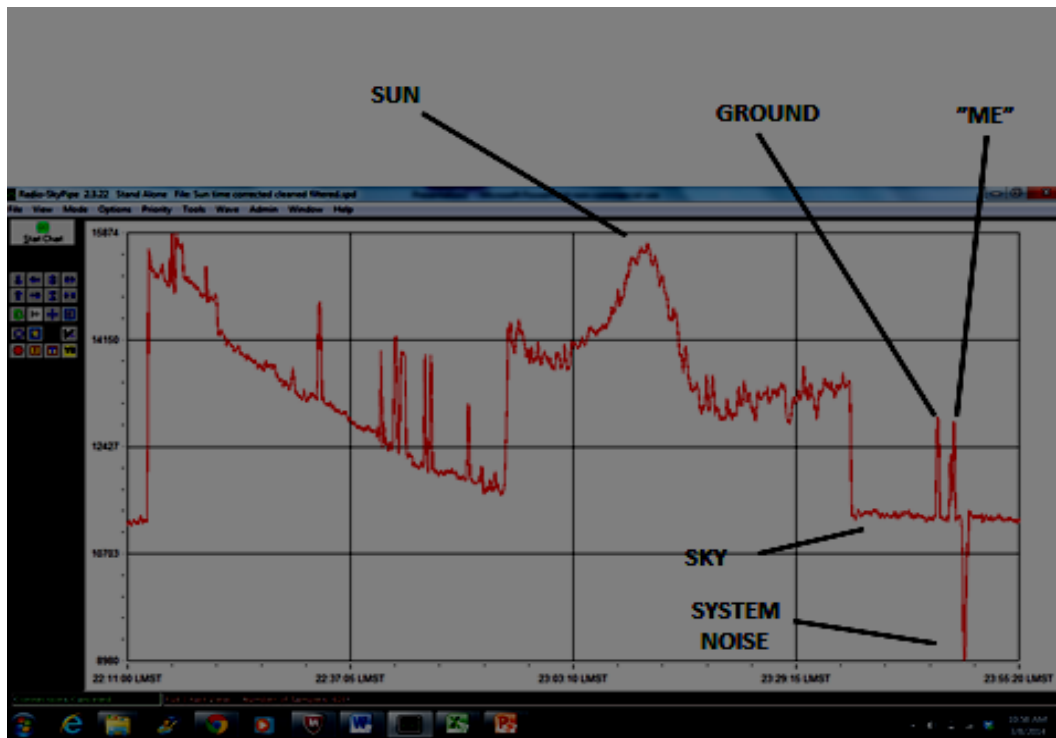

FIGURE 14

Further, typical ham radio receivers have Automatic Gain Control (AGC) circuits.   These AGC circuits automatically boost low amplitude signals and automatically depress high amplitude signals. For qualitative observations (e.g., is there a signal? does it increase when it sees a radio emitter like the sun?), the function of the AGC probably does not significantly affect the results. But, for quantitative observations (e.g., what is the signal strength of Cassiopeia A compared to the sun? what is the signal strength of clear sky?), the operation of the AGC system distorts the actual signal strength. Consequently, for quantitative observations, it is desirable to disable the AGC circuitry. Because the R7000 receiver has such a long history in radio astronomy, exactly how to disable the ACG circuitry without affecting the other functions of the receiver have been worked out in detail.xiv Essentially, a line to a resister in the AGC circuit is cut and a jumper with a toggle switch is connected (at the arrow in Figure 15) to the two cut ends. When the toggle switch is in one position, the line passing through the resistor is disabled so that the AGC circuit is disabled. With the toggle switch in the opposite position, the line passing through the resistor is enabled and the AGC circuit operates as normal.

FIGURE 15

Another issue with the ICOM R7000 receiver is that it has a relatively narrow maximum bandwidth of 175 kHz. As mentioned above, ideally a receiver should have a bandwidth large enough to accommodate the entire frequency band of interest. In the case of a Ku band total power radio telescope, ideally the receiver should have an input bandwidth of the entire 950 – 1450 MHz range of 500 MHz. Obviously, 175 kHz is a lot smaller than 500 MHz. However, both the 611 MHz and Ku band radio telescope seem to work adequately even with this relatively narrow bandwidth.

One small advantage to not having a large bandwidth is that you avoid the radio interference that can come from having a large bandwidth that picks up stray electromagnetic signals along with the radio astronomy signal of interest. Because the bandwidth of the ICOM R7000 is so narrow, if you find that you are picking up spurious radiation at a particular frequency, you can tune to another frequency where the spurious radiation is not present.

Impedance Matching "Problem"

The TV components of the Ku band radio telescope (Pickup/LNB, coax cables) have impedances of 75 ohms. The ham radio components (ICOM R7000 receiver) has an impedance of 50 ohms. So, when the coax cable

that connects the receiver to the coax is connected, there is a slight impedance mismatch. Optimally, this mismatch can be dealt with by using a balum. But, Whit Reeve, a venerable SARA radio astronomer and electrical engineer has does measurements of the amount of signal degradation resulting from this impedance mismatch and has found it to be negligible. So, for practical purposes this impedance mismatch can be neglected.

Strip Recording Software

The ICOM R7000 receiver produces an output signal representative of the signal strength received from space (along with any other interference that it picks up or produces itself). It is highly desirable to record this signal over time as a function of signal strength versus time. A particularly good electronic strip recording software is produced by SARA member Bill Sky and is titled Radio-SkyPipe software.xv Besides being very good strip recording software generally, Radio-SkyPipe software is specially adapted to allow the recording of radio signals with time stamps of the user's local right ascension. This makes it very handy for analyzing data.

For example, Sagittarius A has a right ascension of $17^h\ 45^m\ 40.0409^s$ and a declination of $-29°\ 0'\ 28.118''$.   If the radio antenna were aimed along the north-south axis, then raised to a declination of $-29°\ 0'\ 28.118''$ and the recording started, if a large increase in the signal were found at the right ascension of about $17^h\ 45^m$, the observer can be pretty assured that the signal being received is coming from Sagittarius A and not from some other, likely local, source. Radio-SkyPipe software is available at www.radiosky.com for $49. The Radio-SkyPipe software also has built-in filtering and data management features. Another nice feature of the RadioSkyPipe software is that it can produce an output in comma limited format that can be imported into an Excel spreadsheet where it can be manipulated, including applying filtering tools available in Excel, and used to produce Excel charts and graphs.

COSTS
Ku Band Total Power Telescope

	Already Have Computer	Need to Acquire Computer
Ku Band Antenna and LNB	$0	$0
Cables – RG6 Coax Cable – 100'	$82 from DigiKey	$82 from DigiKey
Channel Master 0747 Power Supply	$20 from channelmasterstore.com	$20 from channelmasterstore.com
ICOM R7000 Receiver	$325 on Ebay	$325 on Ebay
Computer	N/A	$300
Radio-Sky Pipe II Software Strip Recorder	$50 from RadioSky.com	$50 from RadioSky.com
Miscellaneous Parts	$50	$50
Total	**$477**	**$777**

FIGURE 16

Figure 16 shows a parts list and their associated costs for the Ku Band Total Power Telescope of this description.

Setting Up the Ku Band Radio Telescope - Finding the Sun

As mentioned above, an interesting target for the Ku band radio telescope, particularly at the beginning to get some experience with the radio telescope, is the sun. But, because of the narrow beam width of the antenna as described above, it is important to know where the sun is (or at least is going to be) in order to aim the telescope properly to see it. There are several websites that calculate the sun's coordinates on any day and time and for any location.xvi
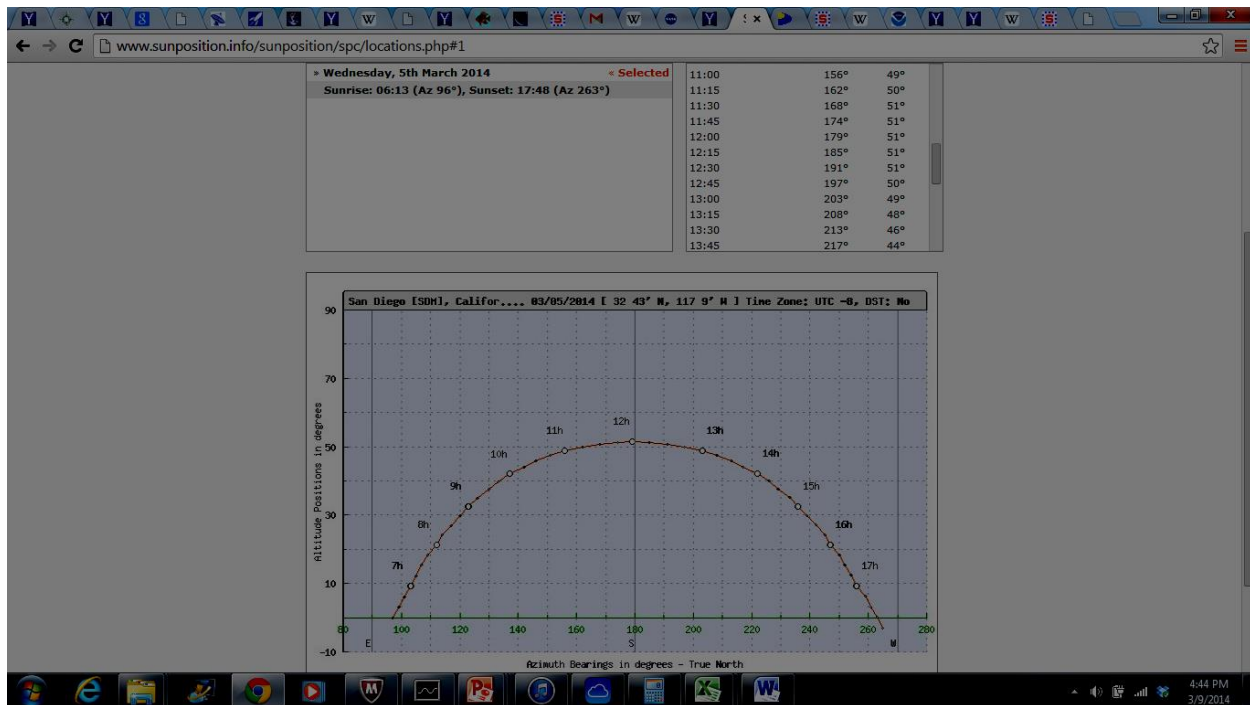
Figure 17

Figure 17 is a chart for my location for March 5, 2014. As can be seen, the sun was at 180° south from me (true south, not magnetic south) at a little after noon at an altitude (elevation) of 51°. Therefore, if a little before noon on March 5, 2014, I aim my telescope true south at an elevation of 51° and start taking data, as the earth rotates, the sun will pass through the beam of my antenna and I should be able to "see" it.

Setting Up the Ku Band Radio Telescope - Aiming the Antenna

As described above, having a narrow beam width produces a practical problem, namely, the importance of being able to accurately aim the antenna. For example, the beam width of the RadioShack U8000 stacked array antenna at 611 MHz is about 30°. So, if I'm looking at a point source such as Cassiopeia A, my aim at Cassiopeia A needs to only be "in the ballpark" of Cassiopeia A since the beam width is so large compared to the very tiny point source.

Typically, a radio telescope antenna is aimed at the sky and uses the rotation of the earth to trace the path through the heavens of the signal it receives from space. For practical purposes, it is best to aim the antenna along the north-south axis so that the radio telescope is aligned with sidereal time. Once the antenna is aligned along this north-south axis, it is moved up or down in elevation.

As is well understood in the astronomy community, a virtual celestial map is superimposed on the heavens. The virtual map has labels of the longitude called 'right ascension" and labels for the latitude called 'declination." Aligning the antenna along the north-south axis aligns the antenna with sidereal time so that the right ascension that the telescope is aligned with can be determined simply by looking at the local sidereal time.

Converting elevation to declination involves understanding what your latitude is. If you are at the North Pole, the latitude is 90° north and the North Star is directly overhead. Consequently, directly overhead corresponds to 90° of declination. In San Diego where I live, my latitude is about 33° (precisely 33.2298 with a longitude of 117.2776). Consequently, the North Star is about 33° above the North horizon. Using simple geometry, directly overhead is 57° of declination. So, when aiming the antenna along the north-south axis, for objects above about 57° of declination, it is best to aim the antenna north and then move the antenna to the desired declination in a northerly direction. Conversely, when aiming the antenna at objects having declinations of less than about 57°, it is best to aim the antenna south and then move the antenna to the desired elevation in the southerly direction.

However, as can be seen in Figure 6, the beam width of a typical 0.46m (18") Ku band antenna, such as you would have attached to your house, at 12.2 GHz is about 4°. To put this into perspective, the angular diameter of the moon or sun is about 0.5° (about 30 arc minutes) so that the beam width of the antenna is about eight times as wide as the diameter of the sun or moon. As shown in the photograph of the sun in Figure 18 (taken through two pieces of welding glass), the sun in the sky is surprisingly small!
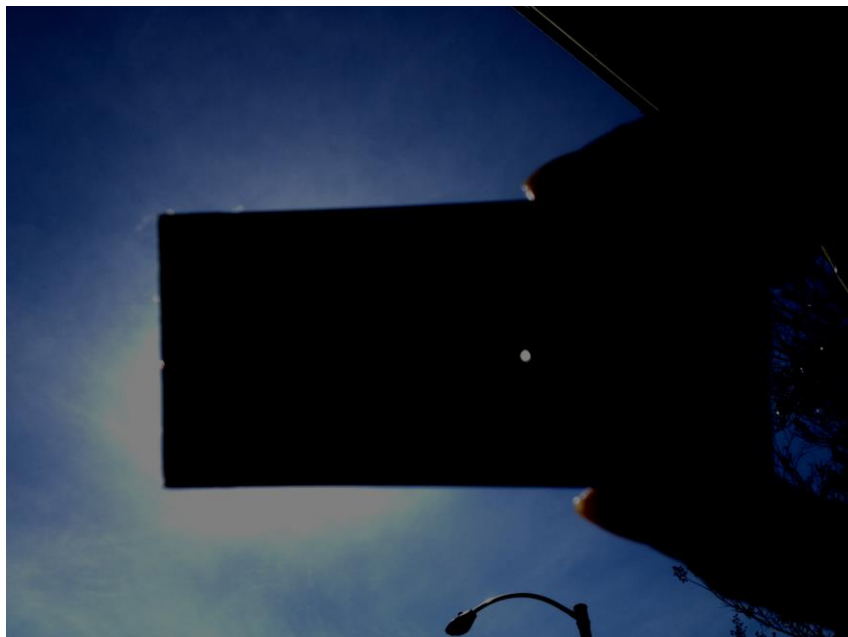
FIGURE 18

As a result, although the beam width of the Ku band antenna is about eight times larger than the angular diameter of either the sun or the moon, a 4° beam width is still quite small and even the sun or moon can be hard to find. Consequently, being able to "find" a point source such as Cassiopeia A or even the much larger sun at these frequencies requires considerable more precision in aiming than is required at 611 MHz.

Further, typical Ku band antennas are of an offset design. In a standard parabolic dish antenna, as shown in Figure 19, the pickup and LNB are at the focus of the dish along a line that runs from the source to the center of the dish.
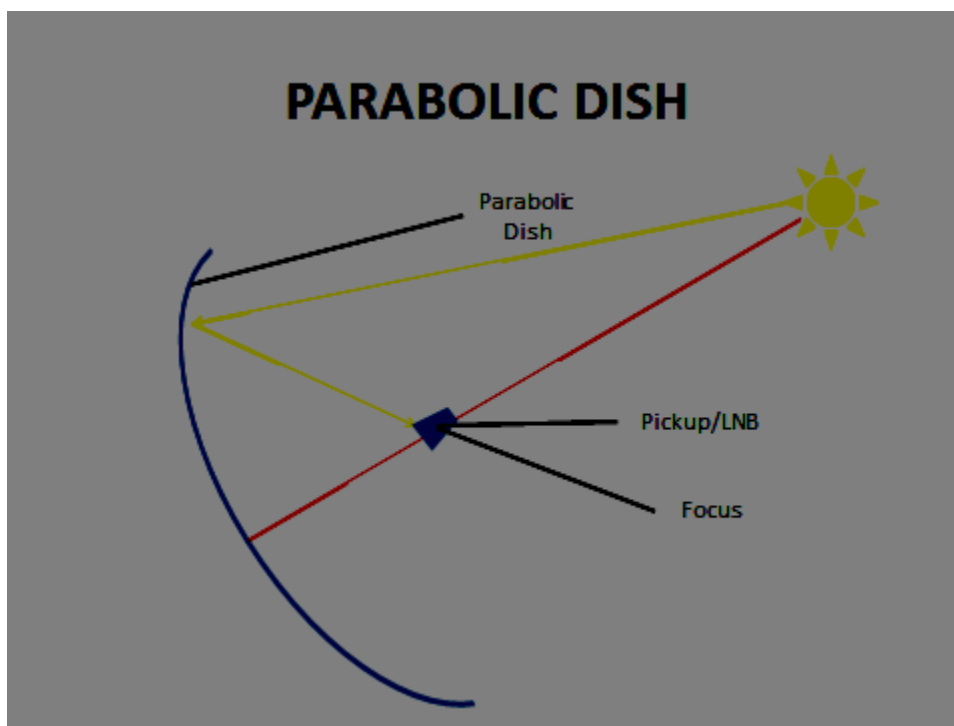

FIGURE 19

With an offset parabolic dish, shown schematically in Figure 20, start by imagining a giant "traditional" parabolic dish with the pickup and LNB at its focus which would be above the center of the dish. But, in such a "traditional" parabolic dish design, the pickup and LNB block a portion of the signal contacting the antenna. (For an example of a "traditional" parabolic dish, see one of the antennae for the Very Large Array in New Mexico.xvii) In an offset dish, the dish is a portion of the imaginary giant dish that is relatively far from the center of the imaginary dish. The offset portion is still parabolic and still reflects the radio signal that impinges on it to the pickup and LNB. But, the pickup and LNB no longer block the signal (which is the key advantage of offset dishes). As a result, the entire signal impinging on the offset antenna is reflected to the

pickup and LNB. (For an example of an enormous offset dish, see the 100m telescope at the Green Bank Observatory.xviii)
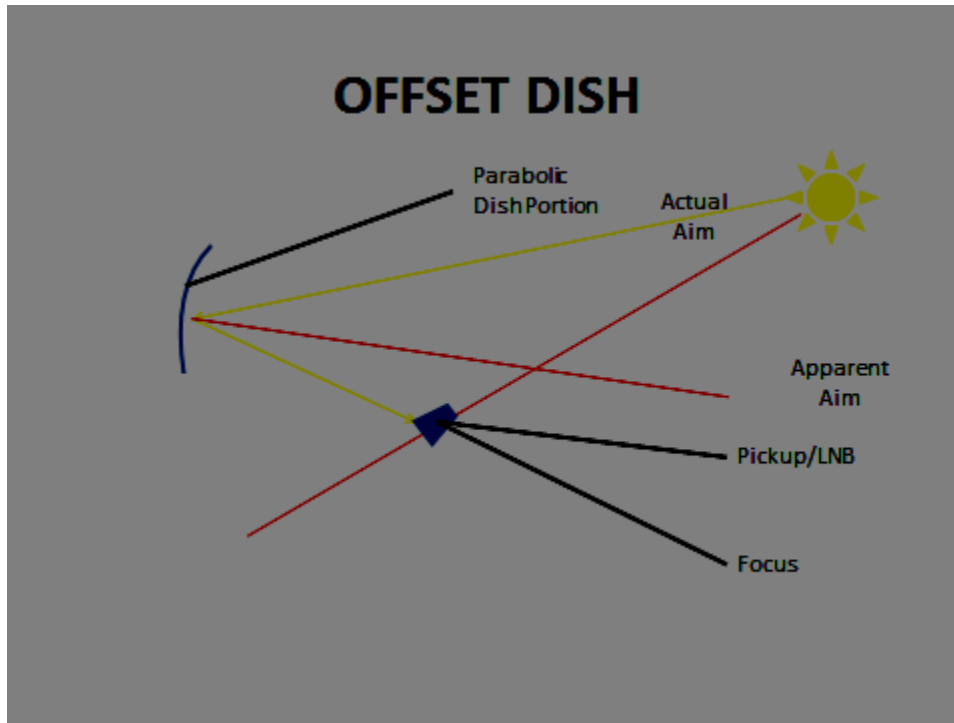

FIGURE 20

While offset dishes have the advantage that the pickup and LNB don't block any of the signal impinging on the dish, they have the disadvantage that they are notoriously hard to aim.xix For example, when a "traditional" parabolic dish such as is shown in Figure 19 is aimed at the sun, the dish is properly aimed when the sun shadow cast by the pickup and LNB is directly in the center of the dish. However, with an offset dish when aimed at the sun, no part or only a tiny part of the shadow of the pickup or LNB should cover the dish. Since the sun is typically the first thing imaged with a new radio telescope to see if it is working (after all, if you can't "see" the brightest thing in the sky, your telescope has a problem!), as I explain later, I can tell you from experience that "finding" the sun with an offset dish can be a frustrating experience!

I have found that I can improve my aiming "odds" with an offset antenna by first determining where the particular offset dish is aimed. A key tool in this regard is a commercial satellite finder that has an audio transducer in addition to an S meter. Such a satellite finder is shown in Figure 21. The satellite finder is attached to the coax cable coming from the Pickup/LNB and may also be connected to the receiver by a piece of coax cable. The satellite finder has its own battery so there is no need to run external power to it for its own operation or to power the Pickup/LNB. As the dish is scanned across the sun, not only will the signal strength indicated on the S meter increase, but there will also be a change of tone produced by the audio transducer so that the tone increases in frequency as the signal strength increases.

FIGURE 21

Armed with the satellite finder, it is possible to find when the dish is aimed at the sun by scanning the dish around and across the sun until the optimal signal strength is found as indicated by the reading on the S meter and also by the sound from the audio transducer. Once this position is found, a "short cut" way of aiming the dish at the sun is to observe where the sun's shadow is on the dish as shown in Figure 22. In Figure 22, the sun's shadow is located just barely on the lower edge of the dish as indicated in the center of the red oval. Once this spot is found, it is easy to aim the dish at the sun by moving the dish until the sun's shadow moves to this same location.

FINDING THE "SWEET SPOT"

FIGURE 22

Here is a word of caution. Many of today's Ku band dishes have multiple Pickup/LNB devices as shown in Figure 23 which is the Pickup/LNB combination for the DirectTV dish shown in Figure 22. These different Pickup/LNB devices are offset from other Pickup/LNB devices so that they are each aimed at a slightly different location along the celestial equator. While this is a convenient feature when it comes to detecting satellites (a single dish can pick up signals from more than one satellite simultaneously), this same feature makes for confusing aiming of the dish! If left intact, this combination actually aims the dish at several different locations in the sky at the same time! So, while one Pickup/LNB may be picking up the signal of interest (e.g., the sun), the other Pickup/LNBs may be picking up noise (and it won't be clear which of the Pickup/LNBs is picking up the sun!). As a result, with this configuration, it is difficult or impossible to know where you are aimed when you are picking up a strong signal. So, you will have extreme difficulty matching the measured signal strength with precise locations in the sky.

So, if you have a dish with more than one Pickup/LNB device, I recommend that you disable all but one. Specifically, you should disable all the Pickup/LNB devices except for the one most centrally located. In the configuration of Figure 23, disable all the Pickup/LNB devices except for the one shown on the farthest right (which is the central Pickup/LNB device). To disable the unselected Pickup/LNB devices, remove the screws holding the back plate of the Pickup/LNB devices. This will expose the coax cables coming from each Pickup/LNB to a combiner device that combines all the signals sent to it onto a single output coax cable that passes out of the antenna. Simply disconnect the coax cables from the unselected Pickup/LNB devices from the combiner device. This leaves only the selected Pickup/LNB connected to the combiner device.

FIGURE 23

Once you can reliably aim the antenna at the sun, a method that can be used to learn how to aim the antenna, either in addition to or in the alternative of the method described above, is to aim the antenna south as described above. Then move the antenna in elevation until it is aimed at the elevation through which the sun will pass at noon. Confirm that you are getting signal from the sun as described below.

Once you have confirmed that you are aimed at the sun, take a metal carpenter square and, as shown in Figure 24, place it across the front of the antenna from the arm holding the Pickup/LNB up to the top of the dish. The short arm on the square is laid along the top edge of the dish and stabilizes the square on the face of the dish. As a result of this configuration, the long arm of the square forms a flat surface across the face of the dish. A low-cost goniometer such as can be acquired at a hardware store is placed on the flat long arm of the square. If the goniometer has a magnetic base, the goniometer is magnetically attracted to and held in place on the carpenter's square. The reading on the goniometer indicates the angle of tilt of the dish relative to vertical. But, because the dish is offset, where the dish is "aimed" is not perpendicular to the face of the dish! The formula to calculate the elevation of where the dish is aimed is:

Target Elevation = Angle of Tilt + Angle of Offset.

So, rearranged to solve for the needed Angle of Tilt to produce the desired Target Elevation produces:

Angle of Tilt = Target Elevation − Angle of Offset.

Using a Target Elevation of 60° and a dish with an Angle of Offset of 22° yields an Angle of Tilt of 38°. Consequently, the dish needs to be moved so that its Angle of Tilt, as measured by the goniometer, is 38°.

Here is a bit of a word of warning with respect to the Angle of Offset. Many, but not all offset Ku band satellite dishes have an offset of 22°. Ideally, you can get the exact offset figure for your dish from the manufacturer. But, I have found that in practice, it is difficult to get the technical specifications for specific dishes. So, if you use an Angle of Offset of 22° but are not finding your target (remember, the beam width is only about 4°), move the dish up and down when the target is aligned to the south until you 'see" your target (e.g., the sun) to determine the actual offset for your antenna.

FIGURE 24

Further, you have the choice of having a more-or-less permanent mount for your telescope or a mobile mount (i.e., one that can be picked up and moved from place to place). Without fully appreciating the difficulty involved in locating a target (e.g., the sun) with an offset dish, I chose the mobile mount. With hindsight, this was probably a mistake, at least initially. If not a mistake, I should have at least built a more robust mobile aiming system as described below.

The advantage of using a permanent mount is that the antenna can be mounted in a first orientation and then moved systematically to find the sun in order to determine the specific offset of your dish. Further, the antenna can always be returned to an original or reference position so that you aren't starting from a different starting point each time you use the telescope or if you get frustrated aiming it. One large and frustrating problem with using a mobile mount is that every time the telescope is set up, the mobile mount must be reoriented. This orienting takes place not only on alt-azimuth axes but, because the mobile mount is mobile, there is also the possibility (probability!) that the ground under the mount is not level. As a result, either the elevation or azimuth axis or both may be skewed!

Once the sun is "found," the orientation of the sun with respect to the dish can be determined by, for example, sighting along the arm holding the pickup and LNB to determine its orientation to the sun. Thereafter, to "find" the sun again, as a "short cut," the antenna is just moved to that orientation. This is particularly helpful when using a mobile mount and taking data from the sun.

As described above, the position of the sun can be calculated for any location and for any day and time as explained above. If your aiming system has reference capabilities, once you gain confidence in your ability to aim the dish, you can calibrate the dish by aiming it at the sun and correcting your reference marks ("registering" the reference marks) to correspond to the sun's elevation and azimuth. Thereafter, to find the sun (or any other target of interest), its position is determined by using one of the websites that calculates the sun's position (or a star chart). Then, the dish is moved so that its coordinates are aligned with the mount's reference scales.

For optimum results for drift scan observing, the antenna should be aimed either true south or true north. In this way, the antenna is aligned with the local sidereal time. But, compasses are typically magnetic compasses that point to the earth's magnetic north pole rather than the earth's true north pole. The earth's magnetic north pole is displaced from its true north pole. As a result, there is a difference between what the magnetic compass reads and the true readings with respect to determining direction. This difference is called magnetic declinationxx (not to be confused with the "declination" associated with right-ascension and the celestial coordinate system). At my location in San Diego, the magnetic declination is 11° 58" east. So, I need to adjust my aim of the antenna by about 12° *to the east* to correctly align the antenna to the correct north

south alignment. If I don't make this correction, my aim will be off by nearly 12° or about three full beam widths!

Also, Ku band dishes are typically made of a ferromagnetic metal. As a result, if you bring a magnetic compass near the dish (for example, as you might do to aim it), the metal in the dish will affect the pointing of the needle. So, you need to keep your magnetic compass away from the dish while you are aiming it. This makes it a little more difficult to aim the dish, but your aim will be bad if you don't do it. In addition, don't use the compass in your cell phone to aim your antenna. I learned by experience aiming my 611 MHz telescope that these compasses are not particularly accurate!

Because the Ku band antenna has a relatively small beam width, unless you can repeatably aim the antenna, using it for even relatively simple operations such as doing scans of the sun, will be frustrating. So, I have learned that it is important to have a good and reliable aiming mechanism. One solution is to use a professionally made alt-azimuth positioner such as is shown in Figure 25. The positioner shown is a commercial grade positioner used to aim satellite or broadcast dishes for remote broadcasts for commercial TV stations. Obviously such a heavy-duty positioner is overkill for a Ku band antenna. But, if you can get one, they are great! (Check EBay, ham or other electronic swap meets.) Alternately, there are lower cost professionally made positioners such as those made by for space communication antennas (e.g., Yaesu G-5500). Also, an article titled "An Affordable Az-El Positioner for Small Antennas" in *Satellite Handbook* published by ARRL describes a low-cost (~$250 or less!) azimuth-elevation system built from two simple Radio Shack *Archerotor* or Channel Master *Colorotor* antenna rotators.

FIGURE 25

In the absence of a motorized alt-azimuth positioner as described above, a robust manual positioner can favorably be used. Such a manual system is described in an article by the SETI League titled "Chippewa Valley Astronomical Society star party

introduces the Little Bitty Telescope™ Version 2 and LBT Experiment No. 1."xxi

In hindsight, I think much of my initial frustration with aiming the Ku band radio telescope would have been eliminated with the use of such a robust manual aiming system.
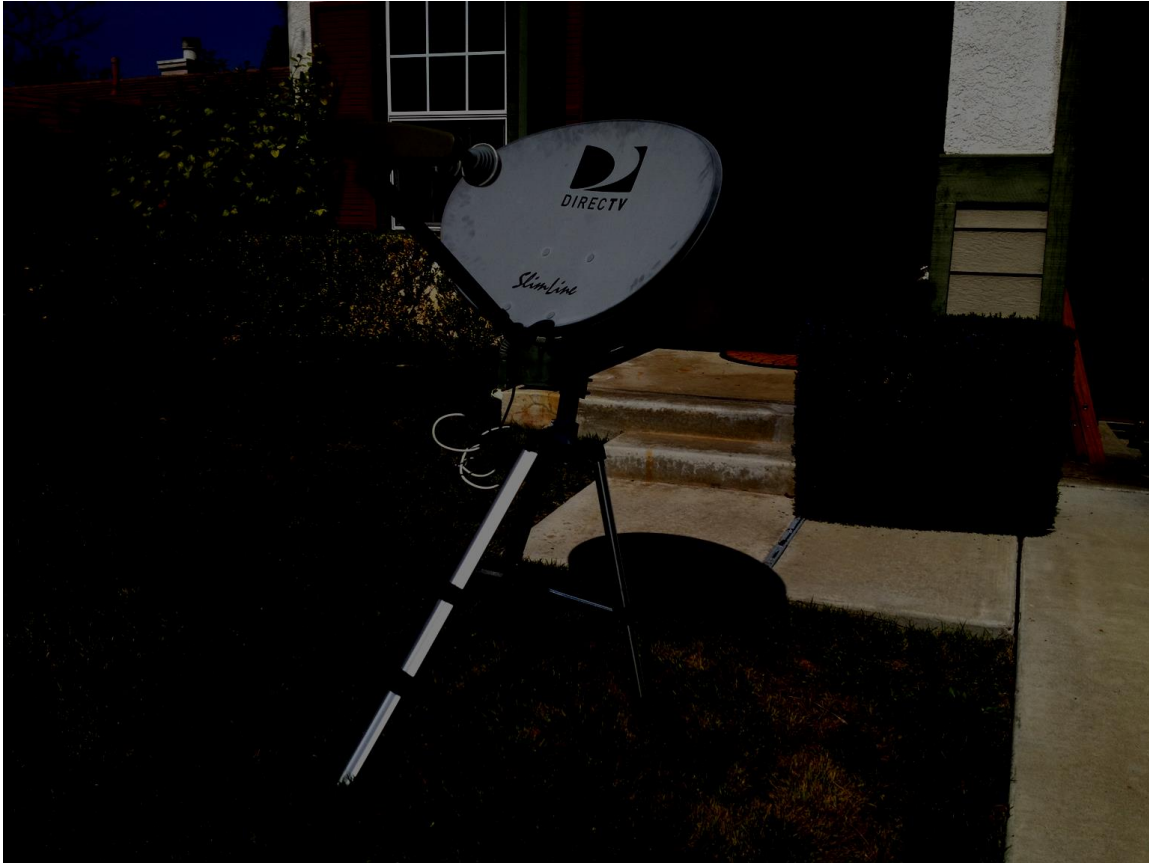
FIGURE 26

Once the antenna is aimed at a target of interest or at an elevation that would allow a target to drift through the beam of an antenna in a drift scan (Figure 26), the receiver is set to the desired settings to receive the down converted signal from the LNB. As mentioned above, the signal sent from the LNB to the receiver is in the range of 950 – 1450 MHz. But, because there is a blocked section in this range on the receiver, you can't tune the receiver to 1000 – 1050 MHz. So, the receiver may be tuned to from 950 – 999 and 1051 – 1450 MHz. This corresponds to original received frequencies of 12. 2 – 12.25 and 12.3 – 12.7 GHz.

The ICOM R7000 receiver has several bandwidth settings, the largest of which is 175 KHz. These settings are made by moving several switches on the back of the receiver into a configuration that produces the bandwidth of 175 KHz. Further, the receiver has AM, FM and SSB modes. Since we are not looking for any modulated signals, we are not interested in the FM or SSB mode. Instead, we are looking at the amplitude of the received signal. So, we set the receiver to the AM mode.

In addition, the receiver has a squelch control. Since our radio signals are typically going to be low amplitude signals, it is important that the squelch be turned all the way down. Otherwise, the squelch control will block the low-amplitude radio signals that we are interested in.
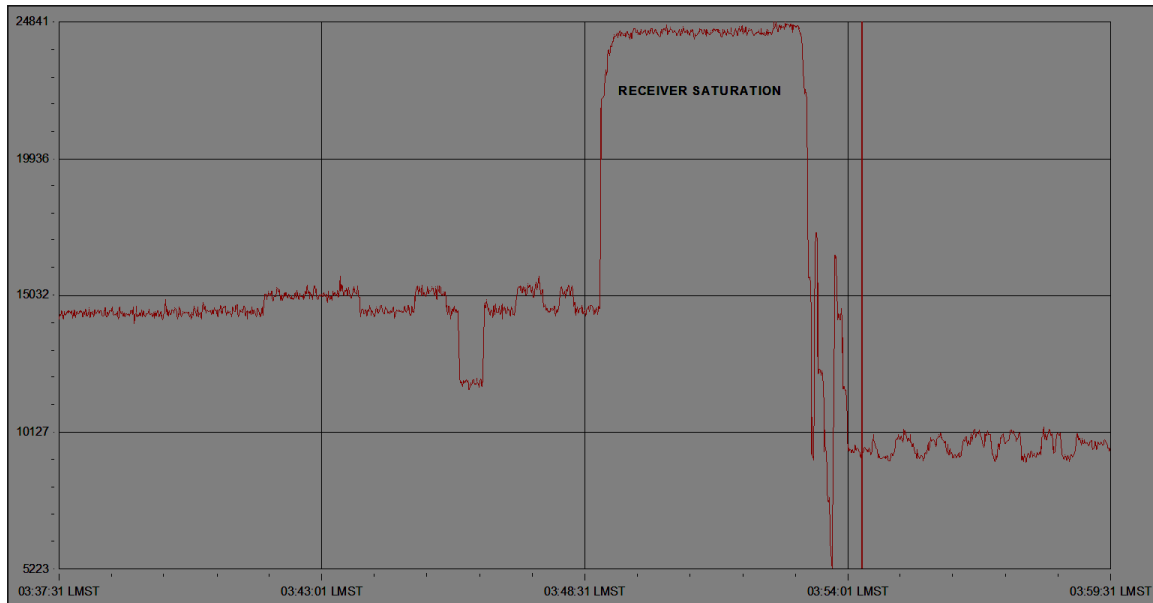

FIGURE 27

Also, because our signals are weak, it is tempting to crank the gain all the way up to amplify the inherently weak radio signals as much as possible. But, as shown in Figure 27, it is easy to saturate the receiver and thus get no amplification at all. So, I recommend starting with a moderate amount of amplification. When using the Radio-SkyPipe software in its default settings, I typically adjust the gain so that when aiming the antenna at the clear background sky as a calibration exercise, the chart recording reads about 12000 on the software scale. This produces a good level of amplification and allows relatively strong signals (e.g., those coming from the sun) to not saturate the receiver.
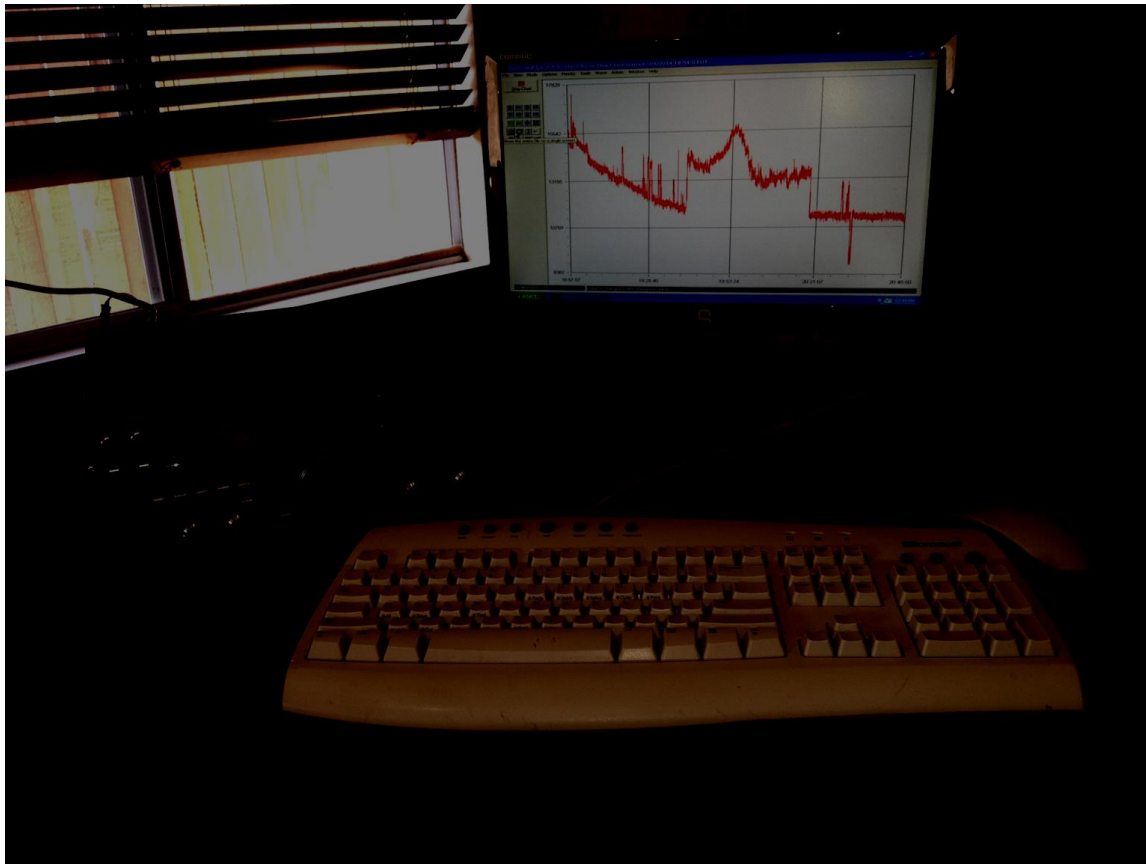
FIGURE 28

Once the Ku Band Total Power Radio Telescope is set up as described above, data can be collected as shown in Figure 28.

Practical considerations - The Effect of Weather on the Ku Band Radio Telescope

Amateur radio astronomy currently requires us to look at the sky from locations on the earth. This requires us to look at the sky through the atmosphere. One obstacle to seeing the sky clearly at the radio frequencies of the Ku band is the absorption of the radio signal by molecules making up air. Beginning at about 10 GHz and rising thereafter through the microwave range, the atmosphere becomes progressively less transparent because air molecules absorb the radio energy and convert the energy into rotation of the air molecules.xxii In particular, water molecules absorb radio energy at these frequencies. Consequently, the ability to "see" the sky at microwave frequencies is influenced by clouds and even humidity.

Further, where your observing location is and where in the sky you are looking necessarily influences how much of the atmosphere the radio signal you are trying to capture has to pass through.   If the radio source

is directly overhead, the thickness of the atmosphere through which the radio signal must pass is simply the thickness of the atmosphere overhead, about 60 miles of progressively thinning atmosphere.xxiii But, for radio objects near the horizon, the radio signal may pass through several hundred miles of atmosphere. Fortunately, this absorption at Ku band frequencies is not severe (otherwise it would greatly affect your ability to watch your satellite TV channels!), but it is noticeable. This leads to opportunities to do research. Several interesting projects that can be done with a Ku band radio telescope to study this effect are described briefly hereafter.

Practical Information

When Ku band satellite dishes are discarded, the cables connecting them to their respective houses are usually just cut. As a result, if you want to use such a discarded dish, you need to put a new connector on the cut end. To connect to the connectors typically placed on RG 6 cabling, usually F connectors are used. Installing good quality F connectors using the rugged compression fittings found on most RG 6 lines used in satellite systems requires a somewhat pricey tool (~$150!). So, if you don't want to invest in such a tool, I found you can go to your local satellite system installer and get some help.

In my case, I went to my local satellite system installer and met Joe Arafat shown in Figure 29 in front of his business. When I explained that I was converting discarded Ku band satellite antennas into telescopes for looking at the radio sky, and took the time to explain how the telescope works and what it would be looking at, I found that Joe loves science! He was quite interested in my project, had his technician install all the F connectors I needed and gave me quite a bit of RG 6 cable to use in the project! Further, he offered to help me however he could in the future including helping me find additional dishes if I want. I very much appreciate Joe's help and I suspect that there are many others like him in the various satellite installation businesses around. I suggest you seek them out and find other "Joe's" to help you!

FIGURE 29

Also, the coax cables will have F connectors as described above. But, the input to the ICOM R7000 receiver requires an N connector. So, you will need to get an male F to male N connector to make this connection.

Further Practical Information

Set out in the End Notes are several useful links to valuable information for others considering this or similar projects.**xxiv**

Calibration and Taking Data

Once the Ku band radio telescope is taking data, it is useful to calibrate the telescope. The telescope acts like a thermometer. Because of this, there are two easy calibration sources illustrated in the charts of Figures 14 and 30. First, the antenna can be pointed at clear sky. Clear sky is an area clear of clouds (see the discussion of weather issues above) where there is not much radio activity going on. One such place is the area around the North Star. The cosmic background radiation corresponds to a 3° K temperature. Since a 3° K source is about as cold as anything in the universe, it's black body radiation strength at 12.2 – 12.7 GHz will be about as weak as any possible cosmic radio signal. So, the signal received by the Ku band radio telescope when aimed at these clear sky areas is going to be the weakest possible cosmic signal and provides a baseline reference for the background radio strength. In the chart of Figure 14, I have labeled this calibration level "SKY" and in Figure 30, "Clear Sky."

The second source for calibration is the ground. If the ground has a temperature of 30° C, the ground will have a temperature of 303° K. The blackbody radiation strength for this temperature at 12.2 – 12.7 GHz will be considerably stronger than the 3° K clear sky source. This will provide another calibration reference for your data. In the chart of Figures 14 and 30, I have labeled this calibration reference "GROUND." Notice also that your own body temperature is not too far from 30° C. So, if you put your own body in front of the antenna, as I did for the data shown in Figure 30 that I labeled "ME," you can see yourself!

Also, the level of "System Noise" described above is the floor of what signal can be received. As a result, its level can also be used as a sort of calibration level as well.
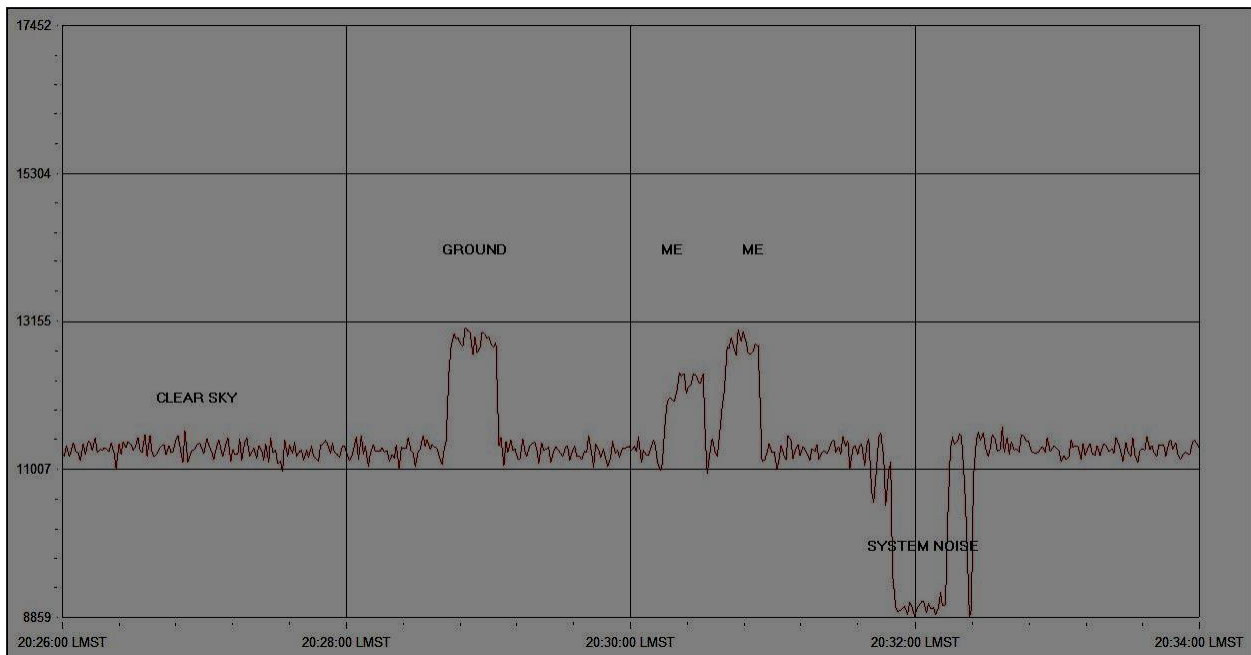

FIGURE 30

Data

Figure 14 is an example of an actual data run for the Ku Band Total Power Radio Telescope that illustrates many of the issues associated with data runs. This data run was taken as a drift scan. At the far left of the chart, the initial signal level represents the signal received when the receiver was first turned on but not yet connected to the antenna. This signal level represents the noise inherent in the receiver.

When the antenna was connected, the signal strength immediately jumps. At this time, I was physically moving the antenna trying to find the sun. Since I had turned the receiver on from being cold, the steady decrease of the signal from this initial jump probably represents the electronics settling down. As a result, I recommend that when taking data, the receiver be allowed to thoroughly warm up before data is taken in order to let the electronics settle down. The spikes moving to the right represent me doing calibration exercises as explained above primarily aiming the antenna at the ground.

The large jump in signal strength about mid-chart occurred when I aimed the dish true south and at about 51° of elevation. As discussed above, I think the large increase in signal strength is due to picking up "noise" from one or more of the commercial satellites operating near "south" at their geosynchronous elevation for my location also of about 51°.

Finally, as labeled "SUN," the sun transits the antenna. Despite the fact that the sun and one or more satellites appear to be in antenna's field of view, the sun is a stronger signal than the satellites. I can be reasonably certain that this peak is the sun first because it has the profile of a drift scan crossing a point source and it appeared exactly south when it was predicted to be there. The total width of the peak appears to be about 12°. Remember that the predicted ½ power beam width of the antenna is about 4°. But, it appears that the peak represents more than just the ½ power level of the sun's signal. Hence, the peak is larger than 8° (twice the 4° ½ power beam width predicted) and the measured ~12° width of the peak appears to be consistent with this.

The big drop in signal strength moving to the right from the observation of the sun occurred when I moved the antenna away from the sun back to clear sky. The spikes along the signal correspond to the calibration exercises I described above.
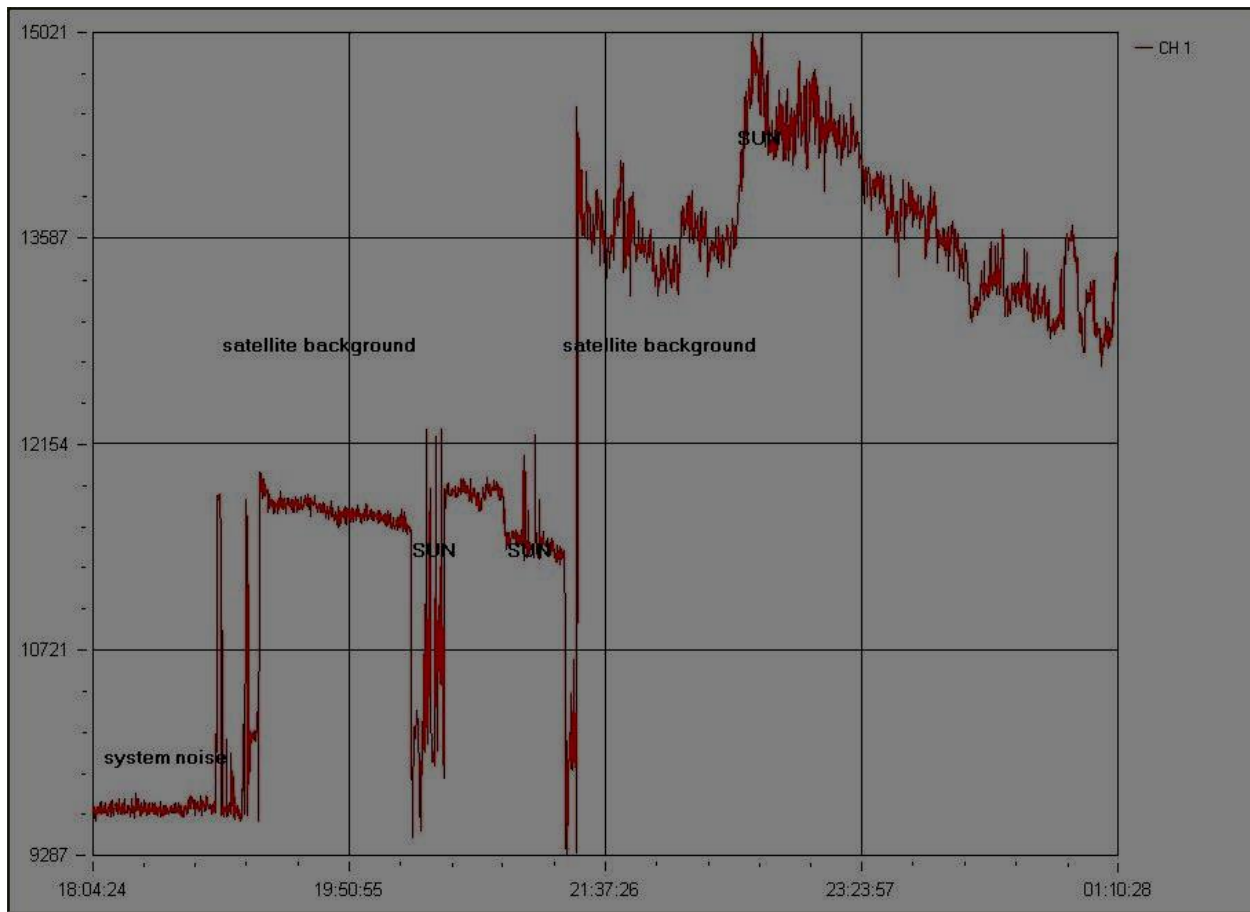
FIGURE 31

Figure 31 is another drift scan of the sun. In this recording, I have placed the satellite finder in the system between the dish and the receiver. So, starting at the far left, the signal level represents the system noise. The spikes moving to the right represent me moving the dish to an elevation of about 51°. As explained above, I believe these relatively higher signal levels are produced by the satellites positioned at about 51° of elevation. Moving even more to the right, there is an increase in signal strength relating to me moving the dish across the sun. The satellite finder degrades the signal level received at the receiver when it is placed inline. But, the satellite finder in this position indicates the received signal strength on both its S meter and audibly so that I am confident that these relatively higher spikes correspond to the signal received from the sun.

About half-way across the chart, I removed the satellite finder. This can be seen as a deep dip in the signal strength. Then, I reconnected the coax cable from the Pickup/LNB to the receiver. As a result, with the satellite finder no longer degrading the signal strength, the signals strength of the "noise" at about an elevation of 51° (corresponding to the communication satellites located there) is indicated. Shortly

thereafter, the sun drifts through the beam width and produces the peak I labeled "Sun." As the sun drifts through the beam, the received signal strength decreases.
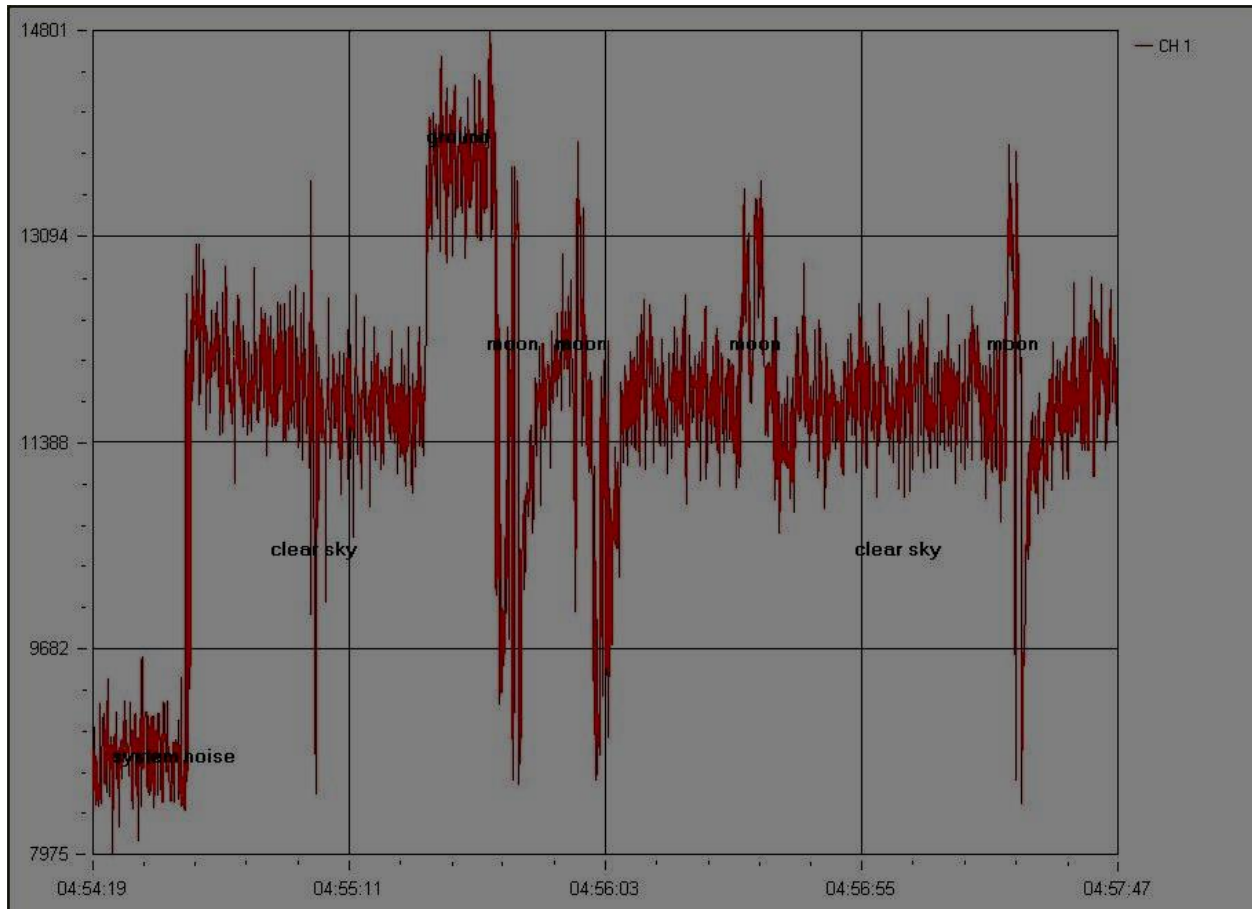

FIGURE 32

Figure 32 is a recording of data from the moon that I produced holding the dish in my lap on a chair and aiming the dish by hand. This recording was taken with the satellite finder inline between the Pickup/LNB and the receiver. As a result, the signal received by the receiver is degraded by the satellite finder so that these signal levels are less than would have been produced had the satellite finder not been in place. At the far left of the recording, the system noise is indicated. Then, I placed the satellite finder inline and connected the coax cable to the receiver. This produced an increase in signal strength even though the satellite finder degraded the signal as described above. Moving to the right, I aimed the dish as clear sky which produced the downward spike that I labeled "clear sky." Moving back from "clear sky" produced an increase in signal strength.

Thereafter, I pointed the dish at the ground with produced a high signal level I labeled "ground." Then I aimed the dish at the moon using the satellite finder's audible tone to indicate when the dish was aimed at the moon.

This produced the spikes I labeled "moon" as I scanned around the moon using the satellite finder to indicate when I was aimed right at the moon. The deep downward spike on the far right is a result of my aiming the dish back at clear sky around the north star.
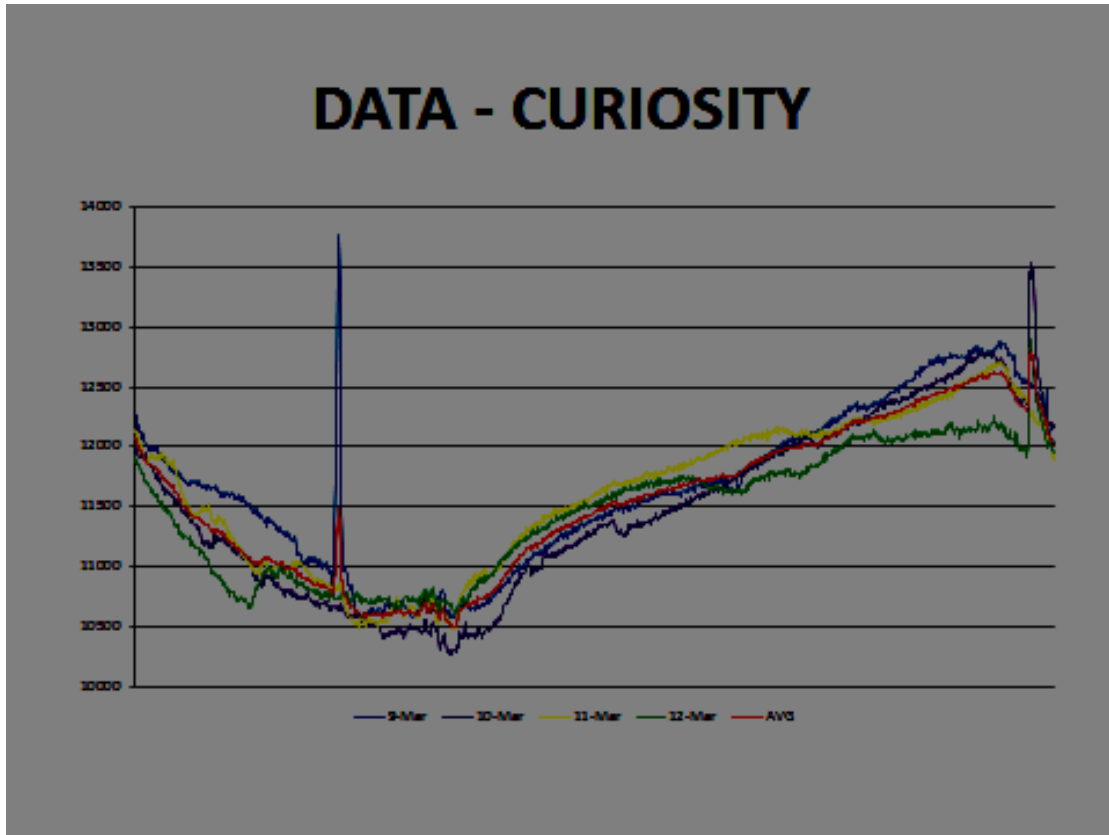

FIGURE 33

Figure 33 is a chart of four consecutive 24 hour recordings (March 9 – 12, 2014) with the dish aimed north and at about 60° of declination along with a line, in red, indicating the average of the four recordings. As can be seen, there is a repeating pattern. When I compare this signal with its corresponding right ascension time stamps to a sky chart, I believe the peak at the far right represents the galactic plane. The large spike on the left on one of the recordings was produced when my neighbor fired up his 55 Chevy with its unshielded ignition system. I am not sure what produced the large spike on far right but believe it to also be some external short-term noise.

Projects

Here are suggestions for some of the many projects that can be done with this Ku band total power radio telescope:

- A drift scan survey of some or all of the sky.

- With respect to the Sun:

  o Measure the antenna beam width by measuring the width of the signal from the sun as the antenna drift scans past the sun.

  o Track the sun at noon below and through the ecliptic (and through the "satellite belt") over time.

- With respect to the Moon:

  o Is the moon signal produced by accelerated charge particles, black body radiation, atomic level change or reflected from the sun? How would this be indicated in a radio signal?

  o Track the moon as it moves through the ecliptic (and through the "satellite belt") over time.

  o Does the measured signal strength change with the phases of the moon?

- With respect to the atmosphere/weather:

  o Measure the signal strength from satellites (e.g., one of the satellites close to south for your location) under different sky conditions (clear sky vs. heavy rain, low humidity vs. high humidity).

  o Measure the signal strength from the sun or moon - high in the sky (radio signal has to pass through less atmosphere) vs. near the horizon (radio signal has to pass through much more of the atmosphere).

  o Measure the signal strength coming from empty sky (cosmic background radiation) at different elevations (i.e., directly overhead corresponding to the least distance through the atmosphere the radio signal must pass and taking measurements at elevations moving toward the horizon where the radio signal has to pass through the most atmosphere).

Next Steps

I have just begun to take data with Ku band radio telescope. So, I would like to continue taking data including more data of the sun and the moon with the ICOM R7000 receiver without the satellite finder inline. I would also like to so more drift scans of the Milky Way and see whether the "Curiosity" data described above is actually the Milky Way. However, in order to more easily "find" the sun and moon, I need to improve the aiming of the dish. As it stands now, it is still a frustrating and inconsistent exercise to aim the antenna at the sun (the brightest object in the sky!) much less the moon. So, I will be implementing better aiming systems including possibly putting the commercial satellite positioner shown in Figure 25 into operation. But, I have learned a lot in this project so far and am confident that I will be able to solve this aiming problem.

Also, now that I have a working Ku band radio telescope, I would like gang several of them together into arrays. One array I would like to explore is to aim several dishes south but have each one aimed at a different elevation so that data from each is taken at the same time. In this way, several drift scans are produced simultaneously that can be reconstructed relatively quickly into a sky survey.

Further, I have been experimenting with replacing the venerable ICOM R7000 receiver with a software defined radio. I am using a FunCube Donglexxv and SDR# software defined radio softwarexxvi with encouraging results. So, this is definitely an area that I will be continuing to explore.

Conclusion

This is a good and relatively easy project. The available targets are less than those available for the 611 MHz telescope and the aiming problem makes it a little frustrating. But, perhaps a little better planning in advance with respect to the aiming problem could have solved this problem. With the aiming problem solved, the interesting projects described above can be done as well as others that can be thought of. I am looking forward to doing more with this scope!

---

i   http://en.wikipedia.org/wiki/James_Clerk_Maxwell

ii http://en.wikipedia.org/wiki/Maxwell%27s_equations

iii http://en.wikipedia.org/wiki/Nikola_Tesla

iv http://www.nrao.edu/whatisra/hist_jansky.shtml

v Id.

vi

vii http://www.spacehike.com/radiowaves.html

viii http://www.aoc.nrao.edu/epo/teachers/ittybitty/

     http://nightsky.jpl.nasa.gov/news-display.cfm?News_ID=270

     http://www.setileague.org/articles/lbt.pdf

ix http://en.wikipedia.org/wiki/Channel_37

     http://www.universetoday.com/101885/the-curious-channel-37-must-see-tv-for-radio-astronomy/

[x] ARRL Antenna Book, 21st Edition, 19-21

http://www.qsl.net/pa2ohh/jsparabolic.htm

http://en.wikipedia.org/wiki/Parabolic_antenna

[xi] : http://www.satsig.net/ssazelm.htm

[xii] Image by Reed Michaelson – Northwest Public Radio

[xiii] http://www.mpifr-bonn.mpg.de/1041051/Porcas_Intro_Radio.pdf

[xiv] http://home.comcast.net/~shannip/icr7000mods.pdf

[xv] www.radioeyes.com

[xvi] I like http://www.sunposition.info/sunposition/spc/locations.php#1.   This on-line calculator gives a map showing the sun's right ascension and elevation over time and also produces a list showing, in 15 minute increments, the sun's altitude and azimuth. Also, it allows you the option of getting the azimuth data in either true or magnetic north format.   http://www.sunearthtools.com/dp/tools/pos_sun.php is another useful website.

[xvii] http://www.vla.nrao.edu/

[xviii] https://science.nrao.edu/facilities/gbt

[xix] http://www.satsig.net/22-deg-offset-dish.htm

[xx] http://www.ngdc.noaa.gov/geomag-web/#declination

[xxi] http://www.setileague.org/articles/lbt.pdf

[xxii] http://astro.u-strasbg.fr/~koppen/10GHz/tengigs.html

[xxiii] http://www.grc.nasa.gov/WWW/K-12/airplane/atmosphere.html

http://en.wikipedia.org/wiki/Earth%27s_atmosphere

[xxiv]   Excellent   tutelage   on   Radio   Astronomy: https://www.astron.nl/~mag/doKUwiki/lib/exe/fetch.php?media=radio_astronomy_lec_3_ma_garrett.pdf

Good Information: http://astro.u-strasbg.fr/~koppen/10GHz/tengigs.html

http://www.ap.smu.ca/~lonc/radiotel.html

http://www.setileague.org/articles/lbt.pdf

http://www.aoc.nrao.edu/epo/teachers/ittybitty/procedure.html

http://astro.u-strasbg.fr/~koppen/10GHz/docs/Cleary1999.pdf

xxv http://www.funcubedongle.com/

xxvi http://www.sdrsharp.com/

SID Monitoring using Raspberry Pi

Author: Ciprian Sufitchi, N2YO

Abstract

As technology advances and becomes more and more affordable, research/crowdsourcing projects such as Sudden Ionospheric Disturbance (SID) monitoring could run 24 hours a day on inexpensive devices. Traditionally, a computer (PC) equipped with a good quality sound card is required to receive VLF signals, process them, store and draw data, and report it in a public database. For a continuous operation a PC is not an ideal platform though, being unreliable and expensive. Attempts to use microcontrollers such as Arduino were successful, as presented at the Annual SARA Conference in 2013 ("Sidruino") however they generally require an external VLF receiver. Raspberry Pi, a credit-card-sized single-board computer developed in the UK by the Raspberry Pi Foundation based on Linux as operating system, could be an attractive alternative – it is inexpensive, fast enough to perform Fast Fourier transform on incoming audio signal from the audio board, can be powered from batteries and it is supported by a large group of open-source enthusiasts around the world. The paper will focus on external hardware able to receive a wide VLF spectrum and a few SID monitoring applications running on Raspberry Pi.

An Introduction to Raspberry Pi

The designing process of Rasberry Pi started in 2006, but the initial sales commenced only in February 2012. In November 2013 the Raspberry Pi Foundation announced that the *two millionth* Pi shipped between 24 October and 31 October.

The Raspberry Pi is essentially a computer that has a Broadcom BCM2835 system on a chip, which includes an ARM 700 MHz processor, VideoCore IV GPU, and was originally shipped with 256 MB of RAM, later upgraded to 512 MB. It does not include a built-in hard disk or solid-state drive, but uses an SD card for booting and persistent storage.

Raspberry Pi is manufactured in 2 configurations – A and B. The most important differences are summarized in this table:

	Model A	Model B
Memory	256 MB	512 MB
USB 2.0 ports	1 (direct from BCM2835)	2 (from USB integrated hub)
Onboard network	None	10/100 Mbps Ethernet
Power ratings	300 mA (1.5 W)	700 mA (3.5 W)
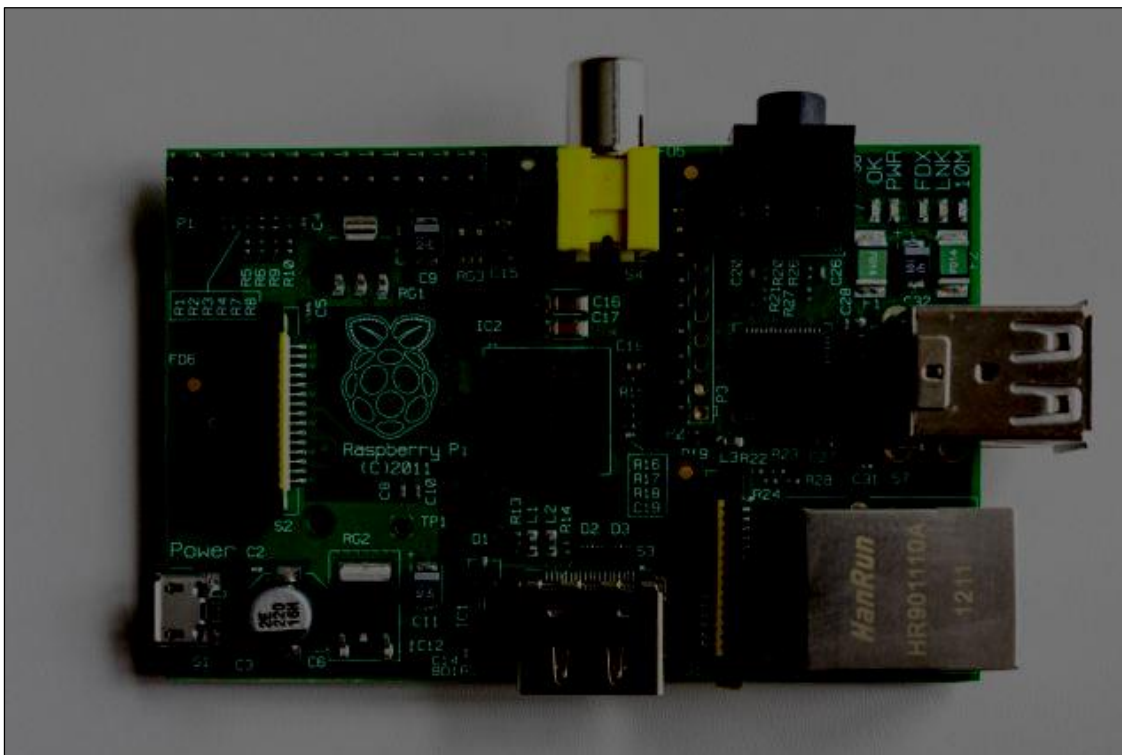
Both models A and B feature a HDMI connector to connect to a high resolution monitor, a RCA connector for composit video signal, an audio output (no input), a micro USB connector for power supply (5 V), a SD card reader located on the opposite side, a GPIO connector, a CSI connector camera, and a DSI display connector. The system supports standard USB keyboard and mouse.

The operating systems currently supported are Arch Linux ARM, Debian GNU/Linux, Gentoo, Fedora, FreeBSD, NetBSD, Plan 9, Raspbian OS, RISC OS, Slackware Linux, and others.

The target price for model A is $25 and for model B is $35 however the selling price is usually higher, when a 5V power supply, a SD card with operating system, then taxes and shipping are added.

Considering that the computing power is good enough to run Fast Fourier algorithms, Raspberry Pi could replace successfully a dedicated PC running Windows doing SID monitoring. The main problem is the sound input, which is missing in the native hardware configuration. Additional hardware (USB cards or specifically R-Pi designed cards) should be utilized for an appropriate configuration. The best option for SID monitoring is the *model B* which allows to dedicate an USB port for a sound card, while the other is available for keyboard. Also, the Ethernet port will be required to report observations online.

Microsoft Windows users may find a bit difficult to handle Linux, however a minimal set of commands will be required to have the system performing the tasks. Ideally users should not utilize any graphical interface, although Raspberry Pi can provide a GUI similar in appearance to MS Windows (called the X-Window environment).

Hardware: USB Sound Cards

Since the audio subsystem on the Raspberry Pi card is rather poor and there is no input connector readily available, the most affordable solution would be an external USB sound card. Many sound cards are available on the market, but the final selection should take into account three important criteria: sampling rate (should be at least 96 kHz), compatibility with Linux systems, and the price (as we are trying to put together an inexpensive SID monitor). After some research and experiments, I found an inexpensive USB audio card available for around $11 on Amazon, Newegg, and other online stores: SYBA SD-AUD20101.

Although the specifications claim that the board is able to sample at 192 kHz with 24-bit resolution, in reality the maximum speed is 96 kHz, which is good enough to receive the strong VLF signals above 24 kHz that can be received anywhere on the continental US. The USB card features a VIA Envt VT1620A audio controller, a USB 2.0

connector (type A), a stereo output jack (S/PDIF capable) and a mono microphone-input jack. No external power is required.

The USB dongle is immediately recognized by Windows 7 and by Rasbian Linux, no additional software (drivers) is required for configuration.

This board has been used with great success on Windows platforms together with the standard SuperSID hardware and software. However it turns out that this card, as well as many other USB audio cards, if not all, do show some challenges with Linux, especially on less powerful computers such as Raspberry Pi when sampling rate is higher that the standard 44/48 kHz values. One problem, as pointed by some users, is that USB isochronous data transfer (as used by soundcards) does not work properly on the Raspberry Pi. USB data packets are silently dropped and this renders the capture side of the device unusable (typically 1% of the audio packets are lost). A work-around recommended by the Raspberry Pi literature is to add dwc_otg.speed=1 to /boot/cmdline.txt which makes all USB (and the ethernet) run at USB 1.1 speed (12Mbit/sec). This enables USB sound capture to work reliably with many cards, but usually prevents the USB keyboard and/or mouse from working. Although this change may work with some programs, it may not work with others, as that will be discussed in the software section. As of May 2014, programmers are currently working to fix the issues with performant USB audio cards compatibility on Raspberry Pi systems and for sure software updates will make this inexpensive card work very well with any software quite soon.

Hardware: Raspberry Pi dedicated audio cards

The audio cards specifically designed to fit Raspberry Pi connectors avoid the limitations of the USB connection discussed before. However not many such audio cards have been designed as of yet (May 2014). One relevant example is the Wolfson Audio Card, produced by Element 14 and Wolfson Microelectronics, offering Raspberry Pi users similar flexibility to a PC soundcard to capture audio alongside their camera, and experiment with stereo digital capture and playback at 192 kHz sampling.
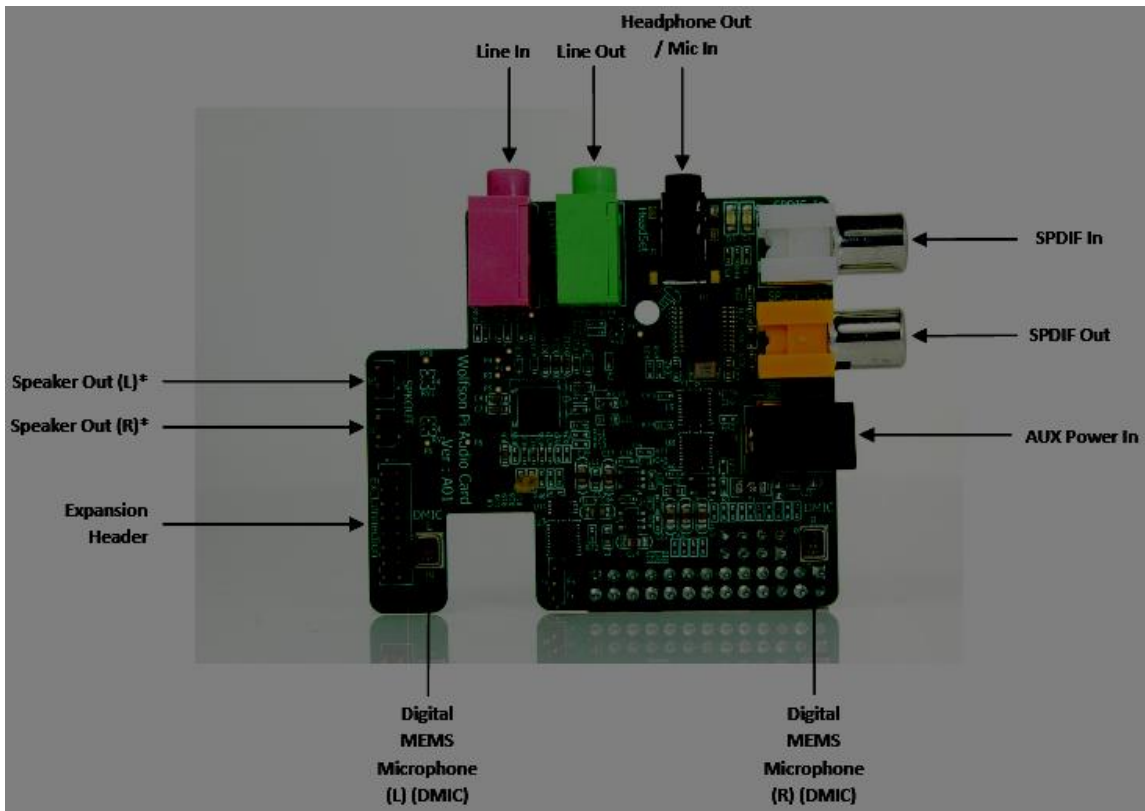
Typical features:

- Analog line-level output

- Analog line-level input

- Digital stereo audio input (SPDIF)

- Digital stereo audio output (SPDIF)

- High quality headphone output, with microphone facility (for headphones with boom microphone)

- Onboard stereo digital microphones

- Ability to play High Definition

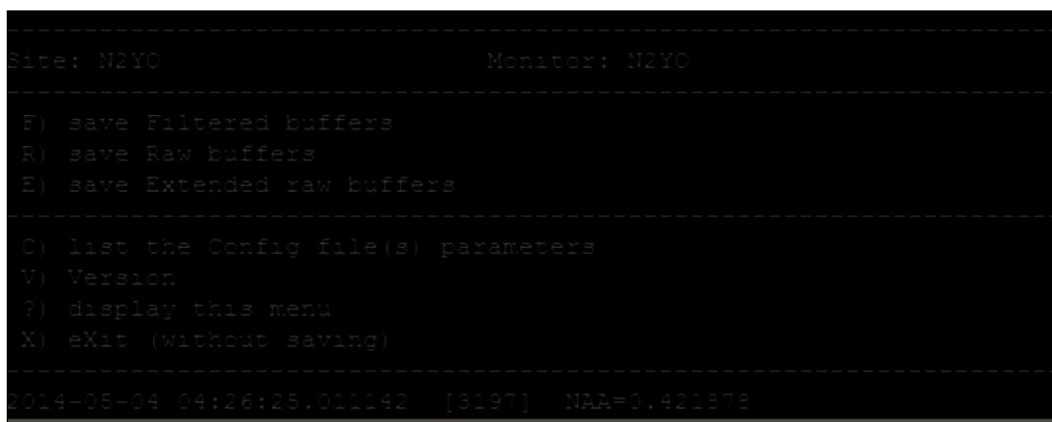- Onboard power amplifier for directly driving loudspeakers.

The card, released only recently (March 2014), is not as cheap as the USB dongle (around $35), and only a few online stores sell it, but considering the performances and the matching parameters and connections with the Raspberry Pi card, the Wolfson Audio Card is highly recommended for a reliable SID monitor.

The critical part is the driver suite which is (as of now) not yet polished to be a stand alone set of file to be installed by users. There are currently two options, one to save the most recent image file from Element14 web site and replace completely the operating system with this new one, precompiled such as the audio card would be fully functional. The other option is to load source files and recompile the kernel. Both methods would provide similar results, but recompilation of kernel is the most flexible choice. Unfortunately the process takes several hours.

The manufacturer has made the following statement: "It is intended that, ultimately, drivers will be fully integrated in future OS downloads, starting with Raspbian. The All-in-One approach will then no longer be necessary."

Software: SuperSID for Linux

The program, wrote in Python by Eric Gilbert from Singapore, is the Linux version of Stanford SuperSID which is available for Windows platforms only. In fact the Linux program is simpler as it does not have a graphical interface. All input parameters are stored in a configuration file, identical with the file used by the Windows program. Once the software is started (running supersid.py), the user is presented with this screen:

A text line is refreshed every few seconds to indicate the current time and the measured signal level from the VLF station(s). The output files have the same structure like the Windows counterpart so the can be uploaded or analyzed in the same way, using the same tools.

The author mentioned a few other features specific to this program:

- Continue recording after interruption

- Auto adjustment of the interval period for better accuracy

- New extended file format with time stamp to the 1.000th of second

- sidfile.py can be used as a utility to manipulate SID files

- Accepts multiple files to display up to 10 days in continue (wildcards possible)

- Can connect to NOAA to draw the day's events

- Can send the graph as PDF by email

The program is free, aligned with a MIT License (MIT). It can be downloaded from GitHub at this address: https://github.com/ericgibert/supersid

Discussions about SuperSID can be found on the dedicated Yahoo group: https://groups.yahoo.com/neo/groups/Super_SID/info

At this time there are a couple of challenges that prevent the program to work properly with audio cards sampling higher than 48 kHz, both USB-type and dedicated, such as Wolfson Audio Card. The author is currently working to fix the problems and I hope at the time of the SARA Conference they would have been resolved.

Software: VLF Tools

The VLF Tools package is a set of command line utilities for processing and storing VLF radio signals that has a wider range of applications, including SID monitoring. The author is Paul Nicholson from United Kingdom and the open source software is released under the Simplified BSD license. The main features of VLF Tools are listed by the author:

- Command line driven, scripted processing;

- Precision timestamped capture and processing;

- Streamable packeted signal streams;

- Whistler detection;

- Signal database;

117

- TOGA measurement;

- Linux, FreeBSD, OpenBSD;

- Open source;

- Real-time, post-processing, or simulations;

- Distributed pipelines, built-in networking;

- SID monitoring with phase and bearing;

- Runs on Raspberry Pi, BeagleBone;

- SDR-IQ and RTL2832U;

Installation may look a little challenging for non-Linux users, but it is well documented on the project's web page: http://abelian.org/vlfrx-tools/notes.html

The programs in this package exchange data with each other using a simple packeted data format. Each packet is timestamped and contains sample rate calibration information. The data is streamable, meaning that a program can begin work in the middle of a stream and does not need to see the start. Signal streams can be exchanged through a choice of files, fifos, lock-free buffers, and network connections.

Here is an example how to create a stream originating from the sound card:

```
vtcard -vv -d hw:0,0 -b16 -r 96000 @raw,20,i2
```

The utility (vtcard) identifies the sound card hardware, sets the sampling speed and creates a stream called "@raw". The buffer is 20 seconds long and uses 16 bit words (20,i2).

While the stream is continuously updated in background, another command can perform the SID monitoring job:

```
vtsid -vc sid.conf @raw
```

The vtsid command simply reads the config file (sid.conf) and uses as input the stream @raw handled by the vtcard utility. The amplitude levels from VLF stations are stored in a local database which can be queried for text outputs or graphical diagrams:

```
vtsidplot -o "png" -m NAA -T2014-05-01,+24h /raw/sid/ > diagram.png
```

This command retrieves data from the database located at /raw/sid, extracts the NAA signal for May 3rd 2014 and generates a png image. The standard output is then directed to the diagram.png file, which can be displayed on any computer with graphic capabilities:

NAA 2014-05-03,+24h /raw/sid/
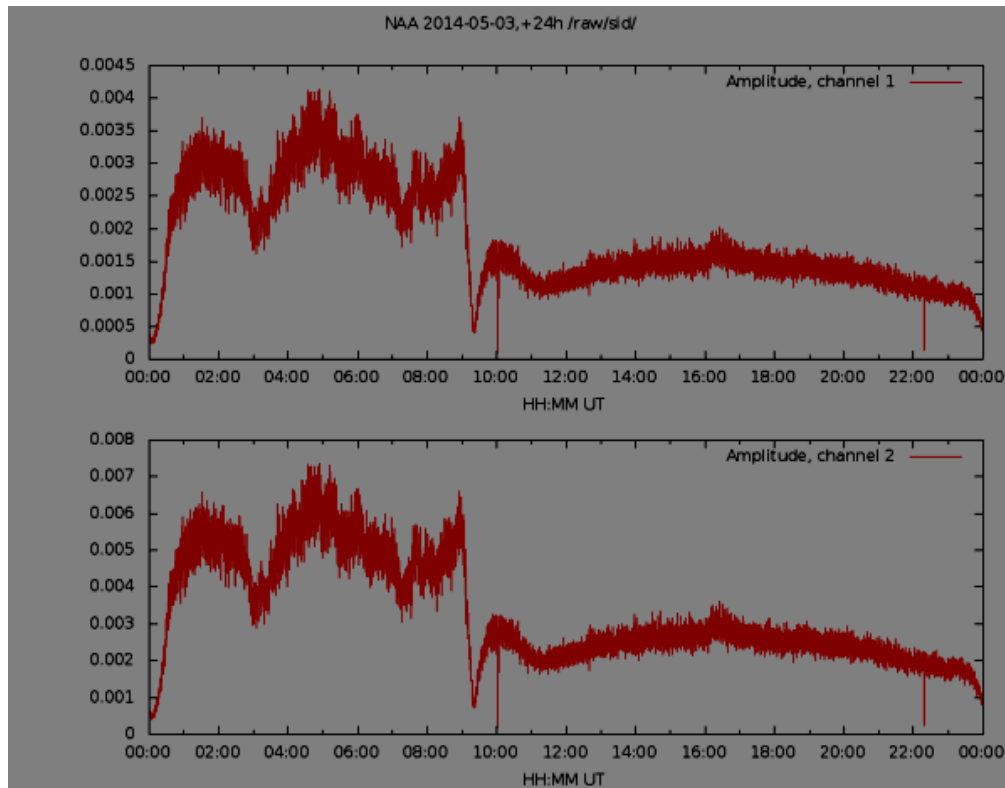
This is just an example how to use VLF Tools that only scratches the surface of this very powerful package. The program works very well with Wolfson Audio Card, however it does not read properly data from the USB dongle apparently because USB isochronous data transfer does not work properly on the Raspberry Pi. Additional tests with other USB cards may be required to identify the origin of this problem.

Conclusions

Raspberry Pi is a very good alternative to a standard PC running Windows. It is less expensive, more reliable, does not need much power, is small and very flexible as it is powered by Linux. However the software that controls the sound cards compatible with Rasberry Pi (drivers in particular) may need a little more work to have the system sampling without errors at 96 kHz or more. At this time the combination SuperSID Monitor + Raspberry Pi Model B + Wolfson Audio Card + VLF Tools is a winner.

References

- Raspberry Pi on WikiPedia: http://en.wikipedia.org/wiki/Raspberry_Pi

- Wolfson Audio Card User Manual - http://www.element14.com/community/docs/DOC-65691/l/user-manual-for-wolfson-audio-card

- Cross-platform Sudden Ionospheric Disturbances (SID) monitor - https://github.com/ericgibert/supersid

- VLF Receiver Software Toolkit - http://abelian.org/vlfrx-tools/

An Off-The-Shelf 611 MHz Total Power Telescope

Part 0x02

Ken Redcap (KD8WOA)

Tom Hagen (NE9Y)

Ed Hendry

1. Introduction

Part 0x01 of this presentation was given at the SARA 2014 West Conference. Part 0x02 will focus on ...

- Analyzing the results from an 8-Bay bowtie UHF antenna for channels 14 - 69 (Antennacraft U8000)
- Configuring/tuning the C# program SDRSharp.exe
- Investigating available software plugins for logging for SDR# (RTL-SDR.Com)
- Testing a second antenna having a yagi configuration for channels 14 - 69 (Antennacraft MXU59)

This project is a work in progress and is my first effort on a radio telescope to detect energy in this frequency range. The telescope is being set up at the McMath Hulbert Solar Observatory (MHO) in Lake Angelus, MI. All electronic components and antennas (2 antenna and 1 USB dongle) required were purchased from Amazon except for the low noise amplifier. All freeware software components were derived from sites with various versions of SDR# like SDRSharp.Com and RTL-SDR.Com. Inspiration for the project comes from Curt Kinghorn's presentation at the 2013 SARA Western Conference on low cost radio telescopes using off- the-shelf TV receive antennas and an article in the August, 2013 SARA Journal about a low cost HI receiver.

1. Background

AS THIS PAPER IS BEING WRITTEN I AM STILL TESTING THE FIRST OF TWO UHF ANTENNAS WHICH ARE BOTH AVAILABLE FROM AMAZON ALONG WITH THE REST OF THE HARDWARE USED EXCEPT FOR THE:

- LNA … $70.00 FROM MINICIRCUITS.COM
- TRIPOD USED TO HOLD THE THE FIRST ANTENNA - ALREADY AVAILABLE AT MHO
- Cables and the hardware required to facilitate the LNA

- HP 8540P LAPTOP (PURCHASED OFF-LEASE) … I AM ASSUMING THAT SOME KIND OF A PC IS 121

AVAILABLE

THE FIRST ANTENNA IS AN ANTENNACRAFT UHF/HDTV ANTENNA FOR EXTREME DEEP FRINGE AREAS - 35IN BOOM/40.5IN WIDTH/36IN V HEIGHT (U8000). THE SECOND ANTENNA IS AN ANTENNACRAFT UHF/HDTV ANTENNA EXTREME DEEP FRINGE AREAS 100IN BOOM/20IN WIDTH/38IN V HEIGHT (MXU59). THE COST FOR THE FIRST ANTENNA IS $71 (PLUS $12 FOR SHIPPING). THE COST OF THE SECOND ANTENNA IS $45 (PLUS $9 FOR SHIPPING).

3. Antennas and LNAs

Due to the size of the antennas, both pieces of hardware shipped to my place of work. There is a reasonably large work area at MHO to setup each antenna. Each antenna had to then be transported separately to MHO (3.2 miles).
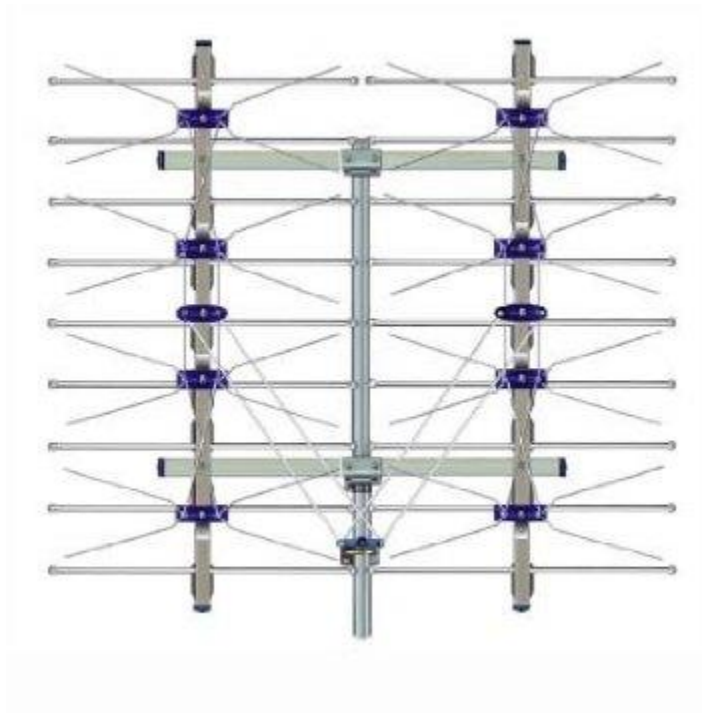
Figure 1 - Antennacraft Antenna (U8000) (X Axis is coming out of the page)

Analysis was found on the web for each antenna dealing with the (dBi) gain. The antenna found was the Antennacraft U-8000 8-Bay Bowtie, modified for 9 FULL-WIDTH Reflector Rods analyzed using 4nec2 (eliminated 1/4-in Gap between each Pair of Reflector Rods).
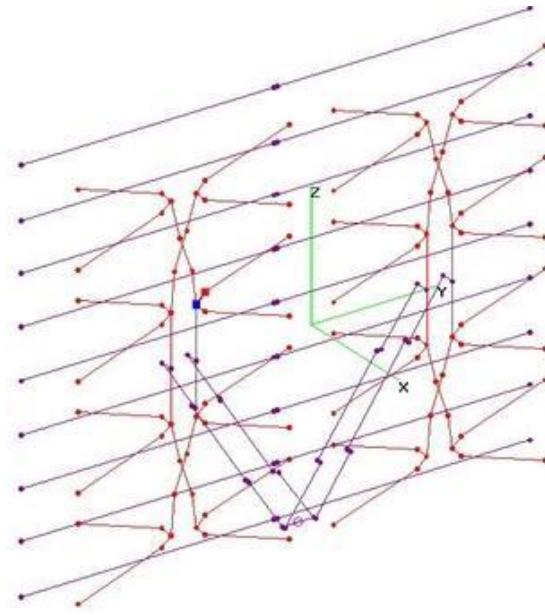
Figure 2 - 3D View Of Antenna With Origin Defined

The wavelength is $300 \div 611 = 0.49$ meters so the height of the antenna is adequate.
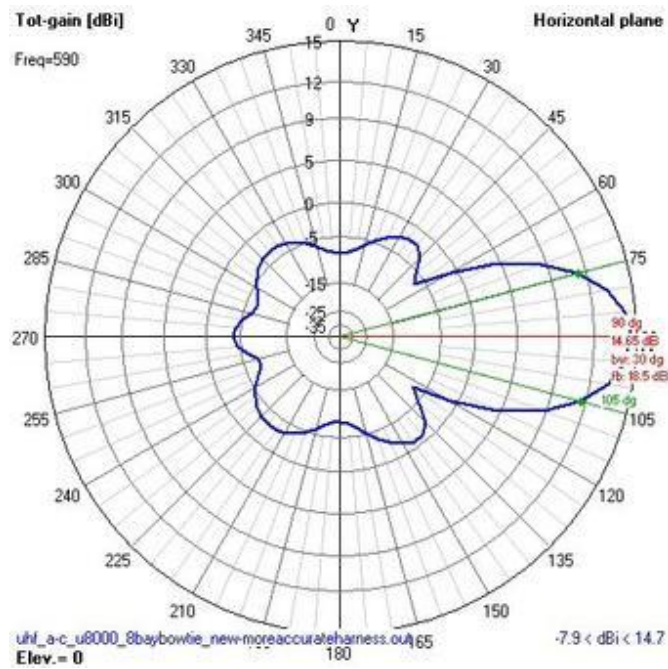

Figure 3 - A-C U-8000 8-Bay - 9 Full-Width Refl Rods Azimuthal Pattern at 590 MHz

Figure 4 - Outside Of Tower 2 Office

After the mount for the antenna was made level, the coax was run into the office of Tower 2.

Figure 5 - The Antenna Connected To Tower 2

Next is the Antennacraft MXU59 yagi antenna. Finding similar analysis for this antenna was not as easy. I strived to match the boom length and a similar reflector for the analysis.
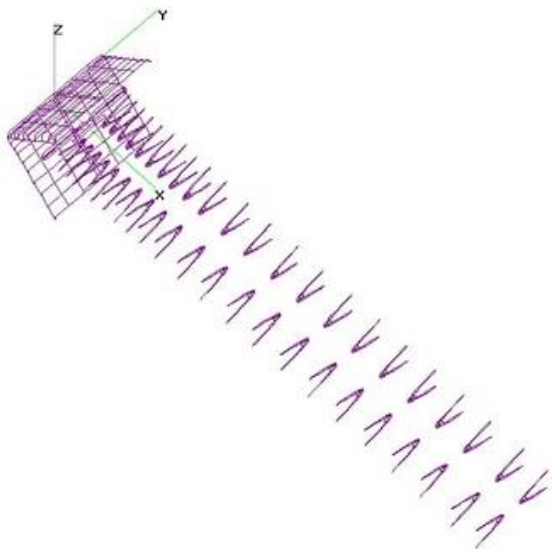
Figure 6 - 3D View Of Yagi Antenna With Origin Defined
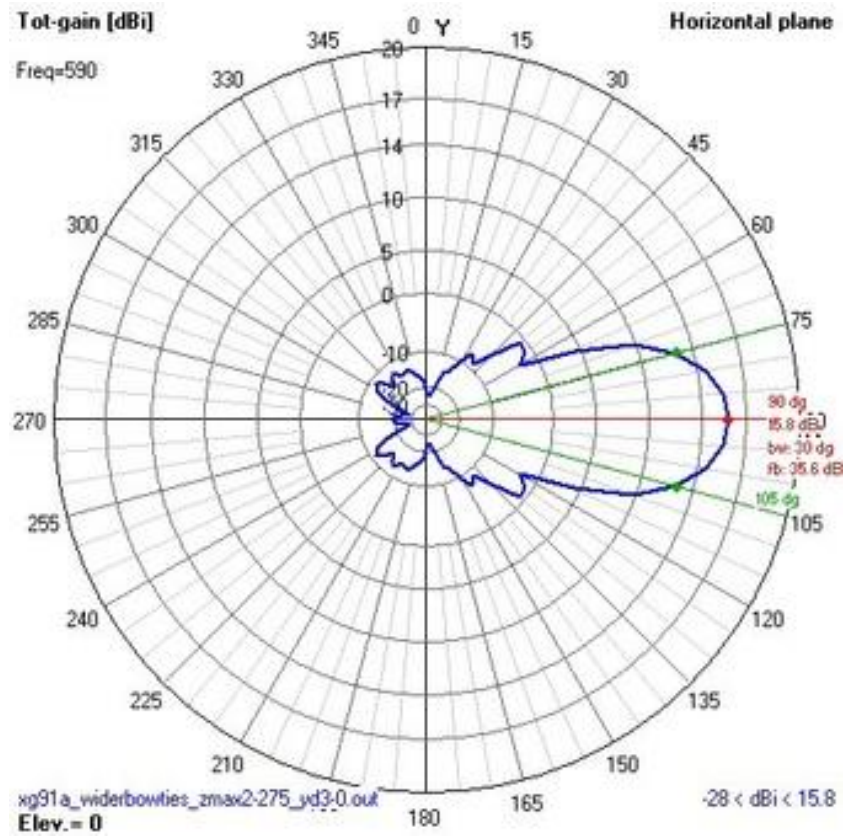
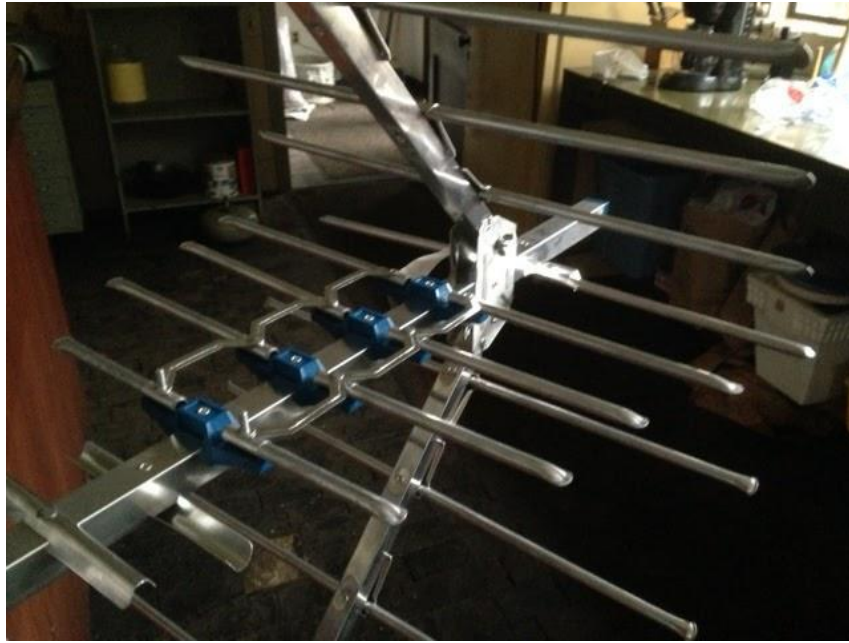Figure 7 - Yagi Azimuthal Pattern at 590 MHz

Figure 8 - Proposed Yagi Antenna
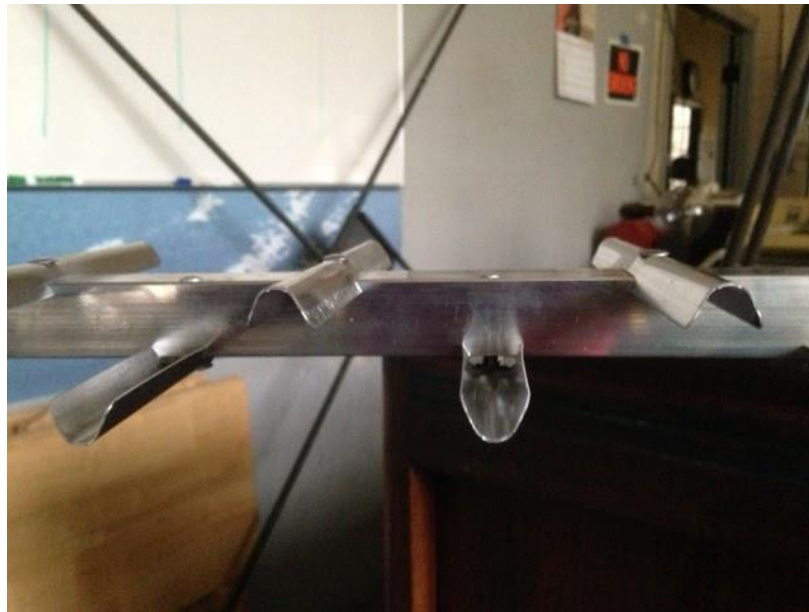
Figure 9 - Driven Element

Figure 10 - Director Elements

After discussions with Curt and Tom each antenna will be tested in a standalone configuration and in an interferometer configuration (approximately 100 feet apart).

A Lenovo laptop (running XP Pro) is used to run the SDR# software. Please note that the software is also running on a Windows 7 HP laptop. The websites used for the software and plugins are SDRSharp.Com and RTL-SDR.Com. Click on the DOWNLOADS link (SDRSharp.Com) to access the page. About halfway down the DOWNLOADS page under the caption 'Important note for RTL-SDR users' is a link.

http://sdrsharp.com/downloads/sdr-install.zip

This particular install includes the zadig tool which is required to load the USB drivers for the dongle (zadig.akeo.ie). When running these tools under Windows 7 (or 8) make sure that it is done as administrator (right click the object you are executing and one of the options should be 'Run As Administrator').

The ZIP file is 152 KB. It contains the folder 'sdr-install' which contains httpget.exe (command line internet FTP like copy command), unzip.exe (QED) and install.bat (sets up files to run SDRSharp. Install.bat works find under XP Pro but under Windows 7 (or 8) please run the file as administrator. The bat file creates a folder 'sdrsharp' under the folder where the batch file is being executed.

The two modes under the 'Radio' option in SDR# that I have been using so far are WFM and RAW. Available options include NFM, WFM, AM, DSB, LSB, CW, USB and RAW. Other than the 'Radio' tab, the 'Stop' and 'Configure' buttons I am still practicing with the application. Right now the slowest sample rate is 0.25 MSPS (with the lowest resolution (8 bit)) making the longest record time that I have been able to achieve before the plugin stops recording is 71.5 minutes. This is better than the original 10 minutes that I was initially achieving but is still inadequate for what I am trying to accomplish which is a 24 hour scan.

As an update, a new and improved data logging plugin is currently being tested - it was downloaded from a site somewhere in Russia (rtl-sdr.ru) and the link was on the RTL-SDR.Com website. Click on the "SOFTWARE v" drop down near the top of the page and click on the "LIST OF SDRSHARP PLUGINS." From there scroll down to "Modified Recording Plugin." I have downloaded the file and unzipped it with no ill effect. All that has to be done is rename the DLL that is being replaced and then copy the updated DLL into the SDR# folder. But then there appeared to be a catch - there is an error message when starting SDR# indicating that the new DLL for data logging is not compatible. This can be fixed by removing the contents of the SDR# folder and download a fresh copy of SDR#. Before starting SDR# replace the existing SDRSharpWavRecorder.dll with the updated version. SDR# should now start with the new version of the recording plugin.

The link below is a good source for documentation on SDR#

http://atouk.com/wordpress/?pageid=237

The LNA (Low Noise Amplifier) is made by Mini-Circuits. The cost is $70.00. The gain at 611 MHz is about 19 dB. The noise figure is 0.5 dB.
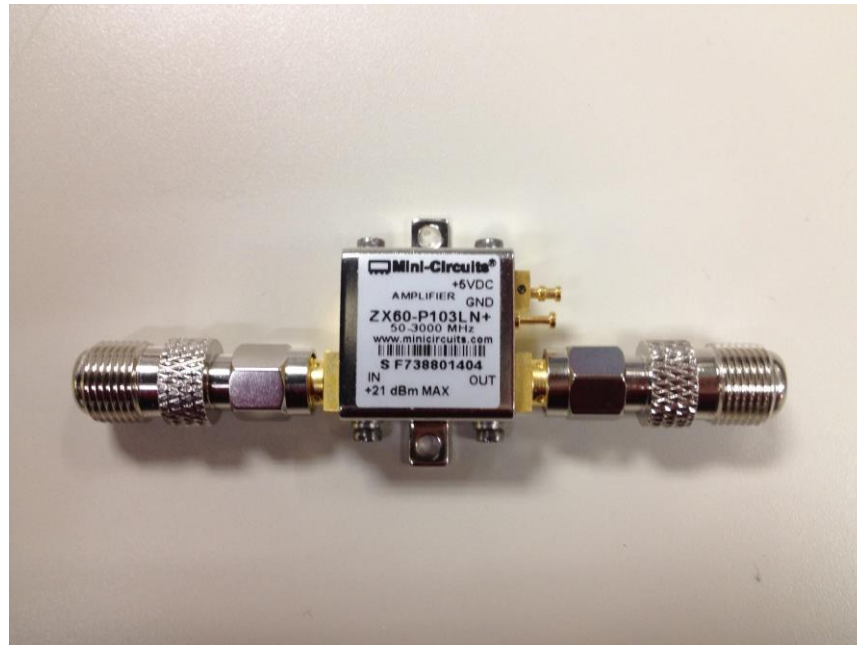

Figure 11 - Mini-Circuits ZX60-P103LN+

A 9 VDC wall wort is used with a 5 VDC voltage regulator. The amplifier is mounted on the arm of the antenna tripod.

4. USB Dongle

There are two (2) IC's that make up the bulk of this device.

R820T

The R820T is a highly integrated silicon tuner that builds in a low noise amplifier (LNA), mixer, fractional PLL, VGA, voltage regulator and tracking filter eliminating the need for external SAW filters, LNA, balun and LDO. It is painful to continue reading the preliminary spec.

● http://superkuh.com/gnuradio/R820T_datasheet-Non_R-20111130_unlocked.pdf

The RTL2832U is a high-performance DVB-T COFDM demodulator that supports a USB 2.0 interface. The RTL2832U complies with NorDig Unified 1.0.3, D-Book 5.0, and EN300 744 (ETSI Specification). It supports 2K or 8K mode with 6, 7, and 8 MHz bandwidth. Modulation parameters, e.g., code rate, and guard interval, are automatically detected.

The RTL2832U supports tuners at IF (Intermediate Frequency, 36.125MHz), low-IF (4.57MHz), or Zero-IF output using a 28.8MHz crystal, and includes FM/DAB/DAB+ Radio Support. Embedded with an advanced ADC (Analog-to-Digital Converter), the RTL2832U features high stability in portable reception..

The state-of-the-art RTL2832U features Realtek proprietary algorithms (patent-pending), including superior channel estimation, co-channel interface rejection, long echo channel reception, and impulse noise cancellation, and provides an ideal solution for a wide range of applications for PC-TV, such as USB dongle and MiniCard/USB, and embedded system via USB interface.

- realtek.com.tw/products/productsView.aspx?Langid=1&PFid=35&Level=4&Conn=3&ProdID=257

There are two (2) brands of this dongle that I found, those made by NooElec (Oscoda, MI) and those made by China (actually, both probably come from China). As far as the markings go the

DVB-T marking is the only marking that the two (2) dongles have in common (and yes, DVB Digital Video Broadcasting USB2.0). So if there wasn't an R820T stamp on the dongle, then the assumption was that the R820T chip wasn't being used …
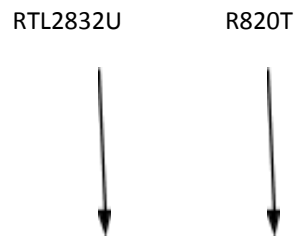

Figure 13 - Generic Dongle ($12)

External physical layout is identical …

Figure 14 - External Comparison
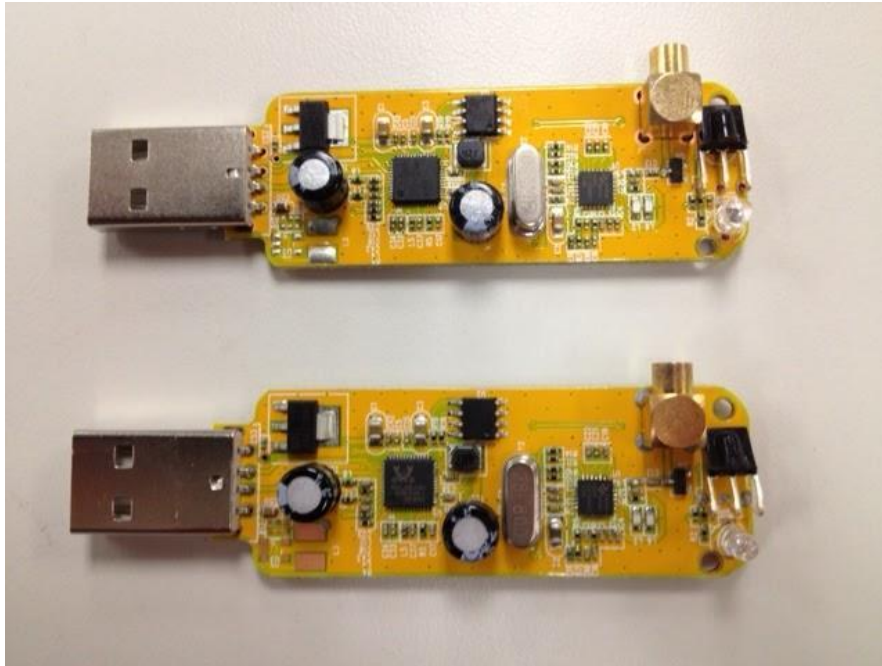
And so is the internal layout, identical ...

RTL2832U   R820T

132

Figure 15 - Internal Comparison (notice the two differences)

As a simple check, each dongle was "plugged in" and the SDR# program was started … There were no issues.

5. Connectors

Although not a definitive list, here is a list of the types of connectors that I have run into since starting this project. I was able to find assembled adapters for ANY connector combination on Amazon. Every one that I purchased was shipped directly from China. Prices ranged from $2 to $9 and with little to no shipping charges - the big unknown was the time for the package to arrive. The only cable that was made at MHO was a cable with male F connections on both ends.

Connector Type	Male	Female
F	IT/P	OT/S

FME	IT/P FME Male	OT/S FME Female
MCX	P	S
RP-SMA	IT/S	OT/P
SMA	IT/P	OT/S

SMA Connector Plug
8mm Hex Nut
Male Pin
Inner thread

Table 1

Acronyms ...

BTA	Bow Tie Antenna
CE	Conformité Européenne
COFDM	Coded Orthogonal Frequency Division Multiplexing
DAB	Digital Audio Broadcasting
dBd	Decibel Dipole (Reference)
dBi	Decibel Isotropic (Radiator) … dBi = dBd + 2.15
dBm or dBmW	Measured power referenced to one milliwatt
dBW	Measured power referenced to one watt
DVB-T	Digital Video Broadcasting - Terrestrial
F	?
FCC	Federal Communications Commission

FM	Frequency Modulation
FME	For Mobile Equipment
IT	Inside Thread
LNA	Low Noise Amplifier
LPC	Lenovo Personal Computer
MCX	Micro Coaxial
Mini MCX (MMCX)	Mini Micro Coaxial
OT	Outside Thread
P	Pin
PCB	Printed Circuit Board
R820T	Rafael Micro DTV-T chip
RP	Reverse Polarity
RTL	
S	Socket
SDR	Software Defined Radio
SMA	Subminiature version A
USB	Universal Serial Bus

Table 2

Figure 16 - RunTeck … Same Chipset

One thing that I did notice was this device appeared to be assembled by hand - the antenna connection was not inline with the PCB.

6. Intermediate Results

Finally turned on logging and walked away for two (2) days. When I returned all that had been generated was one log file of length 2,097,152 KB. Ah yes, the old Windows file length maximum … So it would appear that the "plug in" as installed for recording will not work (one (1) minute of record time in 8 bit PCM mode is about 234 Meg of storage). What is needed here is a slower sample rate … please note that I found a way to cut down on the number of samples per second increasing the maximum record time to just over 70 minutes. Wondering if the drop down for sample rate could be modified to include more "slower rate" values.

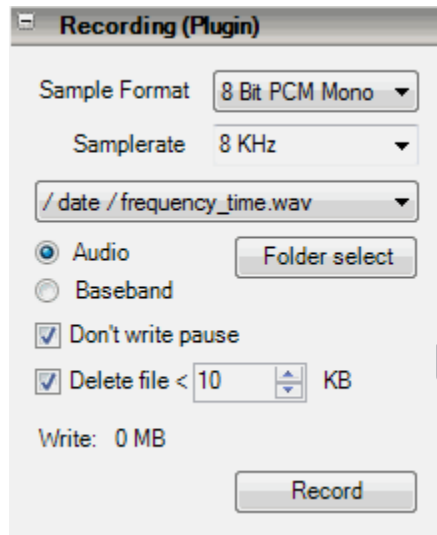The "Modified Recording Plugin" has the following inputs …

Figure 17 - Modified Wave Recording controls

The "Recording Plugin" that comes with SDR# only allows the selection of the "Sample Format" and whether to record audio or baseband or both. Another setting for sample rate is also available under the "Configure" button next to the dropdown used to select the input device.
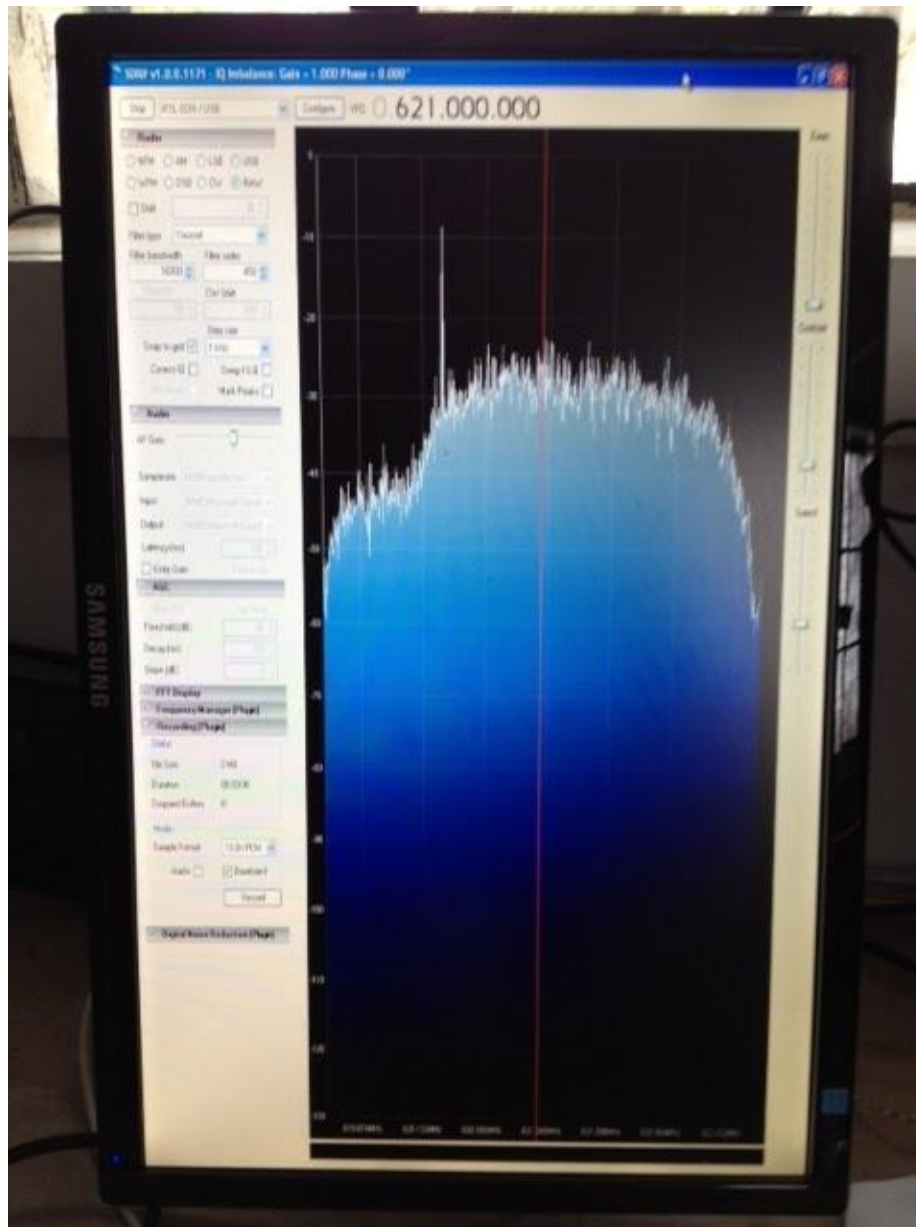
Figure 18 - TV Station Channel 39

(Please note that the spike below 621 MHz is known as the 'Pilot Signal' which most channels have and is being investigated as a possible reference for calibrating SDR#/USB Dongle pairs.)

Tom and I came up with the idea of pointing the scope at a known source (Channel 39 (centered at 621 MHz)) to see how accurate our configuration was. TV stations in the Detroit area emanate from the east so we went from looking north (Cass A) to the east. Success, we were able to see channel 39 …

Another idea to test the accuracy of the two types of USB dongles was to connect each dongle to a signal generator (recently calibrated I might add …) and apply a 611 MHz signal.
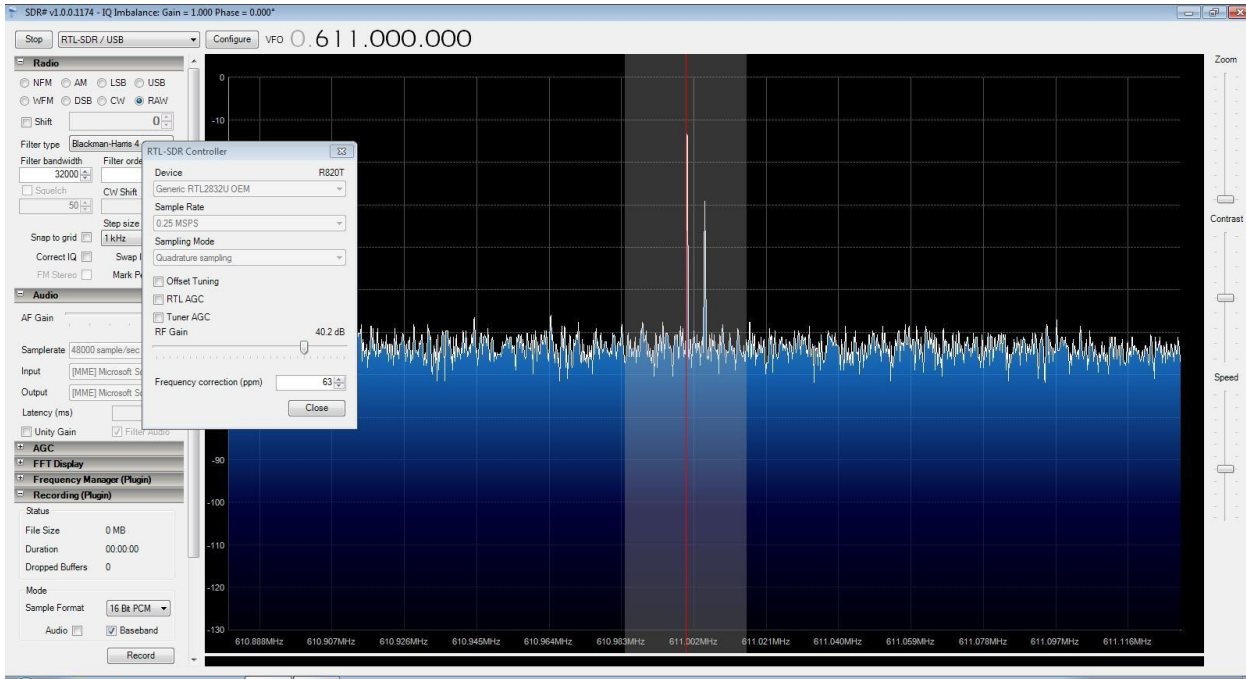

Figure 19 - NooElec Dongle Response To 611 MHz

Clicking on the 'Configure' button there is a setting for 'Frequency correction (ppm)'. The NooElec dongle required a value of 63 to align with the signal generator.

The same test was performed on the generic dongle. The value for 'Frequency correction (ppm)' to get the dongle to align with the signal generator was 82. Once this test was completed on both dongles the next test was to maintain the 'Frequency correction (ppm)' value and apply a 1 GHz signal. The hope was that the dongles would align with the 1 GHz signal without modifying the 'Frequency correction (ppm)' value … and there was great rejoicing … Please note that the 1 GHz maximum was due to the limitation of the signal generator. The hope was for 1.4 GHz, but we got close enough …
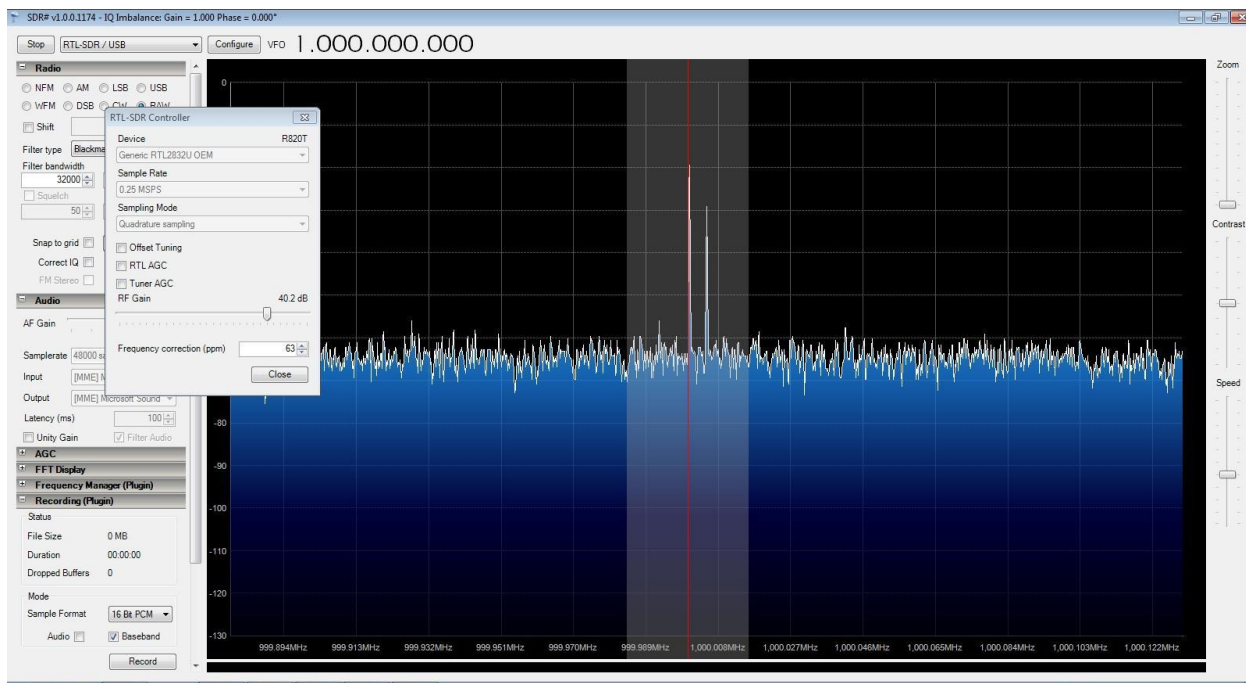
Figure 20 - NooElec Dongle Response To 1 GHz

7. Moving Forward And Next Steps

For the SARA East 2014 update, it will include …

- Documentation on installing USB drivers (Zadig) for the dongles
- Clean up any loose ends from SARA West 2014 presentation
- Digging into the C# code for SDR#
- Update on the bowtie (Bill Nye) and Yagi scopes
- Update on the mount for the Yagi scope
- Possible testing of the bowtie antenna at the top of Tower 3

8.Conclusion

So far, no road blocks. The only pothole (sorry, I'm from Michigan) so far is being able to slow down the sample rate to increase logging duration time. As the source code for SDR# is reviewed, I believe an answer to longer logging time will avail itself.

The Role of Mass Produced Gregorian Offset Antennas

and Feeds on the Future of Radio Astronomy development

A Review

Mohammed Q. Hassan

Communication Systems Engineer - Arlington, VA

Abstract :

   The rapid developments in modern radio astronomy has led to proposing low cost high production level antennas. While the Allen Telescope array is dependent on 21 ft. offset Gregorian antennas having 42 antennas and the potential of increasing it to the full array of 350 units depending on funding, there is a far more profound project that is better financed internationally with a potential of having 3000 antennas, which is the Square Kilometer Array (SKA). South Africa had the first antenna delivered this March, named the MeerKAT with Phase 1, to have 64 such antennas projected to do science for 2017.

   The SKA offset Gregorian antenna design has a 13.5m (44.4ft) diameter with a 3.8m (12.5ft) subreflector and a receiver indexer for four receivers covering the a broad range of frequencies, from 600 MHz up to 14.5 GHz. Other cheaper designs for 15 m diameter offset Gregorian lighter structure antennas are being designed to reduce the cost and make true mass production possible for the large array

This review paper will show us the challenges put forward to combine several ground breaking concepts leading to a unified design that could be produced in large numbers. Several institutions are collaborating to bring this into fruition.

The Square Kilometer Array (SKA):

The (SKA) is a radio telescope in development in Australia and South Africa which will have a total collecting area of approximately one square kilometer. It will operate over a wide range of frequencies and its size will make it 50 times more sensitive than any other radio instrument. It will require very high performance central computing engines and long-haul links with a capacity greater than the current global Internet traffic. It will be able to survey the sky more than ten thousand times faster than ever before. [1]

With receiving stations extending out to distance of at least 3,000 kilometers (1,900 mi) from a concentrated central core, it will exploit radio astronomy's ability to provide the highest resolution images in all astronomy. The SKA will be built in the southern hemi-sphere, in Sub-Saharan states with cores in South Africa and Australia, where the view of the Milky Way Galaxy is best and radio interference least.

The Organization

The SKA is a global project with ten member countries which aims to provide answers to fundamental questions about the origin and evolution of the universe. In April 2011, Jodrell Bank Observatory of the University of Manchester, in Cheshire, England was announced as the location of the headquarters office for the project. In November 2011, the SKA Organization was formed and the project moved from a collaboration to an independent, not for profit, company. As of December 2012, the members of the SKA Organization are:

- **Australia**: Department of Innovation, Industry, Science and Research
- **Canada**: National Research Council
- **China**: National Astronomical Observatories of the Chinese Academy of Sciences
- **Germany**: Federal Ministry of Education and Research
- **Italy**: National Institute for Astrophysics
- **New Zealand**: Ministry of Economic Development
- **South Africa**: National Research Foundation
- **Sweden**: Onsala Space Observatory
- **The Netherlands**: Netherlands Organization for Scientific Research
- **United Kingdom**: Science and Technology Facilities Council

India's National Centre for Radio Astrophysics is an associate member of SKA. Germany has also indicated its intention to join SKA. More than 350 scientists and engineers- representing 18 nations and nearly 100 institutions are currently on track to construct what will be the world's largest radio telescope, within this major framework.

   With a budget of around USD 2 billion to be covered over the next ten years, it comprises of three different kind of arrays, accomplishing RF centric phased array feeds , like dishes with phased array feeds (DSH), low frequency aperture arrays (LFAA), mid frequency aperture array (MFAA), and wideband single pixel feeds (WBSPFs).

These will come as a result in the following main categories

1- The Sparse Array (LFAA) to cover the very low frequencies 50-350 MHz
2- The Dense Aperture Array (MFAA) 400-1500 MHz
3- Center Fed Parabolic Dishes e.g. (KAT 7 antennas)
4- The Offset Gregorian Dish array 600 MHz-14.5 GHz

The Sparse Array
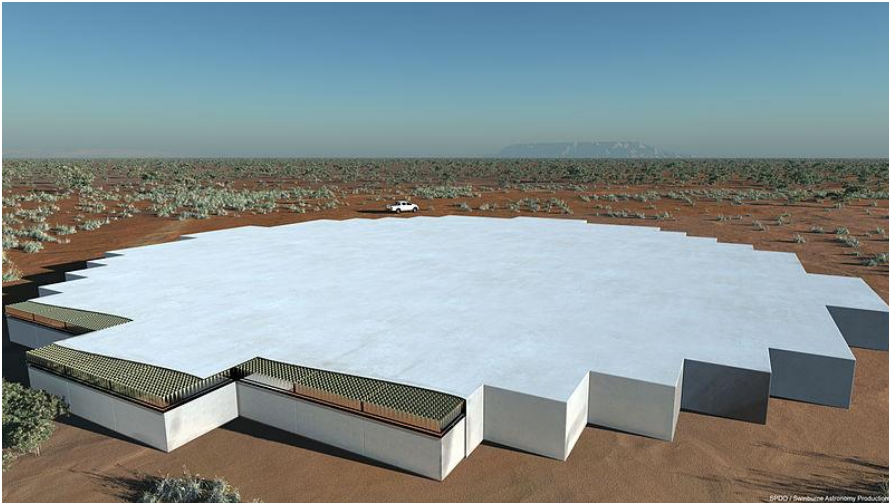
The Dense Aperture Array

Developments in Offset Antenna Technologies:

One of the greatest challenges for the (DSH) group is the mass production of several thousand 15m wide telescopes with identical performance characteristics. Main specs for the large array of dish antennas was to propose an Offset Gregorian design between 12 to 15m in diameters. Our paper will focus on these competing designs and their manufacturing technologies and achieved specifications. Three different prototypes for the SKA dishes are currently being built: DVA-1 in Canada, DVA-C in China, and MeerKAT-1 in South Africa.
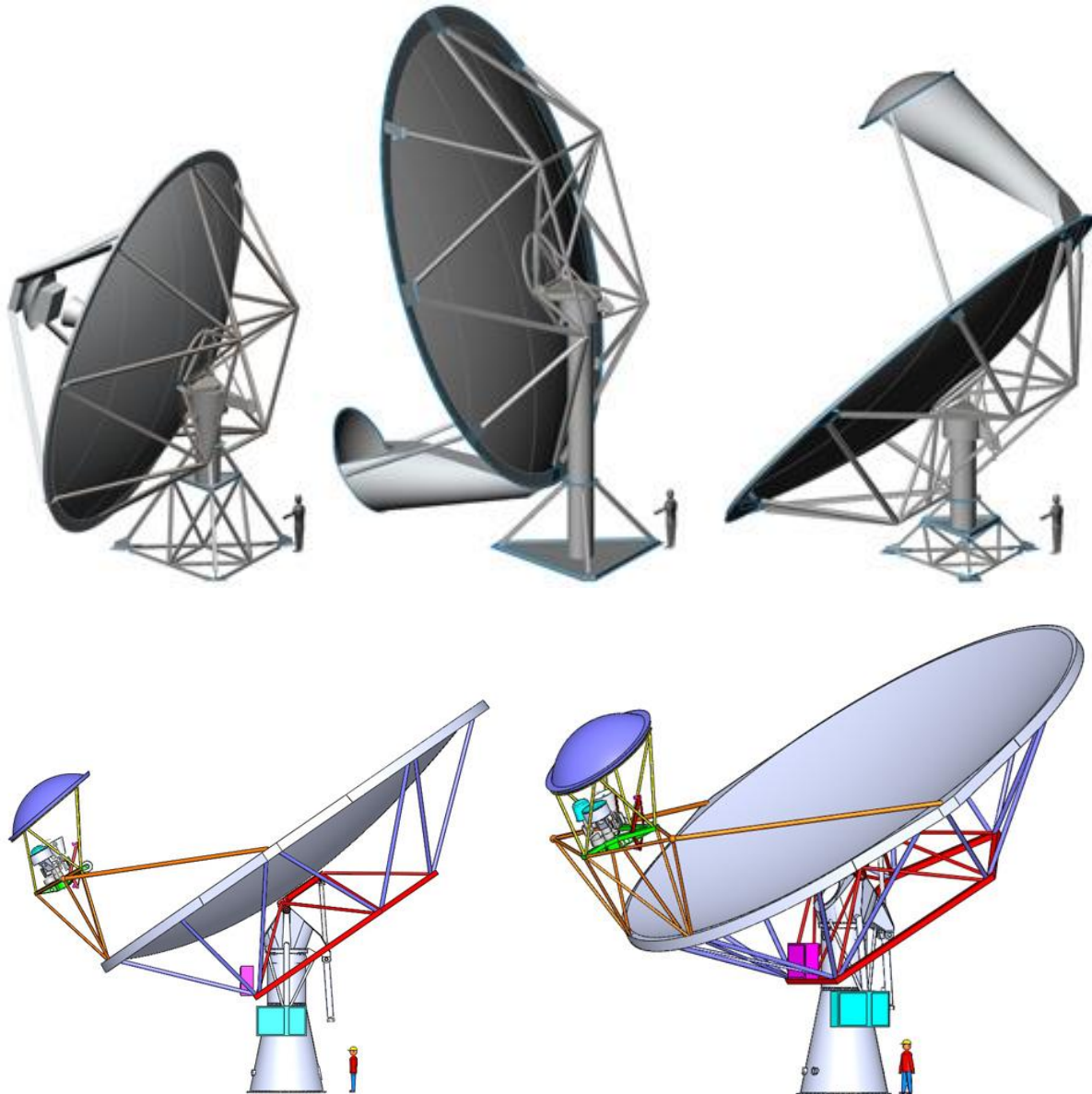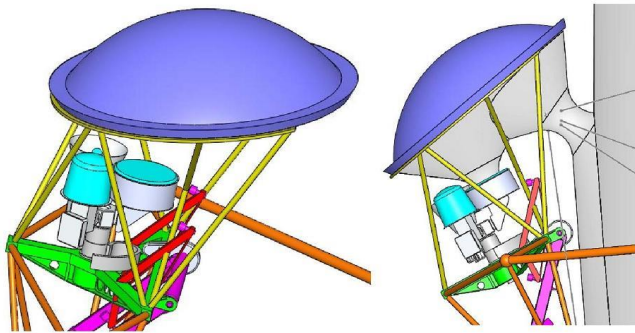
A)-

Dish Verification Antenna (DVA-1) design is being optimized, which is a joint project between Composite Applications in Radio Telescope (CART) program at the National Research Council in Penticton Canada and the Technology Development Program (TDP) in the USA (funded by the National Science Foundation), to build an operational prototype for the SKA project.

The shaped offset dual reflector has 15m by 18.2m dimensions with a 4m subreflector that can allow the frequency performance to go down to 350 MHz, and aperture efficiency reaching **78%** [13], having an **F/D = 0.52** [12] . The main antenna design drivers are to have [3] :

1- Low cost per unit aperture area with low (cost materials, mass design & labor)
2- Very low operational cost for a 30 year life
3- Frequency range of 0.35-10 GHz utilizing 4m subreflector

4- Excellent Ae/ Tsys with accurate surface, controlled spillover and low diffraction

5-

Cooled ATA Feed-5
with focus device

Quad-ridge Uncooled

High gain
corrugated horn type

300 kg, feeds at 483 mm radius
1.340 m focus to mount flange
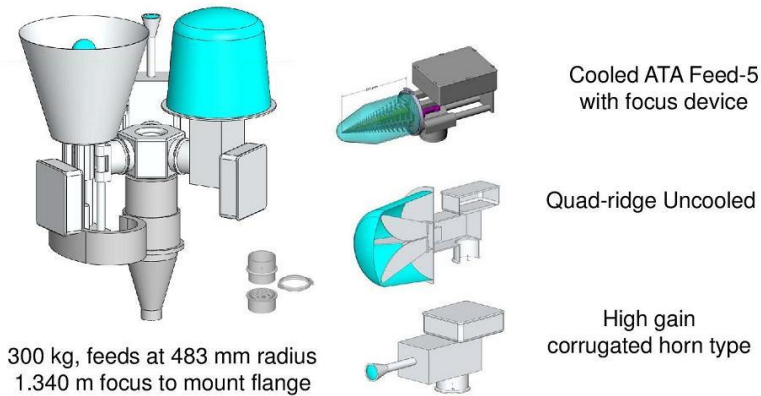
Exceptional dynamic range

The DVA-1 Subreflector System will have a three station feed indexer. The ATA feed could be one of them. The beam path image is shown on the diagram on the left.

Consider that all of these values are still evolving.

Secondary reflector	85 Kg	FRP composite
Secondary support	143 Kg	Alum tube 80 dia x 4 mm tubes
PAF & positioner	350 Kg	Steel
SPFs & indexer	380 Kg	Steel & alum
Feed platform	400 Kg	Steel ? x 6 mm tubes
Platform support spars	200 Kg	FRP Composite
Total forward of primary:	1558 Kg	Not optimized
Primary reflector	2,360 Kg	FRP composite
Primary support spars	686 Kg	Steel
Primary center frame	1,836 Kg	Steel
Primary diaphragm connector	60 Kg	FRP composite
Total full reflector assy:	6,500 Kg	Estimate

The masses for the Elevation Structures are shown in the table below :

B)- Dish Verification Antenna (DVA-C)

The Chinese version of the DVA-1 has been named as the DVA-C . the structure of the main antenna is quite similar except that it lacks the advanced shaping technology which will limit the dish efficiency to slightly over **65%** at the main operational range between 0.9- 6 GHz and dropping at both ends with > 55% at 10 GHz and > 60% at the lowest 0.3 GHz, mainly because of its relative low **F/D of 0.36**.

 The total surface accuracy with wind and at night to be **< 1.2mm** r.m.s.

The reflector weight would be **7050 Kg** for carbon fiber and 7250 kg for the aluminum version, and in both case the weight of the mount of **11250 Kg** would be added. As an alternative to the DVA-1 only two wideband single pixel feeds (WBSPF's) may be used. The first would cover **0.3 – 1.5 GHz** , while the second would cover **1.5 – 10 GHz**. [6]

MeerKAT TECHNICAL SPECIFICATIONS

Number of antennas	64
Configuration	Offset Gregorian
Diameter of main reflector (dish)	13.5 m
Diameter of sub-reflector	3.8 m
Surface accuracy (main and sub-reflector combined)	0.6 mm RMS (root mean square)
Pointing accuracy	5″ under optimal conditions; 25″ under normal conditions
Wind optimal (mean/gust)	10/15 km/h
Wind operating (mean/gust)	35/48 km/h
Wind stow (gust)	68.4 km/h
Wind survival 3 sec gust	144 km/h
Azimuth speed/range	2 deg/s (-185 to +275 deg)
Elevation speed/range	1 deg/s (15 to 88 deg)
Lowest elevation	15 deg
Continuum imaging dynamic range at 1.4 GHz	60 dB
Line-to-line dynamic range at 1.4 GHz	40 dB
Mosaicing imaging dynamic range at 14 GHz	27 dB
Linear polarisation cross coupling across -3 dB beam	-30 dB
Sensitivity UHF-Band (0.58 – 1.015 GHz)	220 m^2/K required (expect to achieve better)
Sensitivity L-Band (0.9 – 1.67 GHz)	220 m^2/K required (300 m^2/K achievable)
Sensitivity X-Band (8 – 14.5 GHz)	200 m^2/K required
Aperture phase efficiency	0.91 (at 14.5 GHz)
Surface accuracy	0.6 mm RMS
Pointing accuracy	5″ (optimal conditions, 20 min); 25″ (normal conditions, 24 h)
Pointing jitter	<15″ RMS
Reflector noise contribution	<1K
Reflector reflecting efficiency	>99.5% (main and sub)
Azimuth	2 deg/s (-185 to +275 deg)
Elevation	1 deg/s (15 to 88 deg)
Indexer	4 receivers, 1 min switchover

C)- The MeerKAT Antenna

The Advanced MeerKAT antenna is a very advanced design made from 40 aluminum panels by primary industry partnerStratosat Datacom (Pty) Ltd leading a technology consortium including international partners (GD Satcom, USA) and Vertex Antennentechnik (Germany).

At least 75% of the components making the MeerKAT dish will be manufactured in South Africa by several subcontractors.

[7]
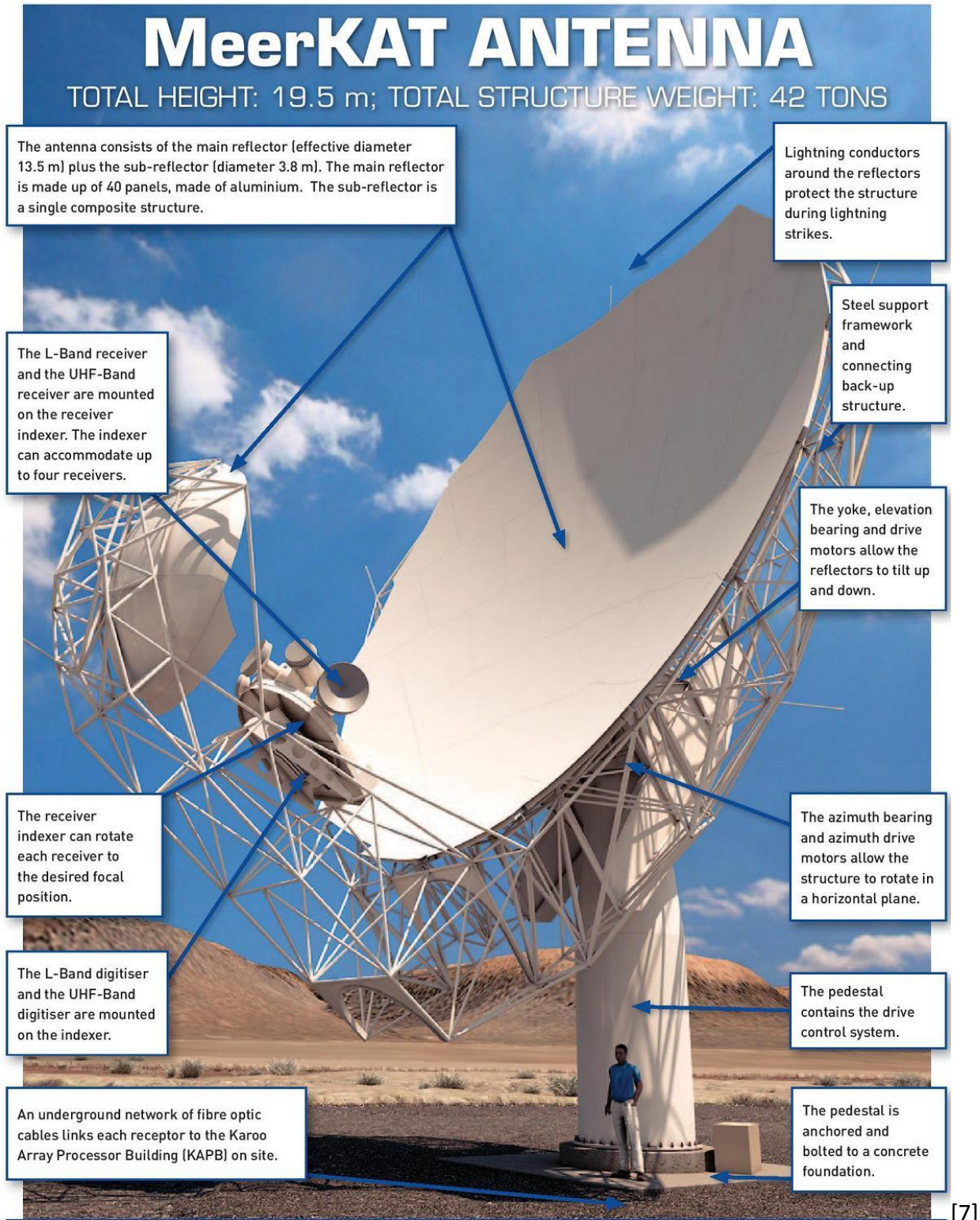
Antenna & Fiber Costs :

One may estimate that the production DVA kind of antenna together with its feed/receiver system going up to 10 GHz to cost around **USD 350K** per unit when manufactured in large numbers. Signal Transmission cost estimates assume **2280** dishes with data rates of 160 Gbps per dish for distances less than 200 Km from the core array center. A greater distances there will be **720** dishes in 40 stations with 160 Gbps per station. Systems costs include budgets for about 1500 km of trenching within the inner 200 Km array and a further 1000 Km of trench to connect stations, at long baselines to a network of 20,000 km of leased dark fiber lines , with an estimated cost of < **USD 150M** [14].

Conclusion :

The comparison of the antenna designs show us clearly that the MeerKAT antenna is more complex and expensive, however offers better surface accuracy that will make it good for over 20 GHz operations , and a true more efficient alternative to traditional circular aperture arrays, making antennas like that of the VLA a design of the past. It made it into production thanks to the experience of its design companies in large radio telescope antennas that included the GBT. However one may expect that design to be implemented for the center of the arrays, while the majority of the dish antennas would come from a unified light weight structure based on the DVA prototypes.

Since NRAO staff are also involved in the new DVA prototypes, it would be nice to have a sample of the production version of 15m resulting design, in addition to an ATA antenna here at Green Bank. SARA'a involvement with the professional community could have a more profound impact on its future, especially when the dawn of mass produced antennas is becoming a reality. Amateur radio astronomy has a much bigger chance of spreading throughout the countries involved with SKA, and integrating globally in a similar way that AMSAT was established with satellite technologies.

References :

1- https://www.skatelescope.org/technology/dishes/

2- http://usskac.astro.cornell.edu/members/index.shtml

3- **SKA TDP & CART and CART 15m offset (DVA-1) Antenna Design**, SKA WP2 Meeting at Oxford UK Oct 27 2010 , Matt Fleming Gordon Lacy

4- http://euclidska.physics.ox.ac.uk/Euclid-SKA/160913/Diamond.pdf, **Square Kilometer Array** : status, Philip Diamond SKA Director-General 16th Sept 2013

5- http://www.bdlive.co.za/national/science/2014/03/27/meerkat-proceeding-on-time-and-on-budget-says-hanekom

6- http://www.skatelescope.org/public/2011-07-13_Dish_Array_CoDR/WP2-020.045.010-TD-002-E_Dishb-ogchina.pdf
SKA DVAC-1 Concept Description : Offset Gregorian Dish Version E

7- http://www.ska.ac.za/download/fact_sheet_meerkat_2014.pdf **South Africa's MeerKAT   Radio Telescope Technical Fact Sheet March 2014**

8- http://www.astron.nl/mfaa2014/Documents/Jonas_MFAA2104.pdf **ZA projects,** **Justin Jonas , SKA South Africa MFAA Workshop –Stellenbosch – February 2014**

9- http://en.wikipedia.org/wiki/Square_Kilometre_Array

10- http://minex-engineering.com/Projects/Sub/skaDesignImg.html

11- http://mwrf.com/systems/rf-black-art-gets-behind-world-s-largest-radio-telescope

12- http://www.astro.cornell.edu/SKATDP/files/Meet_2011Feb_Socorro/DVA1_1_Rev-2_ProjPlan.pdf

13- http://trs-new.jpl.nasa.gov/dspace/handle/2014/42792 , 12-2850_A1b.PDF **An Update on the Mechanical and EM Performance of the Composite Dish Verification Antenna (DVA-1) for the SKA** G.E. Lacy, M.Flemming, L.Baker, W.Imbriale, G.Cortes-Medellin, B.Veidt, G.J.Hovey and D.DeBoer.

14- https://science.nrao.edu/science/Decadal%20Survey/rfi/SKA.pdf, **The Square Kilometer Array** , 1 April 2009 , Contact Author James Cordes, Chair, US SKA Consortium , 607 255-0608 Cornell University, cordes@astro.cornell.edu